

12-22-2021

Distribution and Characterization of Rhyolites of the Strawberry Volcanics – Evolution of a Major Rhyolite Field Associated with Columbia River Basalt Magmatism, Eastern Oregon, USA

Chanel Leigh Dvorak
Portland State University

Follow this and additional works at: https://pdxscholar.library.pdx.edu/open_access_etds



Part of the [Geology Commons](#)

Let us know how access to this document benefits you.

Recommended Citation

Dvorak, Chanel Leigh, "Distribution and Characterization of Rhyolites of the Strawberry Volcanics – Evolution of a Major Rhyolite Field Associated with Columbia River Basalt Magmatism, Eastern Oregon, USA" (2021). *Dissertations and Theses*. Paper 5855.

This Thesis is brought to you for free and open access. It has been accepted for inclusion in Dissertations and Theses by an authorized administrator of PDXScholar. Please contact us if we can make this document more accessible: pdxscholar@pdx.edu.

Distribution and Characterization of Rhyolites of the Strawberry Volcanics – Evolution of a
Major Rhyolite Field Associated with Columbia River Basalt Magmatism, Eastern Oregon,
USA

by
Chanel Leigh Dvorak

A thesis submitted in partial fulfillment of the
requirements for the degree of

Master of Science
in
Geology

Thesis Committee:
Dr. Martin J. Streck, Chair
Dr. John Bershaw
Dr. Jonathan Fink

Portland State University
2021

ABSTRACT

The Strawberry Rhyolites constitute a significant rhyolite field among the largest in Oregon. Aerial coverage of approximately 386 km² and an overall estimated volume of ~67 km³ using a median thickness for each unit. On the other hand, the total volume could be greater than 100 km³ if greater thicknesses apply. The Strawberry Rhyolites, a largely unknown mid-Miocene silicic volcanic rocks, crop out amongst voluminous flood basalt flows of the Columbia River Basalt Group (CRBG) in eastern Oregon. The eruptive activity of the Strawberry Rhyolites is currently constrained to span a period of about 2 million years, ranging from around ~16.2 to 14.3 Ma.

Mid-Miocene rhyolites are part of the Strawberry Volcanics located within the Malheur National Forest near the town of John Day and were first mentioned in the 1960-70s. Still, neither their distribution, composition nor ages were studied in detail until we started to work in the area. Building on our initial reconnaissance data, the main efforts to map rhyolites took place in the context of three Edmap projects from 2019-2021 aided by PSU field study students and covering the area of three 7.5 min quadrangles (Jump-off Joe Mountain, Big Canyon, 1/2 of Logan Valley West, 1/2 of Magpie Table quads) in the NE part of the Harney Basin north of Burns, have shed light on the existence of a diverse set of volcanic units previously lumped into broad single mapping units by earlier regional reconnaissance maps. Hence, there is a much better understanding of the geologic history of the entire northeast margin of the Harney Basin, which plays a significant role in the regional volcanic framework due to this mapping. The focus is to detail the distribution of rhyolite units used for volume estimates,

determine the composition and petrography, and obtain additional age dates to constrain better the eruptive history and generate a geologic map covering the study area.

This thesis summarizes field work, XRF/ICP-MS geochemistry, thin section petrography, and age date analysis by the $^{40}\text{Ar}/^{39}\text{Ar}$ method spanning 2017 to 2020. Nine distinct rhyolite units make up the Strawberry Rhyolites. These are distinguished by their lithology, petrography, and compositions. This study does include a brief overview of other non-Strawberry Rhyolite units found in the area.

Our study has revealed a rhyolite field that is among the largest in Oregon. A minimum of 10 distinct effusive rhyolite units erupted over a 2-million-year period in addition to one mixed, rhyolite-andesite pyroclastic deposit from ~ 16.2 to 14.4 Ma with most $^{40}\text{Ar}/^{39}\text{Ar}$ ages falling in the 15.4 - 14.4 Ma bracket, but stratigraphically highest undated rhyolite units could be slightly younger. The mapped distribution of rhyolites covers 186 km^2 but the estimated original distribution area is likely $\sim 400 \text{ km}^2$ with an estimated volume on the order of 100 km^3 . I present the estimated original distribution area for each rhyolite unit. These estimated areas sum up to a total of 386 km^2 . Using these estimated areas, the largest rhyolite unit is Wolf Mountain (Trwm), covering about 170 km^2 , followed by the rhyolite of Three Cabin Spring (Trtcs) at $\sim 158 \text{ km}^2$. The smallest estimated area is from the rhyolite of Big Bend (Trbb), covering an area of about 8 km^2 . Age dates generated through this study and previously acquired are used in combination with stratigraphic field control to place rhyolite units into an eruptive sequence. The rhyolite of Wolf Mountain is the oldest, dating to 16.16 ± 0.17 Ma, and currently, the youngest age acquired is for the rhyolite of Kent Spring at the age of 14.37 ± 0.02 Ma. Thus, some units are likely to be slightly younger than our youngest radiometric age. An estimated volume is generated for

each unit, with the largest volume obtained for the rhyolite of Wolf Mountain (Trwm), with a value of $\sim 21 \text{ km}^3$. The rhyolite of Three Cabin Spring (Trtcs) follows Trwm with an average volume of $\sim 17 \text{ km}^3$, both units undoubtedly producing the largest volume out of all the Strawberry rhyolites. The smallest volume average produced is from the rhyolite of Buckhorn Spring (Trbs) at a value of about 0.7 km^3 . Volumes are calculated using an estimated range of unit thicknesses and the estimated areas for each unit. By clearly defining a volume for each unit gives a better representation closer to their actual distributions. Rhyolites range from low-silica to high-silica and from phenocryst rich containing $>20\%$ phenocryst to those that are aphyric. All units display glassy-to-devitrified lithologies. Phenocryst assemblages are dominated by plagioclase, some units contain quartz, and mafic silicates often are amphibole, biotite, or both. Orthopyroxene occurs in some units in addition to or instead of biotite and amphibole. Through understanding the Strawberry Rhyolite temporal changes in their mineralogy and composition, the SR units defined can have their age dates and volume relationship interpreted. This age and volume relationship may be a precursor in better determining stratigraphy of rhyolitic volcanic units, which aid in closing geologic time gaps throughout history. The trend depicted is that as the rhyolites are younger, the smaller the volume they produce.

The Nb vs. Zr variation diagram is used to classify samples as I-type or A-type to understand further these implications of the temporal changes in the Strawberry Rhyolites. Our data suggest the following age-volume-composition-lithology relationships. Lower silica, crystal-rich units containing complexly zoned plagioclase, such as Trbs, Trks, erupted early, while crystal poorer and silica-rich units are more

prevalent later. Units with slight A-type affinities such as Trbs, Trks, and the rhyolitic portion of Ttms, erupted the latest. This sequence is compatible with basalt intruding into crust initiating partial melting to produce rhyolites. This is followed by increased heat input from basalt to support near liquidus rhyolite magmas. Interaction of tholeiitic magmas with rhyolites culminates in the production of A-type-like rhyolites. Evidence for this stage is found in the commingling of Fe-rich andesite and rhyolitic magmas to produce the late tuff of Milk Spring. Interaction of basalts with rhyolites culminates in the production of A-type like rhyolites, supporting the association with hot spot activity.

The significance of the Strawberry rhyolite field is highlighted by comparing it to other well-known rhyolite lava flows and fields. Strawberry Rhyolites are now recognized to belong to the rhyolite flare-up associated with the main pulse of the CRBG volcanism. Thus, adding Strawberry Rhyolites to this rhyolite flare-up increased the footprint of this province towards the northwest.

ACKNOWLEDGEMENTS

I must say a huge thank you to the many people who have helped make this possible. First, I would like to thank the USGS for approving and funding two Edmap projects for me, the geologic mapping of Jump-off Joe Mountain and the Big Canyon quadrangle. Also, thank you to the PSU Geology Department for their financial contributions to my research by funding me with the Grant-in-Aid. The project was also supported through the National Science Foundation grant EAR-1220676 to M. Streck. Without those grants, this thesis would not have been possible. Thank you, Washington State University geoanalytical lab, for assisting in XRF and ICP-MS. Preparing samples on their campus is truly an educational and enjoyable experience.

Thank you to several of my fellow alumni from Portland State University who contributed to this project, former Edmap mappers and graduate students Shelby Isom, Matt Cruz, and Rachel Sweeten, as well as for Aaron Steiner for all your data collection and reporting on the region. Thank you for all your hard work to all my field assistants: Pierce Thieme, Mariah Dvorak, Chloe Koolhoven, Bonnie Burke, Natasha Dvorak, Lana Jewell, Owen Daly, Kylie Barber, and Kyle White. Thank you, Portland State University field camp summer 2017, 2018, 2019, and 2020 for all your assistance and everlasting memories. Thank you, Emily Cahoon, for providing endless help, guidance, specifically information about the Columbia River Basalts, regional geology, and field techniques that proved enormously insightful. Pierce Thieme, I could not have completed my thesis without your tremendous help. You assisted me immensely in my ability to produce the best map in ArcGIS, as well as endlessly teaching me how to use other related computer programs to generate other map

features, plots, edits, etc. Without each person's efforts and assistance, this thesis would not be whole. The many years of memories generated throughout all my mapping work are forever held close to my heart.

Many thanks to my advisor, Martin J. Streck, who has consistently provided guidance, assistance, and instruction. For his insight into the geological units present in the field mapping area and insight into field techniques such as identifying minerals in the hand sample, best approach field mapping, collecting data, and reviewing findings while in the field. The patience and kindness he has shown me over the years are cherished greatly.

Finally, I would like to thank my family for supporting me in all my academic endeavors. My family has indeed supported me financially, physically, and mentally. Lastly, I could not have done all of this without the love and support of my chosen family, my amazing group of friends. Thank you for truly being there for me and helping in any way you saw fit. This geologic experience of producing this entire thesis works has been fantastic because of all of you. Thank you!

TABLE OF CONTENTS

ABSTRACT.....	i
ACKNOWLEDGEMENTS	v
LIST OF FIGURES.....	iii
LIST OF TABLES.....	xiv
1.0 INTRODUCTION	1
2.0 GEOLOGIC BACKGROUND and SETTING	3
3.0 METHODS	11
3.1 FIELD STUDY.....	11
3.2 LABORATORY STUDY.....	13
4.0 RESULTS.....	16
4.1 Distribution, Lithology, and Composition of Rock Units in the Study Area.....	16
4.1.1 PRE-TERTIARY UNITS.....	16
I. Itss – Clastic sedimentary rocks: Conglomerate, Sandstone, Siltstone, and minor Carbonates.....	18
II. Kpm – Ultramafic Rocks	20
4.1.2 REGIONAL TUFFS.....	24
I. Trst – Rattlesnake Tuff	24
II. Tdct – Devine Canyon Tuff	26
III. Tdit4 – Dinner Creek Tuff, Unit 4	30
IV. Tdit2 – Dinner Creek Tuff, Unit 2	33
V. Tdit1 – Dinner Creek Tuff, Unit 1	35
4.1.3 LOCAL to REGIONAL BASALTS.....	37
I. Tpv d – Near Vent Pyroclastic Deposits, Basalt to Basaltic Andesite of the Strawberry Volcanics.....	37
II. Tbsv – Basalt to Basaltic Andesite	41
4.1.4 INTERMEDIATE STRAWBERRY VOLCANICS.....	44
I. Tasv – Andesite of the Strawberry Volcanics	44
II. Ttms – Milk Spring Tuff	46
III. Thsd – Holdout Spring Dacite	50
IV. Tmus – Mullen Spring Volcanic Clastics.....	50
4.2 Lithology, Petrography, and Composition of the STRAWBERRY RHYOLITES.....	53
4.2.1 APHYRIC and PHENOCRYST POOR STRAWBERRY RHYOLITE UNITS.....	53
I. Trtcs – Rhyolite of Three Cabin Spring	53
II. Trac – Rhyolite of Antelope Creek.....	58
III. Trbs - Rhyolite of Buckhorn Spring	61
IV. Trcc - Rhyolite of Canyon Creek	63
V. Trks – Rhyolite of Kent Spring.....	66
VI. Trews –Rhyolite of Elk Wallow Spring.....	70
VII. Trbb – Rhyolite of Big Bend.....	73
4.2.2 STRAWBERRY RHYOLITE PHENOCRYST RICH UNITS	75

I. Trbc – Rhyolite of Bridge Creek.....	75
II. Trwm – Rhyolite of Wolf Mountain.....	77
4.3 DISTRIBUTION of RHYOLITES.....	80
4.4 AGE of STRAWBERRY RHYOLITES.....	84
5.0 DISCUSSION.....	86
5.1 VOLUME ESTIMATES.....	86
5.2 TEMPORAL CHANGES in MINERALOGY and COMPOSITION of RHYOLITES.....	89
5.3 COMPARING the STRAWBERRY RHYOLITE FIELD with OTHER MIOCENE and YOUNGER RHYOLITE FLOWS and FIELDS.....	95
6.0 CONCLUSIONS.....	99
7.0 REFERENCES	102
APPENDIX A: Whole Rock Geochemical Data	109
APPENDIX B: Actual Area Sums per Outcrop Mapped	166
APPENDIX C: Abbreviations List	168
APPENDIX D: Geologic Maps of JOJM & BC through the EDMAP Projects.....	171

LIST OF FIGURES

- Figure 1: Color-enhanced, shaded relief location map of northern Harney Basin. Basin boundaries and location of quadrangles of interest (black boxes). The red rectangle indicates the region of investigation. The geologic mapping for this project occurred in Jump-off Joe Mountain, Big Canyon, Logan Valley West, and Magpie Table quadrangles. This map was created on ArcMap to show the location of the study area within Oregon.2
- Figure 2: Map of Paleozoic and Mesozoic rocks of the Blue Mountain terranes. The red stars indicate the investigation's location—modified from LaMaskin et al. (2008).3
- Figure 3: The image on the bottom is the full 1x2 Canyon Mountain geological map (Brown and Thayer, 1966) modified to show the region of study outlined in red and highlighting their unit (T) Strawberry Volcanics in red, which is the mapped overarching Miocene unit. The image on the top left is the study area broken into quadrangles and zoomed in to compare to the mapping results of this study. The image on the top right shows this project's combined geology of Jump-off Joe Mountain, Big Canyon, Logan Valley West, and Magpie Table quadrangles.5
- Figure 4: The image on the left is a map of the northwestern U.S., showing the approximate locations of Yellowstone hotspot volcanic fields (orange), Columbia River Basalts (gray), with Steens Basalt outlined in light orange. The boundary of Yellowstone National Park is shown in yellow. The purple ellipse represents the High Lava Plains (HLP) of Oregon. The red square indicates the field area of this project. The map is modified from Barry et al. (2013), Smith and Siegel (Windows into the Earth: the geologic story of Yellowstone and Grand Teton National Parks: Oxford University Press, 2000), Christiansen (USGS Professional Paper 729-G, 2001), and Long et al., 2009. The map on the right is an enhanced visual of the field area. The map on the right was produced using ArcMap.....6
- Figure 5: Stratigraphy of main-phase Columbia River basalts, modified from Wolff et al. (2008). Column depicts main phase ages which coeval with the Strawberry Mountain Rhyolites. The map was made on ArcMap: Black boxes = this Study area; Blue dot = cities; Light yellow region = Harney Basin; Purple Triangles = dike swarms (CJ= Chief Joseph

Swarm; M=Monument swarm feeding Picture Gorge basalts; S= Steen's swarm). The dashed grey ellipse encloses the present-day area where crustal-depth magma chambers for the flood lavas are inferred to lie. The red ellipse is the likely source area of the Dinner Creek Tuff eruptive center (Steiner and Streck, 2013; Streck et al., 2015).8

Figure 6: Field mapping area for this project. Including the quadrangles Big Canyon and Jump-off Joe Mountain, alongside the western halves of the Logan Valley West and Magpie Table quadrangles. The green box encompasses the area covered in this study. The tan dotted area on the east is the area for which was unmapped in this study. The black dashed lines separate the quadrangle boundaries. The grey hillshade map layer is comprised of all the lidar available for the region- areas without gray do not have lidar data available.10

Figure 7: XRF and ICP-MS geoanalytical process conducted by Chanel Dvorak at Washington State University, Pullman Campus. (A) Rock chips were brought to WSU from PSU in the process of crushing rocks to powders. (B) Round two of crushing rocks into powders at WSU and post addition of dilithium to powdered samples and placed in carbon crucibles. (C) Samples were cooling into beads from being melted in an oven at 1000°C. Further processes are conducted to generate XRF and ICP-MS data.14

Figure 8: Distribution of the units Itss (tan) and Kpm (brown) across the entire mapping area with other units greyed out.17

Figure 9: Sandstone of the Accreted Terranes in hand sample. The left image (sample BC19A45) is pictured with some of the unit's quartz veins throughout the sandstone in Big Canyon. The image of the right (BC19A01) has slightly more of a greenish hue.18

Figure 10: Thin section images of the Sandstone of the Accreted Terranes. The top row images are all in XPL, whereas the bottom is in PPL. (A) is sample BC19A45, (B) BC19A01, and (C) BC19B06. All pictured are in 100X optical zoom.19

Figure 11: Pictured is the Pretertiary Ultramafics, Sample BC19A07.21

Figure 12: Full thin section image of sample BC19A07, Pretertiary Ultramafic unit. The upper image is in XPL, and the lower is in PPL.22

Figure 13: Thin section images of sample BC19A07 all captured in 100X optical zoom. The top row of images is in XPL, and the bottom row is in PPL.23

Figure 14: Image B and C are examples of typical partially welded vitric hand samples of Rattlesnake Tuff, all from the outcrop in image A. Visible features are light to gray pumice clasts in gray glass shard matrix. Image A (Sample CD1988) is in the southern-central region of the quadrangle.24

Figure 15: Distribution of the unit Trst (red) across the entire mapping area with other units greyed out.....26

Figure 16: Image A is an outcrop of Devine Canyon tuff within the Big Canyon quadrangle. The black streaks amongst the outcrop hand samples seen in pictures B and D are fiamme (flattened pumices). Hand samples seen in image C show the variance in color throughout this unit.....27

Figure 17: Full slide thin section image of Devine Canyon tuff (sample JJ18B3.1) shown in PPL. Displays glassy (ash) matrix with quartz phenocrysts.29

Figure 18: Distribution of the unit Tdct (pink) across the entire mapping area with other units greyed out.....29

Figure 19: Zr versus Nb of all regional to local silicic ash-flow tuff units.30

Figure 20: Image (A) sample BC19A26B, (B and C) outcrop and hand sample CD1936A, lastly image (D) sample BC19C40.31

Figure 21: Image of Tdit4 sample BC19A26B. The left image is in XPL, whereas the right is in PPL, represented in 100X optical zoom.32

Figure 22: Distribution of the unit Tdit4 (magenta) across the entire mapping area with other units greyed out.33

Figure 23: On the left is a hand sample of Dinner Creek Tuff unit 2. The right image shows this unit in an outcrop.34

Figure 24: Distribution of the unit Tdit2 (peach) across the entire mapping area with other units greyed out.35

Figure 25: Dinner Creek Tuff unit 1 is found in varying shades of color and alteration, basal vitrophyre, spherulitic tuff, and devitrified. Image A is from sample BC19A61, where B and C are from sample CD1979.36

Figure 26: Thin section image of Dinner Creek unit 1 (sample BC19A61). The images display a glassy (ash) matrix. The left image is in XPL, with the right being in PPL. Images are in 100X optical zoom.	37
Figure 27: Photograph looking at a sizeable basaltic-andesite outcrop in the BC map's northernmost-central region (sample BC19B07).	38
Figure 28: Close-up look at the basaltic andesite outcrop (Sample BC19B07). Highly vesiculated red basaltic andesitic scoria consisting of fine lapilli occasional coarse ash and featuring spindle bombs around and protruding out of the outcrop.	38
Figure 29: Distribution of the units T _{pv} d (light green) and T _{bsv} (dark green) across the entire mapping area with other units greyed out.	39
Figure 30: Photograph looking north at mafic pyroclastic flow, unit T _{vp} d makes up units 1 and 1b in the image. Image label unit 2 and scoria fall deposits (unit 3) make up the flow of the pahoehoe toe. “Covered” means talus conceals outcrop; the black line is the upper extent of the talus. “Reworked” means the unit is slightly modified from subsequent processes. The dashed white line is the presumed contact between units. Photograph by Martin Streck. (Ferns, et al., 2017).	39
Figure 31: (A) Outcrop of T _{pv} d (named T _{bt} in JOJM quad) in roadcut along NF17, icelandite juvenile clasts are pictured. (B) Spindle bomb.	40
Figure 32: Pictured is a full thin section image of sample JJ18A3.1D2. The unit is abbreviated as T _{bt} in JOJM 7.5 min quadrangle from 2018. This thin section is in PPL and showing a glassy matrix containing lithics and is vesicle rich.	41
Figure 33: Basalt of the Strawberry Volcanics, sample BC19B36 in hand sample.	42
Figure 34: Basalt of the Strawberry Volcanics, sample BC19B36 in thin section. Image A is in XPL, B is in PPL, 40X optical zoom.	42
Figure 35: Total alkali-silica classification diagram displaying the samples of basaltic to andesitic compositions from this project.	43
Figure 36: Photograph (A) is an andesite dike (sample BC19B45), with image B representing the dike in hand sample. Image C is from sample BC19A22 displaying a distinct lithological variant of T _{asv} that is fine-grained, black, and fractures conchoidally.	45

Figure 37: Sample numbers and optical zoom are as follows - (A) BC19A50 (100X), (B) BC19A22 (40X), (C) BC19C69 (40X). The top half of the photograph's thin sections are in XPL, with the bottom half in PPL.45

Figure 38: The first image on the upper left is a finely stratified tuff of Milk Spring consisting of the surge and fallout deposits. The hand in the image measures a section of about 5cm thick. The image on the upper right is the outcrop used in the thickness model image found at the bottom of this figure. The bottom image was generated using Google Earth and knowledge of this field location in the JOJM quadrangle. Ttms cropping out in this location measures about 35 m in thickness.47

Figure 39: (A)-(B) Milk Spring Tuff of the south-central region of the Jump-off Joe Mountain quadrangle. The basal surge and fallout deposits are about 1 m thick and overlain by an ignimbrite incorporating larger lithics. (C) Fallout tuff and surge deposit in a nearby section of the Milk Spring Tuff.48

Figure 40: Milk Spring Tuff in hand sample BC19C56 displays lithics made up of multiple units.48

Figure 41: Milk Spring Tuff in thin section, XPL on top with PPL images on the bottom. Note prominent lithic fragments in B and C with lithologies of andesites of the Strawberry Volcanics. All images are from sample BC19C56, with A and B in 100X optical zoom. Lastly, with C and D in a 40X optical zoom.49

Figure 42: Left upper image is of the fine-grained epiclastic debris flow member in outcrop off NF17. The right image is a close-up image of this unit's block and ash flow member, the Mullen Spring Volcanic Clastics. The lower image is the same outcrop but detailing its unit thickness.51

Figure 43: Geologic field map highlighting the units Tmus (pale turquoise) and the unit Thsd (purple). These units are superimposed on the entire mapped extent, with most other units greyed out, besides for Tasv and Ttms for context regarding the zoomed-in image.52

Figure 44: Outcrop and hand sample images of Three Cabin Spring rhyolite sample CD1977 on the left. With the right image being a Trtcs obsidian member image from the LVW quad.53

Figure 45: Thin section of a sample of devitrified Three Cabin Spring Rhyolite (Sample CD1830), with visible flow banding, in PPL.54

Figure 46: Photos are of the Rhyolite of Three Cabin Spring, the left image being from the JOJM quadrangle near Round Mountain where sample CD1875 was collected. The image on the right was generated using Google Earth and knowing where this unit crops out in the study area. This outcrop location is in the MPT quadrangle along the northwestern margin. Trtcs crops out in this location and covers the entire hillside stretching into its neighboring west quad of JOJM. Using this model, Trtcs unit thickness measures about 768m. The large size is in part a result of a fault that runs between these two locations. The fault is north-south trending and dipping to the east. A typical unit thickness will range from 40-180m.....55

Figure 47: Ba vs. Sr variation diagram for the Strawberry Rhyolites, highlighting samples of unit Trtcs (red).56

Figure 48: Nb vs. Zr variation diagram for the units found in this study. This plot classifies samples as I-type or A-type using the discrimination techniques of Whalen et al., 1987. The samples that plot outside the box have A-type affinities, and samples with Zr less than 250 ppm and Nb less than 20 ppm are classified as I-type. The coordinates of the box are X=250, Y=20. The undefined unit is regarding a (perlitic) rhyolite sample found in the MPT quadrangle. This has yet been defined as a discrete unit, as this map is still in progress by PSU graduate student Rachel Sweeten.56

Figure 49: This figure represents plots A through F (Figure 50 with plots G through J) trace elements vs. SiO₂ wt. % plots for the SV rhyolites. Plot A: Eu/Eu* vs. SiO₂ wt. %. Plot B: Ba ppm vs. SiO₂ wt. %. Plot C: La ppm vs. SiO₂ wt. %. Plot D: Sr ppm vs. SiO₂ wt. %. Plot E: Rb ppm vs. SiO₂ wt. %. Lastly, Plot F: the ratio La/Yb ppm vs. SiO₂ wt. %.57

Figure 50: This figure represents G through J plots (see Figure 49 for A through F) trace elements vs. SiO₂ wt. % plots for the SV rhyolites. Plot G: Nb ppm vs. SiO₂ wt. %. Plot H: (Zr+Nb+Y+Ce) ppm vs. SiO₂ wt.%. Plot I: TiO₂ wt. % vs. SiO₂ wt. %. Lastly, Plot J: Zr ppm vs. SiO₂ wt. %.58

Figure 51: The image on the left is the obsidian member of Antelope Creek Rhyolite, and the right image is devitrified. Photos are from hand sample CD1879.59

Figure 52: Photos are from the exact outcrop location in the JOJM quadrangle where sample CD1879 was collected. The image on the left highlights the obsidian member of Trac, and the top of the hill is where its devitrified member is found. The image on the right measures from the top of the outcrop to the road, recording a thickness of 129m. Just east of this outcrop, an NW trending fault dips to the NE towards this outcrop. The fault could be accounting for some displacement thus thickness, where a typical Trac outcrop thickness ranges from 30-70m.60

Figure 53: Obsidian of Antelope Creek rhyolite as full thin section image, showing about 4% phenocrysts, clear quartz and plagioclase, and dark shaded acicular biotite.60

Figure 54: Hand samples of rhyolite of Buckhorn Spring unit (A) BC19C30 sample and (B) BC19C37 sample.61

Figure 55: This image representing Trbs highlights this unit's highest peak and most exposed region in the BC quadrangle. About 1km west of this peak, a fault runs north-south for about 7km in length, dipping east. This extensional faulting and the youth of the Trbs unit itself would account for its significant cliffside exposures. Trbs typically has a thickness of about 20-120m.62

Figure 56: Images of the Rhyolite of Buckhorn Spring in thin section from sample BC19C30. The row of images on top is represented in XPL, and the bottom row is in PPL. Image (A) is in 100X optical zoom, with (B) in 40X optical zoom.63

Figure 57: Outcrop of rhyolite of Canyon Creek located in the map's furthest north-eastern corner (sample CD1943).64

Figure 58: These images represent the rhyolite of Canyon Creek. This unit is very well exposed as it lies on a fault that runs north-south for about 7km in length and dips to the east. The east block, which incorporated the unit Trcc and its outcrop pictured, has also formed a lake in its offset. The top image shows the lake meeting Trcc in outcrop. The bottom right map was generated in Google Earth to measure the unit's exposure. The unit thickness measurement occurred from the south side of the lake to the adjoining peak. Its thickness measures 135 m, which is an accurate high range thickness value for Trcc.65

Figure 59: Thin section images of Canyon Creek rhyolite from float sample BC19A11 with images in XPL on top and PPL at the bottom (A) in 100X optical zoom and (B) in 40X optical zoom.66

Figure 60: Kent Spring rhyolite (CD1932). Overall, the unit is crystal poor and distinguishable by the presence of amphibole.67

Figure 61: These images represent the rhyolite of Kent Spring and its amount of exposure due to faulting in the region. Both images are from the same outcrop, located in the far SE of the BC quadrangle. Four north-south trending faults intersect this unit in an east-dipping extensional domino effect, generating considerable exposure. With Trks remaining relatively local to this area, its typical maximum unit thickness is about 200m. The map image was produced on Google Earth along with geologic mapping knowledge of the region.68

Figure 62: Thin section images of Kent Spring rhyolite sample CD1932. The top row of images is in XPL, and the bottom row is in PPL. Image (A) is in 40X optical zoom, whereas (B) is in 100X optical zoom, shown crystal poor nature with about 1% amphibole crystals.69

Figure 63: Ba vs. Zr variation diagram for the Strawberry Rhyolites, highlighting samples of unit Trks (red). The unit Trks has a distinctly lower Zr ppm than the other SR units.69

Figure 64: The image is of the Rhyolite of Elk Wallow Spring, where the highest elevation is atop Glass Mountain in MPT and is the sample location for RS20MPT03. The map image was generated using Google Earth and used knowledge of where this unit crops out in the study area. Trews crops out in this location and covers this entire, overall wedged between Trtcs and Trac. Using this model, Trews unit thickness measures about 488m. The measurement of the unit may have a deviation as many faults that trend north-south just to the east of this location, crossing into neighboring quads of JOJM and BC. The faults are dipping to the east, generating domino extensional features. A typical unit thickness will range from 40-200m, making sense for this unit's location in the study area.70

Figure 65: Hand sample of the rhyolite of Elk Wallow Spring. This sample is from the top of Glass Mountain in the Magpie Table quadrangle (RS20MPT03).71

Figure 66: Petrographic thin section of Trews from the MPT quadrangle. Flow banded, with prominent acicular phenocrysts of hornblende and plagioclase phenocrysts in a glassy, flow banded groundmass.72

Figure 67: Zr vs. Sr variation diagram for the Strawberry Rhyolites, highlighting unit Trews (green) and Trbc (red) samples. The unit Trews and Trbc are lithologically similar but can be differentiated by their trace elements. Specifically, Zr and Sr, where the unit Trews has an overall lower Zr and Sr trace element concentration than the unit Trbc.72

Figure 68: The image on the left is a typical outcrop of Trbb. The image on the right is a classic representation of this units' phenocrysts percentage.73

Figure 69: Image is of the Rhyolite of Big Bend; the map image was generated using Google Earth and by using knowledge of where this unit crops out in the study area. Trbb crops out in this location and overall only in a small portion throughout the entire map, ~1km². Using this model, Trbb unit thickness measures about 1,039m at maximum. This area is in close proximity to Bear Creek. Large alluvium-filled meadow and creek. Directly to the west, in the quadrangle BC, there are a couple of outlier faults that trend from east to south, where all other faults in the region tend to be normal faults. I suspect that this potentially active faulting is the cause of this rather large unit thickness. Especially regarding Trbb is one of the younger, if not youngest SR unit.74

Figure 70: Thin section image of unit Trbb in XPL from sample LVW-N-19. The thin section image features a very fine-grained matrix encompassing glomerocrysts.74

Figure 71: (A) Hand sample of Trbc, devitrified with amphibole and biotite, clearly visible. (B) Vitric hand sample of Trbc, outcrop just south of Che Spring in JOJM. (C) A smaller outcrop of the Bridge Creek Rhyolite is consistently found amongst a sizeable blocky and more extensive outcrop.75

Figure 72: Thin section of the Rhyolite of Bridge Creek. Full slide images, the left is in PPL, and the right image is in XPL, from sample JJ18A257. The thin section highlights the abundance of clearly visible biotite and amphibole crystals, making up about 3%, with about 8% plagioclase.76

Figure 73: Photos are of the Rhyolite of Bridge Creek (formerly known as the unit Tsvr in the 2019 JOJM map). The left image is from the JOJM quadrangle, NW of Bond Spring.

The image on the right was generated using Google Earth and subsequent knowledge of this unit within the study area. The majority of Trbc crops out in this location covering the entire hill, continuously reaching the NE and SW, covering a stretch of ~7km. Using this model and a prominent location of a continuous outcrop of Trbc, its unit thickness measures about 785m. The sizeable unit thickness estimate is likely due to the extensional faulting throughout the region, exposing a substantial face of Trbc. Thus, a typical unit thickness will range from 40-100m.77

Figure 74: Wolf Mountain rhyolite in outcrop and as hand sample (CD1921).78

Figure 75: Wolf Mountain rhyolite in hand sample. From (A) to (C), the samples go from non-glassy to glassy. Each variety is of the 30% phenocryst-rich variety found in the Jump-off Joe Mountain quadrangle.78

Figure 76: Photos are all from the Rhyolite of Wolf Mountain and are indeed from the south-eastern side of Wolf Mountain in the JOJM quadrangle. The image on the right was generated using Google Earth using knowledge of this unit in the study area. The majority of Trwm crops out to the South in JOJM and the east in MPT quads. By using this model, the unit Trwm thickness measures about 940m. The sizeable, estimated thickness is partly due to the north-south trending fault that dips east and runs directly through this section. In addition, the exposed Trwm is exceptional due to the extensional faulting, exposing a prominent face of Trbc. A typical unit outcrop thickness, however, remains rather large, ranging from 50-200m.79

Figure 77: Thin section images from sample CD1964. The top row exhibits XPL, while the bottom row is in PPL. Image (A) is in 40X optical zoom, with (B) in 100X optical zoom....80

Figure 78: This study's estimated original coverage of each Strawberry rhyolite unit (in color) superimposed on the mapped extent (black).82

Figure 79: Geologic map showing rhyolite outcrops in dark gray and estimated original coverage of all rhyolite units of this study (in color). Dvorak conducted the mapping of the quadrangles Big Canyon and Jump-off Joe Mountain, and current PSU graduate student Rachel Sweeten mapped the Logan Valley West and Magpie Table quadrangles.....83

Figure 80: Plot (A) is a variation diagram for Eu/Eu* vs. SiO2 wt.% for the Strawberry Rhyolites, highlighting the trend of as silica increases the compatible element (Eu) decrease.

Plot (B) is also a variation diagram, highlighting the trace element Ba versus silica content. Circled in red, most of the units have a high Ba value (exception of Trks). This high concentration indicates how compatible they are—the higher the Ba, the stronger the compatibility in alkali feldspar.90

Figure 81: Estimated volume versus age plot of the Strawberry Rhyolites. This plot highlights how as the rhyolite units go from older to younger, they also trend towards larger to smaller regarding volume in size. The larger bold numbers on the plot are the age dates acquired, with the smaller numbers being their estimated volume. The map images below the graph highlight each specific unit's estimated area based on maps produced in the field area.94

Figure 82: Map image incorporates all the rhyolite units or units with a rhyolite component (Ttms)) mapped in this project; all units that are not locally sourced rhyolites are greyed out. This map shows that the presence of rhyolite is more varied and extensive than previously mapped.....95

Figure 83: Figure representing a size comparison to the project area and other rhyolite fields. Each volcanic field is on the same scale to highlight its size differences.98

Figure 84: Geologic map produced through this study incorporates the geology of Jump-off Joe Mountain, Big Canyon, Logan Valley West, and Magpie Table quadrangles, depicting how various the area's units genuinely are.101

LIST OF TABLES

Table 1: Calculated distribution area, from largest to smallest of Strawberry rhyolitic units. The area in this table is based on the estimated size of each unit (Figure 78) and the geometry of the polygons generated in ArcMap from the final map produced from fieldwork in this study.	81
Table 2: This area and volume table is produced by compiling all the field mappings of each Strawberry rhyolite unit, generating an estimated area polygon surrounding all those units, and calculating its overall geometry in ArcMap; the area is outlined in red. Then using this geometry with field compiled data, an estimated volume is produced....	84
Table 3: Compilation of $^{40}\text{Ar}/^{39}\text{Ar}$ age dates of SR units found in this project mapped region. Unit abbreviations are elaborated by unit names in Table 1, or the legend of the project map found in the appendix.	85
Table 4: The Strawberry Rhyolite units are listed according to age, from oldest to youngest. Unit abbreviations are elaborated by unit names in Table 1, or the legend of the project map found in the appendix.	85
Table 5: Calculated volume of Strawberry rhyolitic units, from largest to smallest. The volumes are calculated using each unit thickness multiplied by their respective area.	87
Table 6: Calculated volumes of each rhyolite unit based on the estimated area (see Table 1) and their respective unit maximum and minimum thicknesses that were discerned from fieldwork component and observations from well-preserved rhyolite lavas.	88

1.0 INTRODUCTION

In eastern Oregon, abundant mid-Miocene silicic volcanic rocks crop out amongst voluminous flood basalt flows of the Columbia River Basalt Group (CRBG). One large rhyolite center found within this large igneous province is located south of the Strawberry Mountain range and is part of the Strawberry Volcanics (Figure 1). Only recent work (Steiner & Streck, 2014) and mapping efforts, including those of this study in the NE part of the Harney Basin north of Burns, have shed light on the existence of a diverse set of volcanic units previously lumped into broad single mapping units by earlier regional reconnaissance maps (Brown and Thayer, 1966). This mapping brought to light the existence of Oligocene dacites with lesser andesites and basalts, mid-Miocene rhyolite, and outcrops of regional tuff units such as the Dinner Creek Tuff that were previously unknown to occur in the area. Hence, there is a much better understanding of the geologic history of the entire northeast margin of the Harney Basin, which plays a significant role in the regional volcanic framework due to this mapping. This region was mapped originally in reconnaissance in the 1960s, where geologic units were poorly delineated, often blanketing whole quadrangles as nearly one unit. For example, more than 90% of the 7.5 min Jump-off Joe Mountain quadrangle is mapped as ‘Ts’ – Strawberry Volcanics – and the adjacent Big Canyon quadrangle is similarly nonspecific. In 2018 and 2019, I mapped portions of the area where mid-Miocene rhyolites are exposed as part of two USGS Edmap projects, and my MS thesis project is based on this mapping. When I started this project, prior PSU thesis work by A. Steiner (2016) had broadly revealed the existence of a major rhyolite field in size comparable to the Coso rhyolites of Inyo County, California that covered about 316 km². Steiner found rhyolite outcrops distributed over four 7.5-minute quadrangles. The work by Steiner also showed rhyolites are comprised of varying

lithological units and defined a preliminary eruptive age range from 16.2 to 14.3 Ma. These rhyolites are part of the Strawberry Volcanics, hereafter referred to as Strawberry Rhyolites (SR). This project builds on Steiner’s work. The main focus is to detail the distribution of rhyolite units used for volume estimates, determine the composition and petrography, and obtain additional age dates to better constrain the eruptive history.

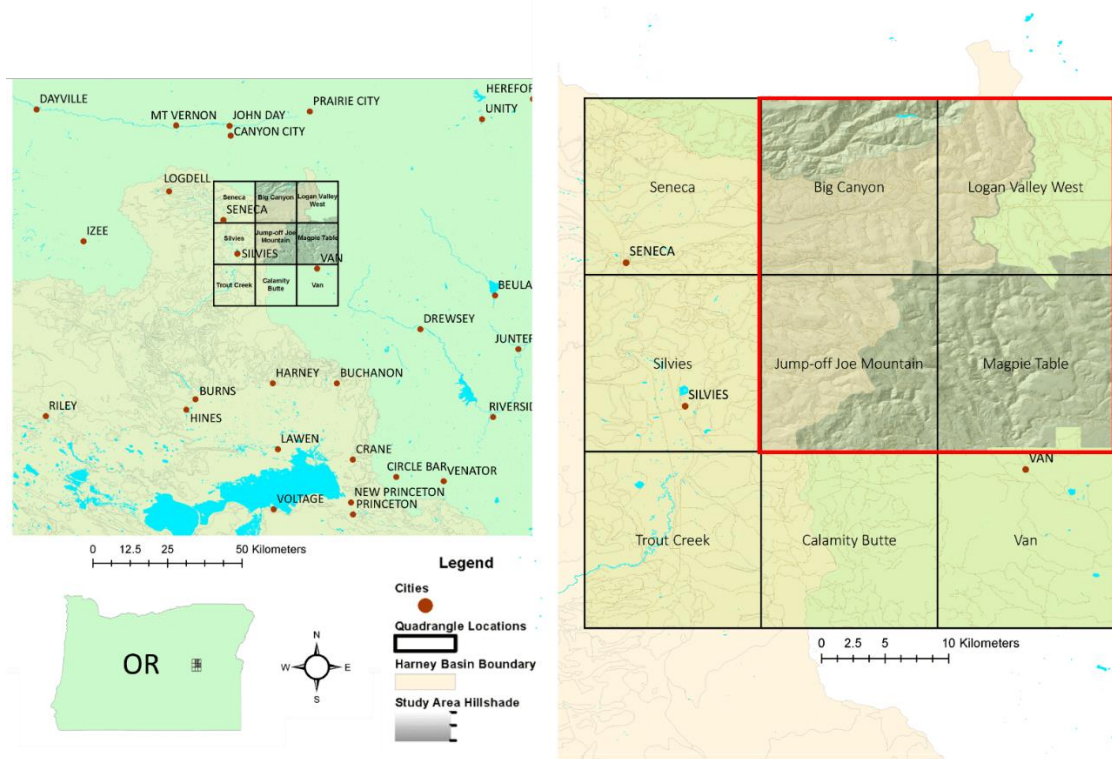


Figure 1: Color-enhanced, shaded relief location map of northern Harney Basin. Basin boundaries and location of quadrangles of interest (black boxes). The red rectangle indicates the region of investigation. The geologic mapping for this project occurred in Jump-off Joe Mountain, Big Canyon, Logan Valley West, and Magpie Table quadrangles. This map was created on ArcMap to show the location of the study area within Oregon.

2.0 GEOLOGICAL BACKGROUND and SETTING

The area of interest consists of four 7.5 min quadrangles: Jump-off Joe Mountain, Big Canyon, Magpie Table, and Logan Valley West, all located along the north-eastern margin of the Harney Basin in eastern Oregon and lie within the Malheur National Forest (Figure 1). The basement rocks of the region consist of accreted island arcs and oceanic crust collectively known as “accreted terranes” (Figure 2).

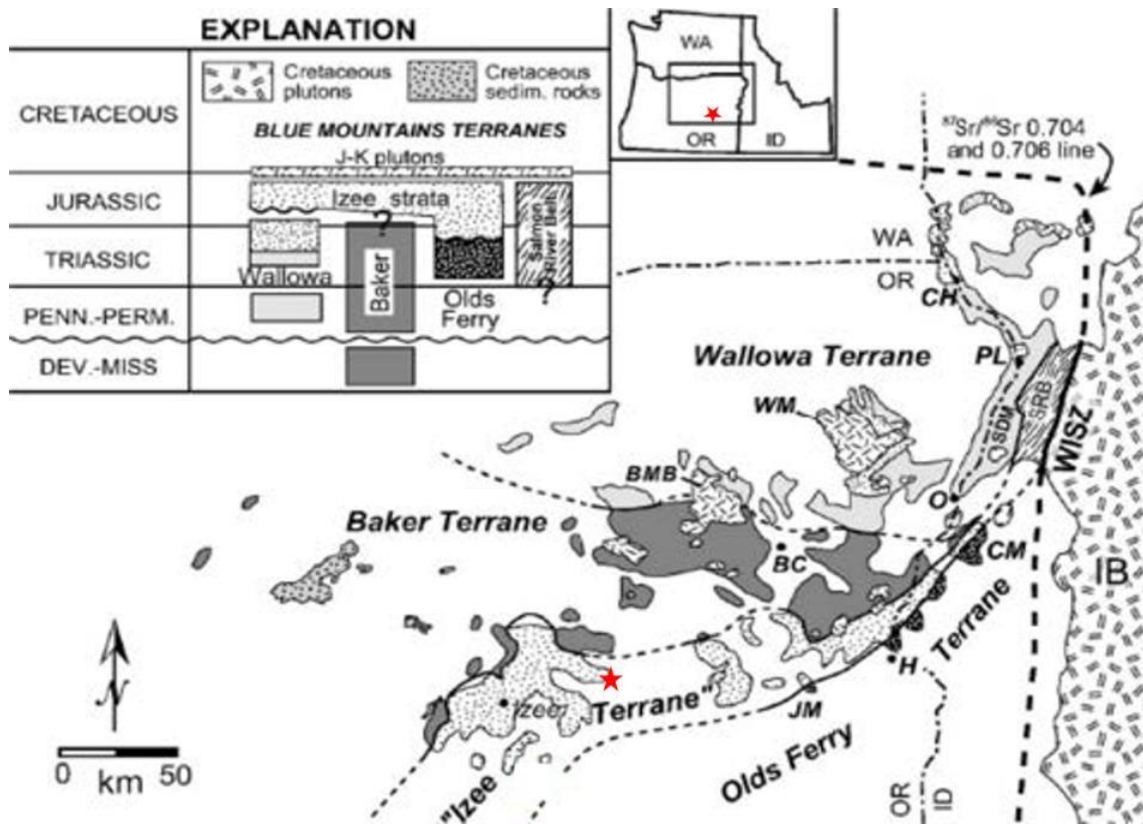


Figure 2: Map of Paleozoic and Mesozoic rocks of the Blue Mountain terranes. The red stars indicate the investigation's location—modified from LaMaskin et al. (2008).

These terranes were accreted from east to west on the North American continent from the late Permian to the Early Cretaceous (Dickinson, 1979; Vallier, 1995; Dorsey and

LaMaskin, 2008; Schwartz et al., 2010). The quadrangles lie within the Izee basin, a forearc basin where roughly 7,000 meters of marine sediments were deposited from early to middle Jurassic and uplifted in the early Cretaceous due to continued accretion of the Blue Mountain terranes (Dorsey and LaMaskin, 20011; Ware, 2013). On Brown and Thayer's 1x2-degree Canyon Mountain quadrangle (1966), nearly the entire study area was mapped as one Miocene unit, 'Ts' – Strawberry Volcanics (Figure 3), with a small sections 'Jtl' – Jurassic sedimentary rocks.

The name “Strawberry Volcanics” was given to the diverse group of volcanic rocks that overlie Paleogene and pre-Tertiary basement rocks over an area of 3,600 km² along the southern and eastern margins of the John Day Valley (Thayer, 1957; Brown and Thayer, 1967). Robyn (1979) determined that the Strawberry Volcanics were generally younger than the main phase of the Columbia River Basalt and are calc-alkaline. It was later found that basaltic to andesitic rocks of the Strawberry Volcanics are predominantly calc-alkaline suite but include a mildly tholeiitic suite much smaller in volume (Steiner, 2013a, 2015). The Strawberry Volcanics also includes rhyolite and minor dacite. Other than FeO*, the calc-alkaline and tholeiitic basalts and basaltic andesites (<55 wt. percent SiO₂) are almost geochemically indistinguishable. Rare basalts resemble the lavas of the Steens Basalt (Steiner and Streck, 2018). Faulting was likely instrumental in forming numerous north-south trending valleys that dot this part of the Blue Mountains province. Quaternary fluvial processes incised canyons and caused several deep-seated landslides, resulting in this part of the Strawberry Mountains' present topography.

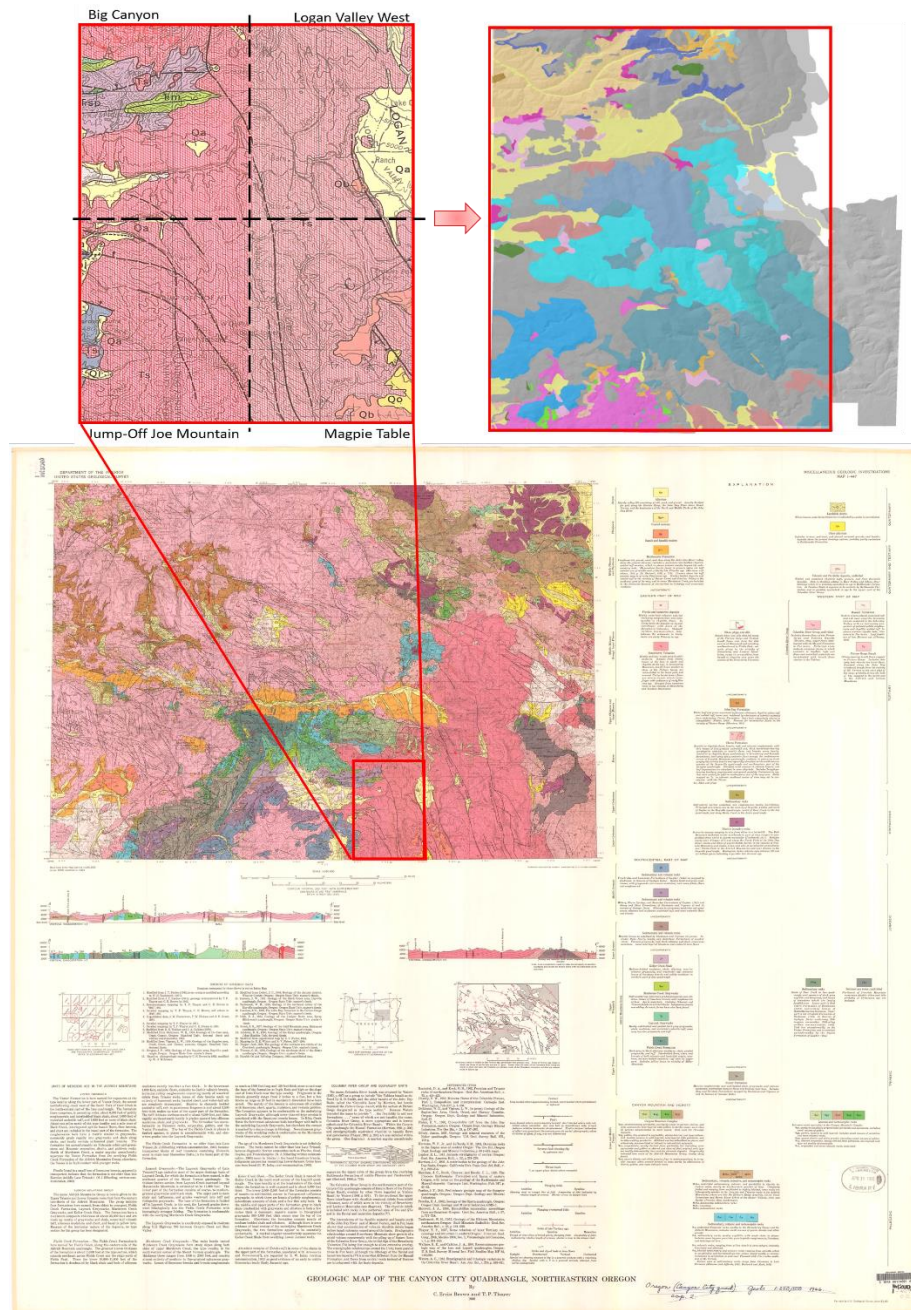


Figure 3: The image on the bottom is the full 1x2 degree Canyon Mountain geological map (Brown and Thayer, 1966) modified to show the region of study outlined in red and highlighting their unit (T's) Strawberry Volcanics in red, which is the mapped dominant Miocene unit. The image on the top left is the study area broken into quadrangles and zoomed in to compare to the mapping results of this study. The image on the top right shows this project's combined geology of Jump-off Joe Mountain, Big Canyon, Logan Valley West, and Magpie Table quadrangles.

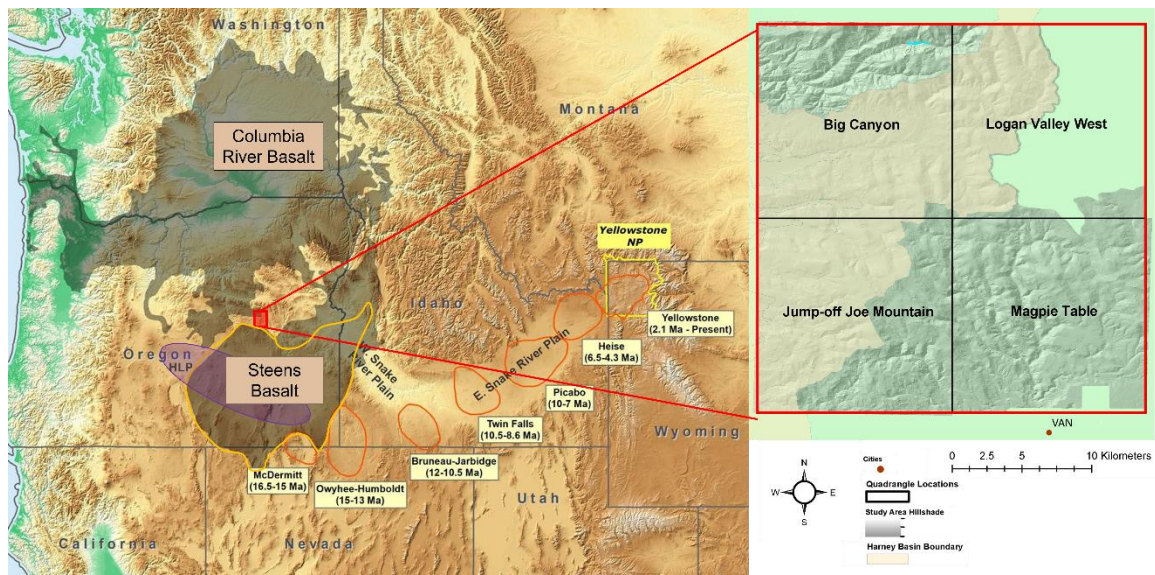


Figure 4: The image on the left is a map of the northwestern U.S., showing the approximate locations of Yellowstone hotspot volcanic fields (orange), Columbia River Basalts (gray), with Steens Basalt outlined in light orange. The boundary of Yellowstone National Park is shown in yellow. The purple ellipse represents the High Lava Plains (HLP) of Oregon. The red square indicates the field area of this project. The map is modified from Barry et al. (2013), Smith and Siegel (*Windows into the Earth: the geologic story of Yellowstone and Grand Teton National Parks*: Oxford University Press, 2000), Christiansen (USGS Professional Paper 729-G, 2001), and Long et al., 2009. The map on the right is an enhanced visual of the field area. The map on the right was produced using ArcMap.

A late Miocene and younger bimodal volcanic group, expressed as basaltic lava flows, rhyolite domes, and ignimbrites, are exposed along the High Lava Plains (e.g., Ford et al., 2013). Along the High Lava Plains, about 60 rhyolitic dome complexes are lined up in a northwestern direction (Ford et al., 2013). These dome complexes can be monogenetic or long-lived and more complex in size. The rhyolitic domes show an age progression from the oldest (~12 Ma) in the east and becoming progressively younger to the northwest, with the youngest eruptions being at the Newberry volcano (<1 Ma). This age progression mirrors the Yellowstone Hotspot track, with younging from the southwest to the northeast (Coble and

Mahood, 2016). In addition, three extensive ($\sim 100\text{-}300\text{ km}^3$) ash-flow tuffs erupted from ~ 10 – 7 Ma. From oldest to youngest, these are the Devine Canyon Tuff (9.7 Ma), Prater Creek Tuff (8.5 Ma), and Rattlesnake Tuff (7.1 Ma) (Greene, 1973; Streck & Grunder, 1997; Ford et al., 2013). Not included within this trend but found in the mapping area is the Dinner Creek Tuff, ranging from 16.1 to 15 Ma (Streck et al., 2015; Isom, 2017). The regional map depicted in Figure 4 highlights the study area amongst the High Lava Plains, the Columbia River Basalts, the Steens Basalts, and the Snake River Plain hotspot track.

Two significant phases characterize the older volcanism within eastern Oregon. The Clarno Formation (54-40 Ma), which is hypothesized to underly the High Lava Plains, crops out extensively to the north and west of the province within the Blue Mountains Terrane (Walker and Robinson., 1990) and the younger John Day formation (38.5-20 Ma) also crops out extensively to the north of the HLP (Bestland and Rettalack., 1994a & 1994b) (Figure 5). Mid-Miocene lavas of the Columbia River Basalt Group overlie the Blue Mountain Terrane basement rocks and the earlier Cenozoic volcanic rocks across central and eastern Oregon and consist mostly of tholeiitic flood basalts that erupted from various dike swarms, and volcanic centers across eastern Oregon, northern Nevada, southern Washington, and western Idaho from 16.8 – 5 Ma (Swanson et al., 1979; Hooper, 1997; Hooper et al., 2002; Camp & Ross, 2004; Camp & Hanan, 2008; Wolf & Ramos, 2013; Coble & Mahood, 2012; Reidel et al., 2013).

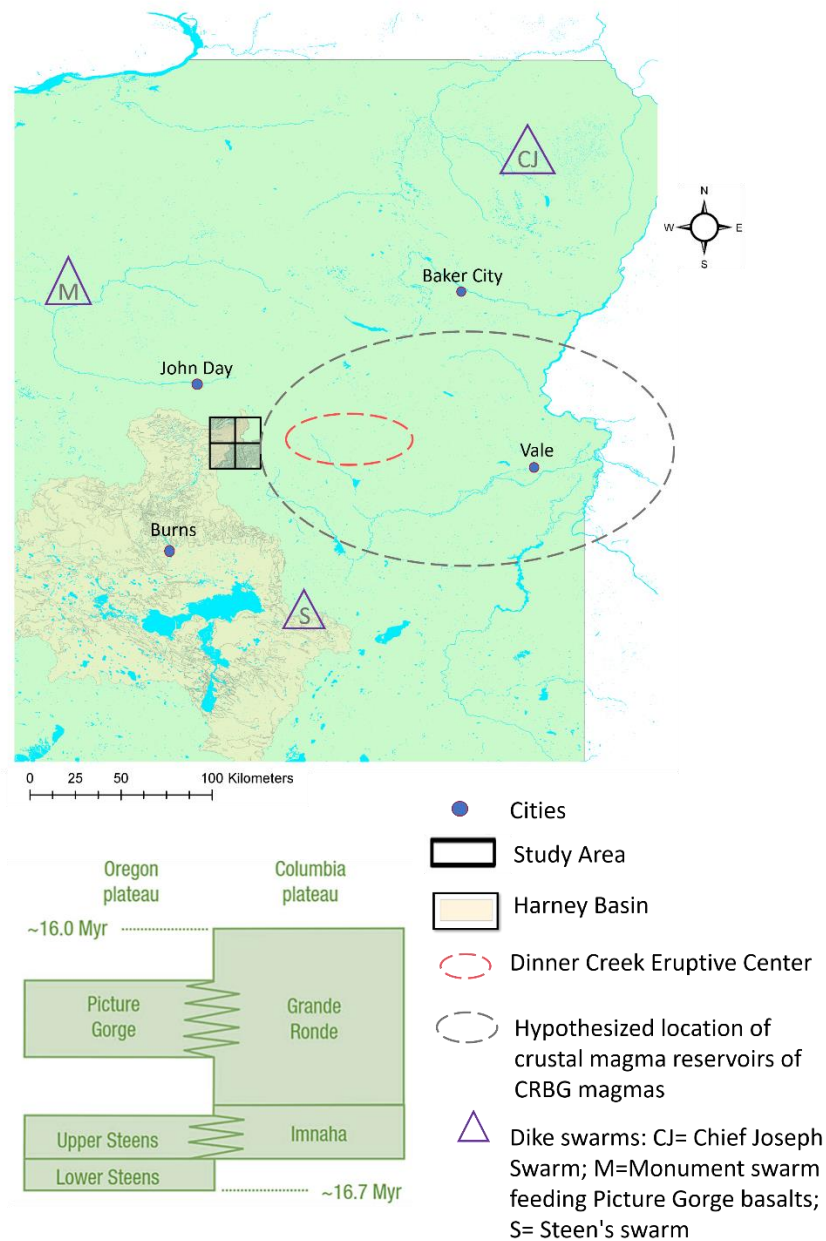


Figure 5: Stratigraphy of main-phase Columbia River Basalt units, modified from Wolff et al. (2008). The column depicts main phase units and overlaps with the other ages of the Strawberry Mountain Rhyolites. The map was made on ArcMap: Black boxes = this Study area; Blue dot = cities; Light yellow region = Harney Basin; Purple Triangles = dike swarms (CJ= Chief Joseph Swarm; M=Monument swarm feeding Picture Gorge basalts; S= Steen's swarm). The dashed grey ellipse encloses the present-day area where crustal-depth magma chambers for the flood lavas are inferred to lie. The red ellipse is the likely source area of the Dinner Creek Tuff eruptive center (Steiner and Streck, 2013; Streck et al., 2015).

Based on the age range of 16.16 to 14.37 Ma from Steiner and Streck, 2013, and ages compiled from this study, the Strawberry rhyolites belong to the relatively recently recognized rhyolite flare-up associated with the main pulse of volcanism of the CRBG (e.g., Coble and Mahood, 2012; Streck et al., 2015). Early eruptions of rhyolites in the southern part of the Strawberry Volcanics are coeval with the CRBG magmatism of the Grande Ronde Basalt. Other Co-CRBG silicic volcanism includes numerous rhyolitic ash-flow tuff that erupted from various volcanic centers across eastern Oregon and northern Nevada (Rytuba & Vander Meulen, 1991; Streck et al., 2015; Benson & Mahood, 2016; Coble & Mahood, 2016; Henry et al., 2017; Cruz, 2017). The nearest known volcanic center to the study area is the Dinner Creek Tuff eruptive center. This center lies north of the town of Juntura near the Malheur Gorge between Castle Rock and Ironside Mountain (Streck et al., 2015), where four rhyolitic-dacitic ash-flow tuffs, collectively known as Dinner Creek Tuff units 1 – 4 (Tdit1 – 4), erupted from calderas 16 – 15 Ma (Haddock, 1967; Woods, 1976; Streck et al., 2015; Cruz, 2017). All Dinner Creek Tuff units reach into the investigated area and are found primarily in the Big Canyon and Jump-off Joe Mountain, Calamity Butte quads (Figure 6).

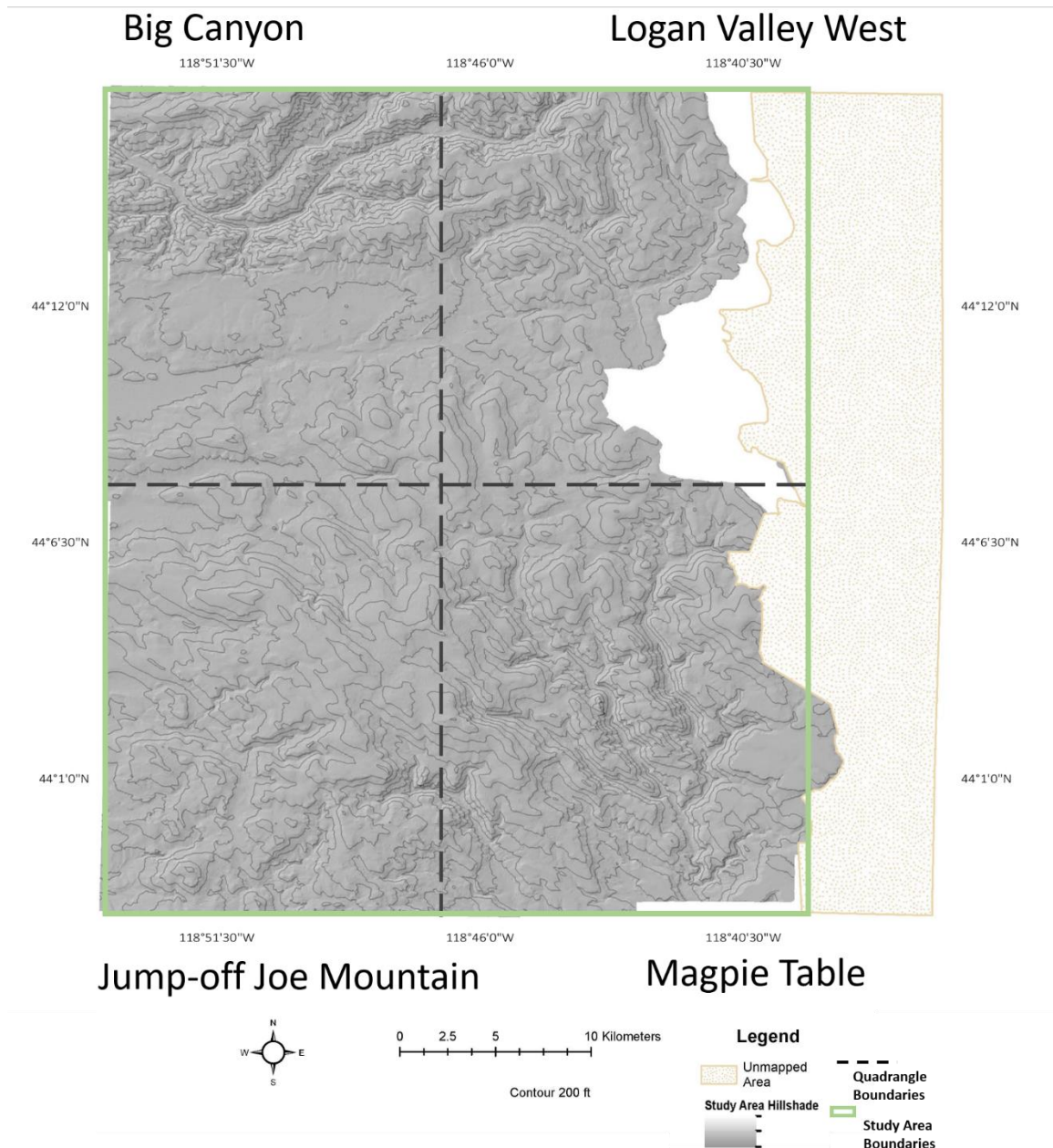


Figure 6: Field mapping area outlined for this project. Including the quadrangles Big Canyon and Jump-off Joe Mountain, alongside the western halves of the Logan Valley West and Magpie Table quadrangles. The green box encompasses the area covered in this study. The tan dotted area on the east is the area for which was unmapped in this study. The black dashed lines separate the quadrangle boundaries. The grey hillshade map layer is comprised of all the lidar available for the region- areas without grey do not have lidar data available.

3.0 METHODS

3.1 FIELD STUDIES

Fieldwork for this study was imperative for achieving the objectives. Some fieldwork predated my entering the MS program at PSU with mapping a portion of Jump-off Joe Mountain quadrangle (JOJM) as part of Portland State's field camp in the summer of 2017. This was followed by receiving a USGS EDMAP grant to continue and finish mapping the Jump-off Joe Mountain quadrangle in the summer of 2018. Results from this EDMAP project prompted me to continue this work as my MS graduate thesis project, which was supported by a second USGS EDMAP grant for the Big Canyon quadrangle (BC). The mapping for Big Canyon was conducted in the summer of 2019, aided by field camp participants of this year. Results from the Big Canyon and Jump-off Joe Mountain quads, along with reconnaissance mapping results by Steiner (2016), suggested that rhyolites extend eastward to about half of the adjacent quads.

The primary access roads to the quads lie east of US Route 395 and are forest roads NF-17, NF-16, and NF-15. In addition, there are graded gravel roads that run throughout the quads from the national forest roads, with numerous minor dirt roads providing access to much of the mapping areas. The entire map areas were covered by road access, and walking transects were strategically placed throughout the quads. A 7.5 min quadrangle map of Big Canyon, Jump-off Joe Mountain, and eastern neighboring quads were utilized in the field using the GPS mapping software "Avenza Maps." Rocks of outcrops or pieces of float were lithologically classified and logged on the topo map, and a subset was sampled for later analysis. A waypoint location of the field stops was recorded using GPS capabilities on a field tablet

using the Avenza Maps software. The locations of the samples were recorded using handheld GPS units and the application Avenza Maps then later exported to ArcMap.

Notes and descriptions were entered in field notebooks as well as photos were taken. Samples were taken primarily at outcrop locations, but it should be noted that some samples were taken from large pieces of float due to some areas having poor or no outcrop exposures. The fieldwork portion of this project was accomplished over a total duration of 16 weeks, split across smaller time segments during the summer of 2017, 2018, 2019, and 2020. Since the EDMAP program only allows two projects to be conducted by the same student, the EDMAP project of Summer 2020 to map portions of Logan Valley West (LVW) and Magpie Table (MPT) quadrangles to the east of JOJM and BC required engagement of another student. Hence, mapping in the Logan Valley West and Magpie quadrangle in 2020 was primarily conducted by Rachel Sweeten (current PSU graduate student) and assisted by Dvorak and other PSU students from the PSU field camp 2020. The EDMAP projects resulted in a geological map of the 7.5 min Jump off Joe Mountain and the 7.5 min Big Canyon quad and a geological map of half of the 7.5 min Logan Valley West and Magpie Table quads, which are still in progress.

I used to distinguish one rhyolite unit from another based on what I learned from the PSU's field camp, being a field assistant to other graduate students, and from my own experience. It is an interactive process that builds on lithological and stratigraphic field observations, followed by analytical data consisting of petrographic, geochemical, and sometimes radiometrically obtained age information. In gathering all the information, one needs to be incredibly organized with all your data (notes, computer files, photos) and allow for the process to take a proper allotment of time. For example, each USGS Edmap map I

produced is a year-long project. The time and process it takes to differentiate units go in stages, with many changes along the way. Initially, it is getting yourself familiar with any known units in and around the area. Determining what distinguishes them from one another and keep thorough notes that are field accessible. Following that is to complete a portion of the field work.

With this initial phase complete, observing rocks in the field leads to a rough schematic of different features that later on are refined after more outcrops have been observed. Each period between field sessions is filled with reviewing samples, specifically the ability to see many of them side by side and use equipment such as binoculars to get a more detailed look. This is also the time to decide which samples are deemed representative of a unit, including consideration of preservation quality prepared for further analysis such as, preparing billets for thin sections and geochemical analysis. With each field session, more details become available, and the process of choosing samples continues. Upon final return from the field again (may be the second or third time), the final decision on important and geologically significant samples is being made. Once analytical data becomes available (~3-6 months), you can start making more solid decisions on which units differ based on their chemical differences and petrographic characteristics. All data feeds into distinguishing the units.

3.2 LABORATORY STUDIES

Seventeen rock samples in 2018, twenty-five in 2019, and twenty in 2020 were analyzed at the Geoanalytical Lab at Washington State University, Pullman Campus. Major and trace element data were acquired using the X-ray fluorescence spectrometer (XRF) and the inductively coupled plasma mass spectrometry (ICP-MS). Data were used to determine their

composition and to differentiate the geologic units. Bulk chemical data are included in the appendix. The sample preparation for the analysis went as follows. First, rock samples were crushed into chips using the rock crusher at Portland State University. At WSU, the chips were crushed into a powder in a tungsten carbide swing mill (mill material is low Ta, Nb steel avoiding contamination of these elements). The powder was then combined with dilithium tetraborate ($\text{Li}_2\text{B}_4\text{O}_7$) in a ratio of 2:1, dilithium tetraborate to sample. The sample was then fused into a bead in an oven at a temperature of 1000°C . The beads were re-grinded into powder, and 1 gram of powder was separated to make the ICP-MS bead. Two beads per sample were then made at 1000°C , one for XRF and one for ICP-MS analysis. The XRF bead was analyzed in the XRF machine, and the ICP-MS bead was dissolved for the final analysis.



Figure 7: XRF and ICP-MS geoanalytical process conducted by Chanel Dvorak at Washington State University, Pullman Campus. (A) Rock chips were brought to WSU from PSU in the process of crushing rocks to powders. (B) Round two of crushing rocks into powders at WSU and post addition of dilithium to powdered samples and placed in carbon crucibles. (C) Samples were cooling into beads from being melted in an oven at 1000°C . Further processes are conducted to generate XRF and ICP-MS data.

Forty-two petrographic thin sections were prepared from JOJM quad units over the years 2017 and 2018. The samples that were analyzed signify prominent map units throughout the quadrangle. Jump-off Joe Mountain quad consisted of four regional ash-flow tuffs and twelve compositionally varying Strawberry Volcanic units. Thirty-eight petrographic thin sections were prepared for petrographic analysis from the Big Canyon quad. The samples selected for thin sections come from seventeen distinct map units throughout the BC quadrangle. All thin section billets were cut from the samples using a trim saw at Portland State University. The billets were roughly 4 cm in length, 2.5 cm in width, and 1 cm in thickness. After cutting the billets, the samples were sent to Spectrum Petrographics LLC in Vancouver, Washington, for final preparation. Full-sized thin-section photographs were taken with a Sony Alpha A7R II using a macro lens. Higher magnification photos were taken with a Canon EOS 5D Mark II using an Olympus microscope. Thin sections were analyzed at Portland State using a petrographic microscope under the plane and cross-polarized light. Mineral phases, mineral proportions, and textures were recorded for all samples, aiding in categorizing the units. Petrographic analysis of phenocrysts was conducted to provide further insight into each unit and the evidence of magma mixing or crustal contamination. In addition, thirty-four new thin sections were produced in 2020 for the LVW and MPT quadrangles.

Samples of crucial rhyolite units were used for radiometric age determination by the $^{40}\text{Ar}/^{39}\text{Ar}$ method. Two samples located in the Jump-off Joe Mountain quad, JJ-17-08 and MS-17-05, were analyzed at the Noble Gas Mass Spectrometry Lab at New Mexico Tech. Data are composed of age dates on two rhyolite flows, Biotite-Amphibole Rhyolite and Wolf Mountain Rhyolite. The samples were crushed at Portland State University and then sieved

to isolate feldspar phenocrysts for analysis. Sample ages were calculated using FCT-NM (R98) (4E36-14) of 28.201 ± 0.023 Ma (Kuiper et al., 2008). Age data were also collected from one of the rhyolite units from the BC quadrangle, Kent Spring Rhyolite (sample CD1975), at the Oregon State University Ar-Ar Geochronology facility. The sample was crushed at Portland State University and then sieved to isolate feldspar phenocrysts for analysis. Sample MS-14-23 also selected for age determinant is a rhyolite from the ~aphyric Three Cabin Spring unit in the BC quadrangle. Age dating of this sample was performed at the Ar-Ar Geochronology Research Laboratory at the New Mexico Bureau of Geology & Mineral Resources on groundmass. Age data from previous studies (Steiner, 2016) are available for five select rhyolite samples and were used to establish stratigraphic relationships based on correlating units across areas based on lithology and chemical compositions. The analytical results for all these samples can be found in the appendix.

4.0 RESULTS

4.1 Distribution, Lithology, and Composition of Rock Units in the Study Area

4.1.1 PRE-TERTIARY

Based on the 1x2-degree Canyon Mountain quadrangle by Brown and Thayer 1966, pre-tertiary rocks of Big Canyon Quadrangle belong to the Aldrich Mountains Group. Within the Aldrich Mountains Group contains the unit (JK) Keller Creek Shale and (Rsp) Igneous and Metamorphic Rocks and thus is equivalent to Clastic Sedimentary Rocks (Itss) and Ultramafic Rocks (Kpm) of my map produced of the Big Canyon quadrangle, respectively. “The Aldrich Mountain Group is herein given to the Upper

Triassic and Lower Jurassic rocks that form the western two-thirds of the Aldrich Mountains” (Brown, 1966). The unit Keller Creek Shale is well exposed, about 5,000 ft thick. The lower 2,500 ft. of the formation consists of massive to well-bedded, coarse- to fine-grained tuffaceous sandstone with lenses of pebbly conglomerate, shale, thin ashy beds. The Jk unit's upper and middle consists of shale interbedded with graywacke, siltstone, massive coarse- to fine-grained graywacke about 1000 ft thick. These sedimentary units belong in general to the Izee terrane (Vallier, 1986). Unit Kpm of this study is interpreted as sheared serpentinite, mostly derived from peridotite, but with original rock type not readily determinable.

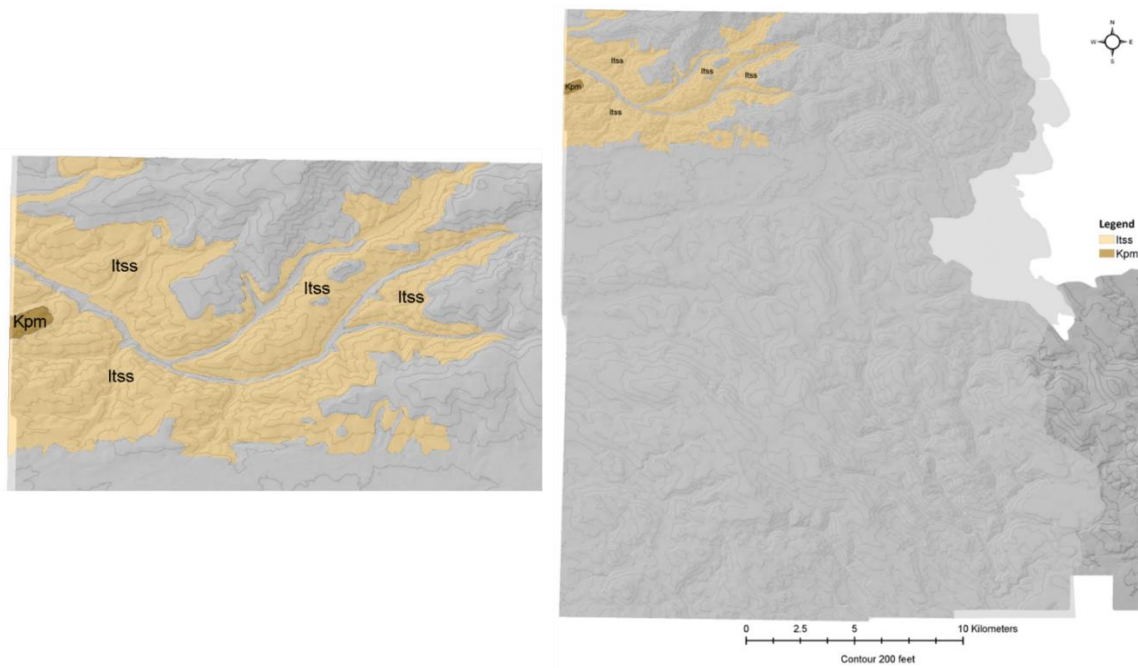


Figure 8: Distribution of the units Itss (tan) and Kpm (brown) across the entire mapping area with other units greyed out.

I. Itss – Clastic sedimentary rocks: Conglomerate, Sandstone, Siltstone, and minor Carbonates (Mesozoic ~252-66 Ma)

The unit Itss makes up a substantial portion of the northern half of the BC quadrangle. The rocks that make up this unit are sandstone, conglomerates, siltstones, and some claystone. Occasional carbonates are exposed near the east side of the BC quad. Overall, this unit was primarily found in the northwest section and the west-central region of the BC map. Outcrops around the Canyon Creek bed exposed tilted bedding. They dip steeply towards the east between 70 and 90 degrees. This degree of dip is constant as you move eastward in the region of study. Overall, the east-west synclinal structure and the anticlinal orientation of geologic features in the far west indicate that this unit can be broken into more than one sandstone unit. However, no discerning factors were documented in the field, and spatial differences between sandstone units were not observed.



Figure 9: Sandstone of the Accreted Terranes in hand sample. The left image (sample BC19A45) is pictured with some of the unit's quartz veins throughout the sandstone in Big Canyon. The image of the right (BC19A01) has slightly more of a greenish hue.

Itss is best identified on slightly weathered surfaces, as the fresh fine-grained interior parts resemble the aphanitic and aphyric Miocene andesite (unit Tasv). When slightly weathered, the Itss has defining characteristics. Displaying the clastic nature with sand grains and rounded lithic fragments are clearly visible with a 10X magnification hand lens. The surface can be dark to light tan or greenish in color, with finer-grained samples dark to light gray. The argillite beds provide most bedding orientations, indicating ample folding of the area during orogenic times. Most of the outcrops have lenticular bedding, alternated between sandstone and mudstone.

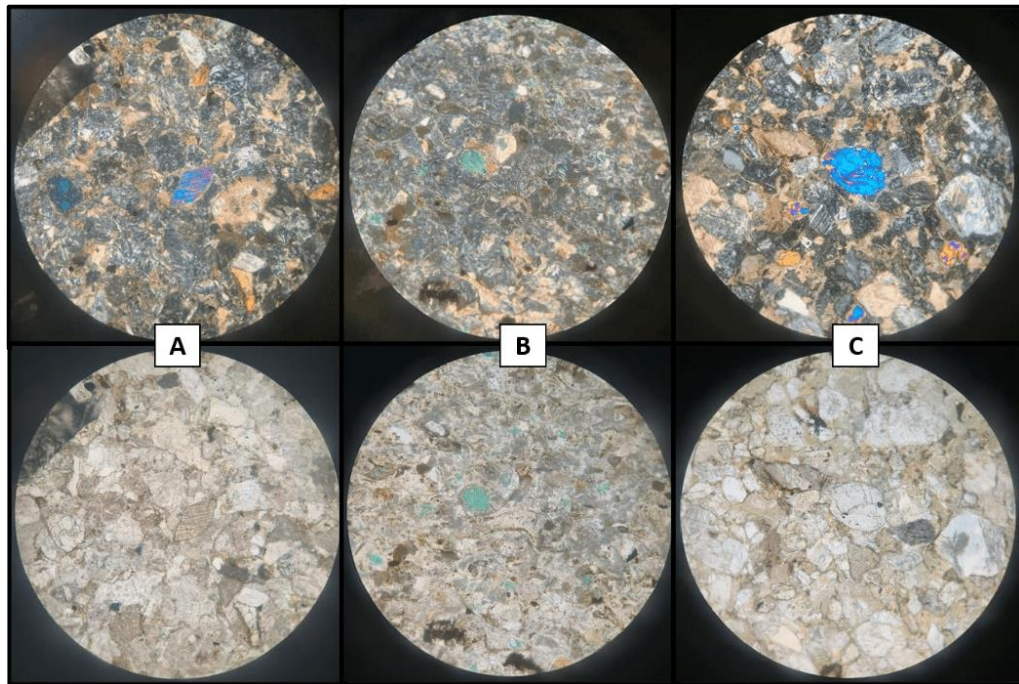


Figure 10: Thin section images of the Sandstone of the Accreted Terranes. The top row images are all in XPL, whereas the bottom is in PPL. (A) is sample BC19A45, (B) BC19A01, and (C) BC19B06. All pictured are in 100X optical zoom.

Thin-section analysis of sample BC19A01 (Image B Figure 10) shows alteration of plagioclase altering to epidote. Itss show pleochroic teal, clay chlorite that leads in hand

samples to the greenish-blue hue of the rock. It is a subangular-subrounded fine-grained sandstone displaying weathered minerals indicative of andesite (pyroxene, plagioclase) or possibly more mafic protoliths. About five percent of quartz grains are present. In image B, chlorite patches indicate alteration of the mafic minerals such as amphiboles and pyroxenes. A whole thin section comprises approximately 5% of dark lithic fragments. In Figure 10, image A, sample BC-19-A-45, is much less altered than image B. Fragments of siltstone, shell fragments, and lithics are seen within this sample. Clinopyroxene and amphibole are also present, characterizing this sample as part of a volcanoclastic unit. The pre-Tertiary unit Itss has an average SiO₂ content of about 65 wt.% but analyzed samples range from ~57.9 to 71.3 SiO₂ wt.%, and Al₂O₃ values range from 13.9 wt.% to 16.5 wt.%. The average CaO content is 6.7 wt.%.

II. Kpm – Ultramafic Rocks (Paleozoic ~541-251 Ma)

The oldest unit found in the project region is a recognized ophiolite and includes mafic-ultramafic rocks, serpentinite, and a chert-argillite mélange (Steiner, 2018). Kpm only was found in a small section to contact unit Itss to the west in the BC quadrangle and appears to consist mainly of what used to be pyroxenite upon outcrop inspection.



Figure 11: Pictured is the Pretertiary Ultramafics, Sample BC19A07.

The Kpm unit in the hand sample appears nearly black or a weathered green hue and is mainly composed of talc and serpentine. Only pseudomorphs after pyroxene up to three cm in size are apparent in hand samples.

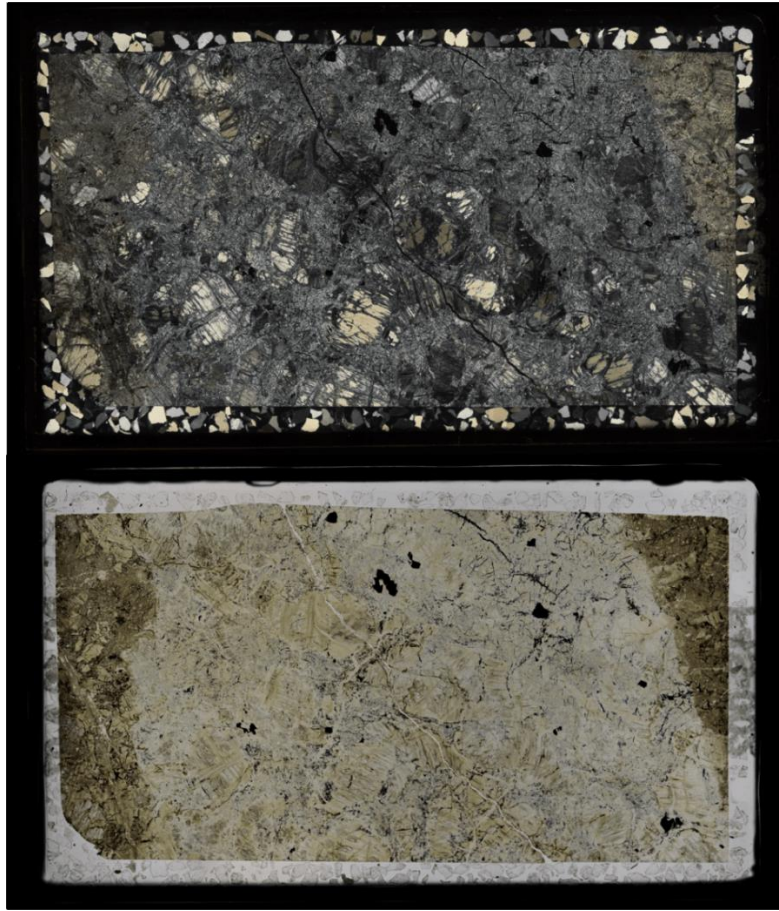


Figure 12: Full thin section image of sample BC19A07, Pretertiary Ultramafic unit. The upper image is in XPL, and the lower is in PPL.

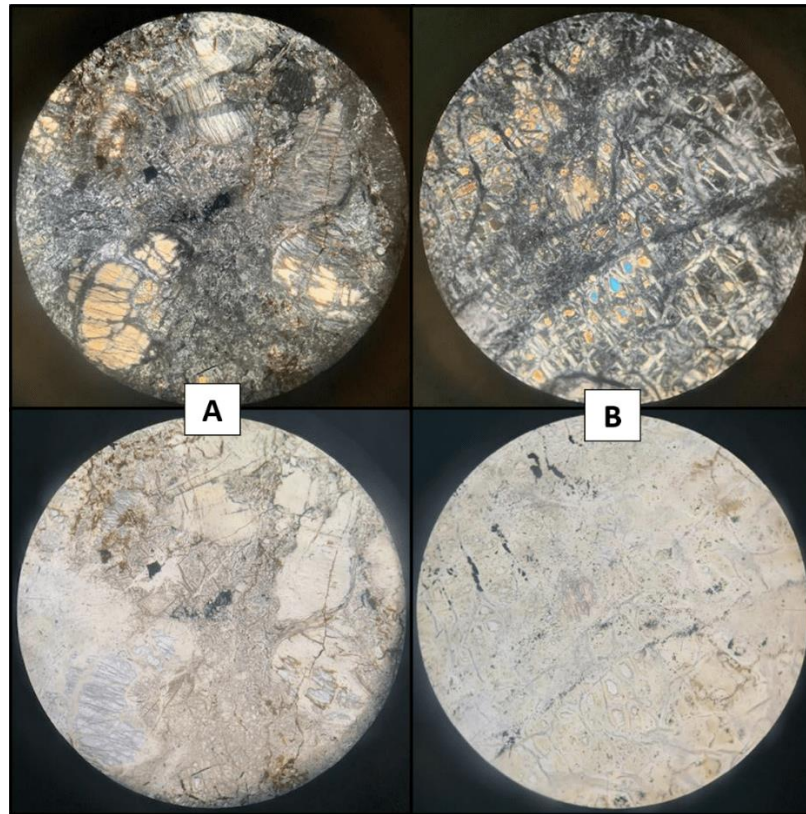


Figure 13: Thin section images of sample BC19A07 all captured in 100X optical zoom. The top row of images is in XPL, and the bottom row is in PPL.

Investigating a thin section of Kpm (sample BC19A07), the sample is indeed classified as pyroxenite. Abundant large pyroxenes have altered to serpentine and talc with a mesh-like texture. Pictured in Figure 13, the weathered pyroxene grains make up most of the field of view. Unit Kpm has a low SiO_2 content of 47.49 wt.%, a FeO^* content of 8.56 wt.%, and a high MgO content of around 40 wt.%. All ICP-MS trace element concentrations are depleted in comparison to neighboring units. On the other hand, the Ni and Cr contents are high, with 2233 ppm and 2872 ppm values. These compositional features support and are in keeping with being initially a pyroxenite.

4.1.2 REGIONAL TUFFS

I. Trst – Rattlesnake Tuff (7.1 Ma)

The Rattlesnake Tuff (Trst) is a widespread, single cooling unit and displays variable welding characteristics from non-welded to densely welded with vapor phase and lithophysae zones (Streck and Grunder, 1995). Most of the RST is high-silica rhyolitic tuff (75-77.5 wt. % SiO₂) but with some dacitic components (62-70 wt. % SiO₂) found in pumices and banded pumices. Dacite pumices occasionally contain mafic inclusions that range from andesitic to basaltic (Streck and Grunder, 1999). Rattlesnake Tuff can be distinguished from other tuffs lithologically and geochemically.



Figure 14: Image B and C are examples of typical partially welded vitric hand samples of Rattlesnake Tuff, all from the outcrop in image A. Visible features are light to gray pumice clasts in gray glass shard matrix. Image A (Sample CD1988) is in the southern-central region of the quadrangle.

The tuff is typically exposed to 5-20 m thick outcrops, which often caps flat-lying plateaus (Streck and Grunder, 1995). However, in my study area, outcrops of Trst typically are less than 10m in thickness and dip at a few (~5) degrees in an easterly direction. Typical hand samples of the tuff are light to middle gray and light reddish to pinkish red, often vitric containing ~1 % phenocrysts. Trst is typically pumiceous, glassy, and ranging from incipiently welded to welded. Pumices can be white, gray, and black, and banding of any combination of these colors. The 7.1 Ma Rattlesnake Tuff overlies Devine Canyon Tuff and Dinner Creek Tuff unit 1 on the northwestern and southeastern corner of the BC quad and some sparse northern and southern regions of the JOJM quadrangle. Trst roughly covers an area of ~108 km² with a minimal calculated volume of ~1 km³. Distinguishable from other tuffs by the vitreous fresh glassy groundmass, white pumice up to 10 cm in length, and virtual nearly aphyric character (~1% phenocrysts mostly alkali-feldspar and quartz). Hand samples of Trst may contain some fiamme when welded. This tuff may display some horizontal parting parallel to the welding plane and is consequently platy in outcrop.

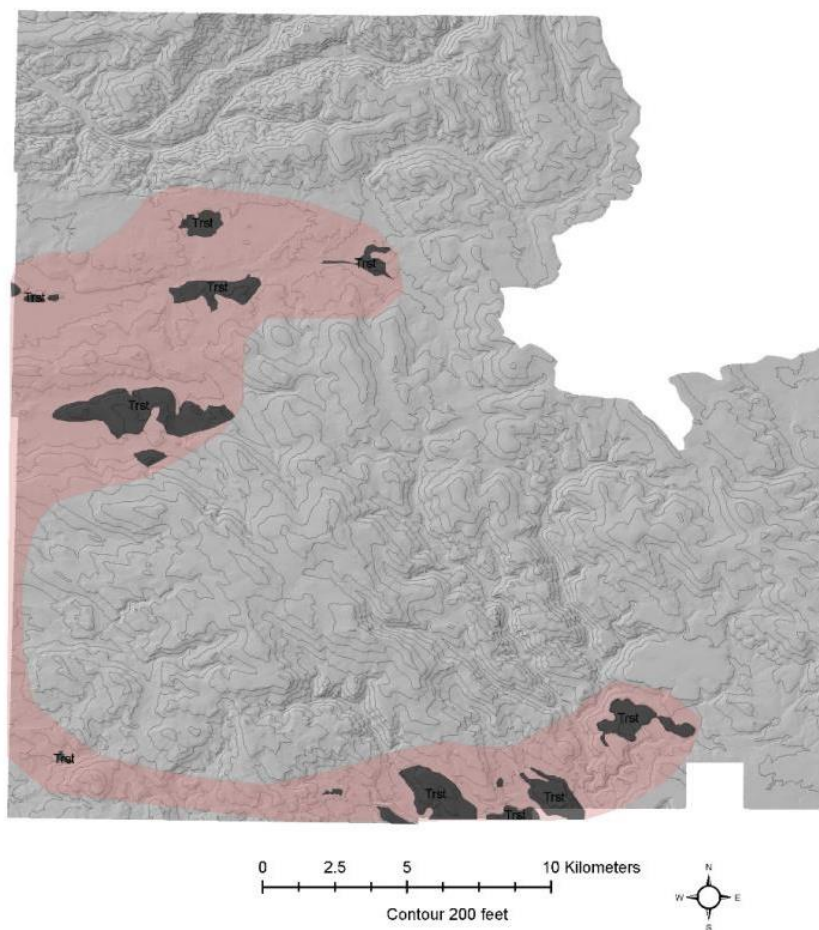


Figure 15: Distribution of the unit Trst (red) across the entire mapping area with other units greyed out.

II. Tdct – Devine Canyon Tuff (9.7 Ma)

The Devine Canyon Tuff is one of the largest late Miocene ash-flow tuffs in eastern Oregon, extending over 20,000 km² (Wacaster and others, 2011) with a reported Ar-Ar date of 9.74±0.02 Ma (Jordan et al., 2000). The Devine Canyon Tuff is part of the High Lava Plains volcanic province. The erupted source is believed to be a caldera located in the Harney Basin, near Burns (Jordan et al., 2004). Tdct is almost entirely composed of rhyolite (74.6-77.6 wt.% SiO₂) with a dacitic component (68.7-68.9 wt.% SiO₂) found as

individual pumices or as streaks within banded pumices, comprised of both rhyolite and dacite (Isom, 2017). The Devine Canyon Tuff is the oldest of the three ash-flow tuff units that erupted from the Harney Basin to the south and overlay Dinner Creek Tuff unit 1 and older volcanic units.



Figure 16: Image A is an outcrop of Devine Canyon tuff within the Big Canyon quadrangle. The black streaks amongst the outcrop hand samples seen in pictures B and D are fiamme (flattened pumices). Hand samples seen in image C show the variance in color throughout this unit.

The Tdct that crops out in the study region is primarily found in the western-central and southwest parts of BC and sparse northern and southern sections of the JOJM quadrangles. Typically, Tdct in my region is about 5-15 meters thick. It can be up to 50 meters closer to the source (Figure 16). Tdct roughly covers an area of $\sim 160 \text{ km}^2$ with a minimal calculated volume of $\sim 1.6 \text{ km}^3$. The tuff is partial to densely welded, typically outcrops as rounded boulders. Eroded Tdct has a unique feature as the abundant phenocrysts generate very sparkly sands. Outcrops are dark grey to light grey in color. This

unit contains vitric, devitrified, and vapor phase zones. The ignimbrite generally exhibits stratigraphic gradation in phenocryst content from phenocryst-poor (<5%) in basal sections to phenocryst-rich (>25%) in the uppermost portion (Isom, 2017). Typically, Tdct contains ~25% crystals of alkali feldspar in a hand sample and noticeable quartz phenocrysts with trace amounts of clinopyroxene and fayalite. The tuff forms a single cooling unit, which suggests the entire magma chamber erupted during a single eruptive episode (Isom, 2017). In the thin section, the tuff is effortlessly distinguishable from other tuffs in the area due to its high phenocryst percentage (Figure 17). Devine Canyon Tuff is slightly peralkaline rhyolite with high Zr (>700 ppm), high Nb (>53 ppm), Ce (152 – 196 ppm), and low Ba (183 – 216 ppm) content. Outcrops of Tdct in the study region vary in their welding degree, but observed sections are mostly densely welded. Vitric groundmass consists of glass shards, pumice, and lithic fragments. Fiamme is also found in several sections within the mapped region. On the other hand, lithophysae or spherulites have not been observed in the tuff. Select samples were analyzed for major and trace elements and plotted in Figure 19 along with other regional tuffs of this study.

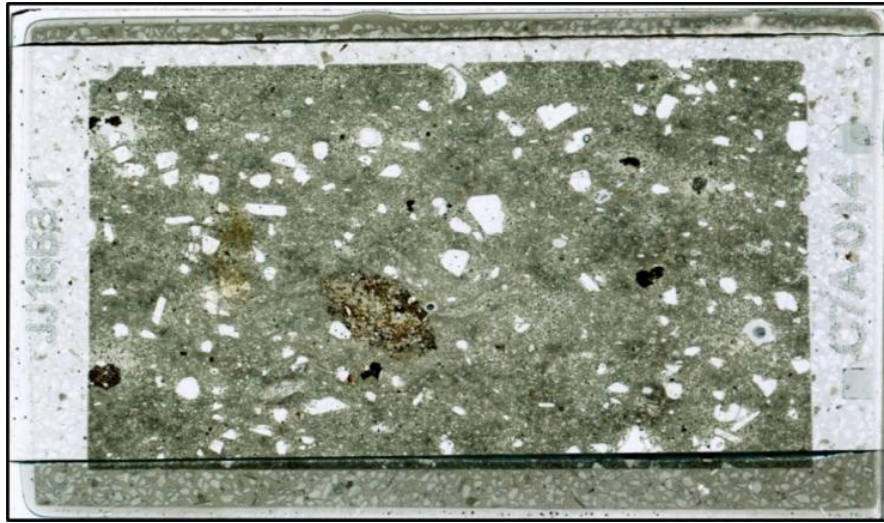


Figure 17: Full slide thin section image of Devine Canyon tuff (sample JJ18B3.1) shown in PPL. Displays glassy (ash) matrix with quartz phenocrysts.

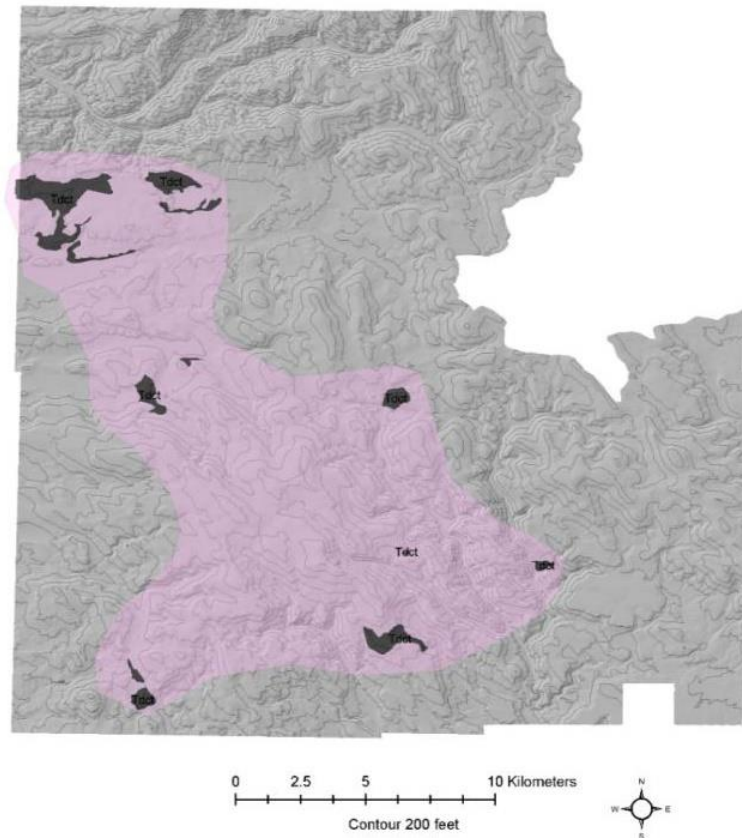


Figure 18: Distribution of the unit Tdct (pink) across the entire mapping area with other units greyed out.

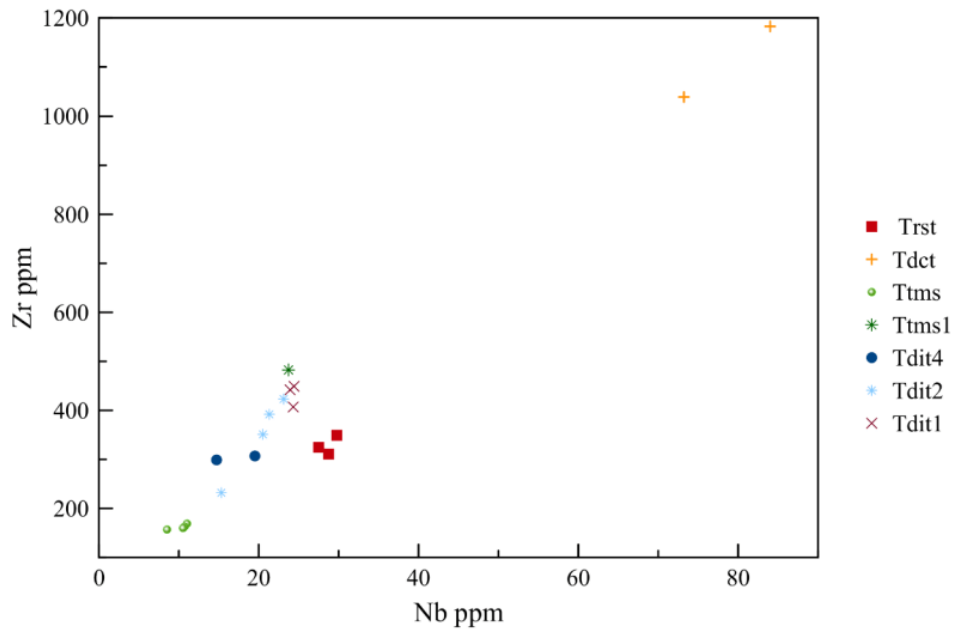


Figure 19: Zr versus Nb of all regional to local silicic ash-flow tuff units.

III. Tdit4 – Dinner Creek Tuff, Unit 4 (15 Ma)

The four Dinner Creek Tuff units are all regionally distributed ignimbrites and erupted during a period of mid-Miocene rhyolitic volcanism coeval to the flood volcanism of the CRBG (Streck and Ferns, 2012; Streck et al., 2015). Source caldera(s) for the four discrete ignimbrites that make up the Dinner Creek are believed to lie in the Castle Rock-Ironside Mountain area northeast of the town of Burns (Rytuba and Vander Meulen, 1991; Streck et al., 2015; Cruz, 2017) The Dinner tuff unit 4 unit is the youngest with an age of around 15 Ma (Streck et al., 2015; Hanna, 2018); it roughly covers an area of $\sim 82 \text{ km}^2$ with a minimal calculated volume of $\sim 0.5 \text{ km}^3$. It is the most mafic of the Dinner Creek units with a bulk composition of dacite but consisting of juvenile components ranging in composition from rhyolite to basaltic andesite. The other Tdit units are rhyolitic tuffs

displaying nearly identical compositions but with subtle geochemical and lithological differences and distinct unit ages (Streck et al., 2015). Hand samples of Dinner Creek Tuff cooling units 1, 2, and 3 strongly resemble one another. When devitrified, samples without eutaxitic texture are difficult to distinguish from samples of devitrified rhyolite lava flows considered part of the lower Strawberry Volcanics (Ferns et al., 2017).

The bulk composition of the Tdit4 tuff deposit is lower in SiO_2 than the other Tdit cooling units due to the substantial comingling of dacite and andesite components with high-silica rhyolite. Given its dacitic bulk composition, Tdit4 is also depleted in most trace elements, except for compatible elements such as Sr, which are enriched compared to rhyolitic units (Streck et al., 2015). For example, sample CD1936A has a Sr value of 135 ppm, whereas Tdit units 1 and 2 found in the quadrangle to the south (Jump-off Joe Mountain) have a lower Sr value, ~30 ppm for Tdit1 and ~90 ppm for Tdit2. Outcrop thickness is roughly 3-8 m. This unit is found throughout the Big Canyon quadrangle, with its largest outcrop occurring in the far southwestern region.

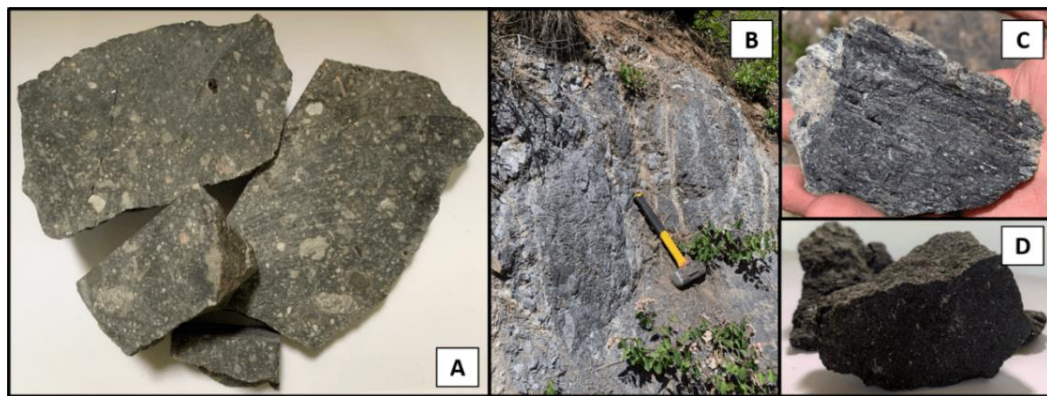


Figure 20: Image (A) sample BC19A26B, (B and C) outcrop and hand sample CD1936A, lastly image (D) sample BC19C40.

Typically, Tdit4 may contain up to ~15% lapilli-sized fragments of juvenile and lithic nature in the hand sample. Lithic fragments appear to be mostly derived from older lavas and tuffs of the surrounding region. This unit is typically much darker in color due to its more dacitic composition and often appears to have a glassy groundmass compared to the other Tdit members (Figure 20). The welded vitrophyre is often more friable in outcrop, making hand samples much more delicate to handle than the surrounding tuff units. In hand samples, fiammes are often seen, welded glass shards, dacitic lapilli lithics, occasionally pumice, and lithics ranging in size from about 1-20 cm. The thin section pictured in Figure 21 is Tdit4 sample BC19A26B from the BC quad. This thin section image is a perfect example of the mafic lithic fragment incorporated in the tuff. Thin sections reveal a phenocryst percentage of ~3-5% feldspar and ~ 1% subhedral pyroxene. The feldspars are primarily plagioclase, as indicated by the albite twinning. The groundmass typically consists of variably welded glass shards.

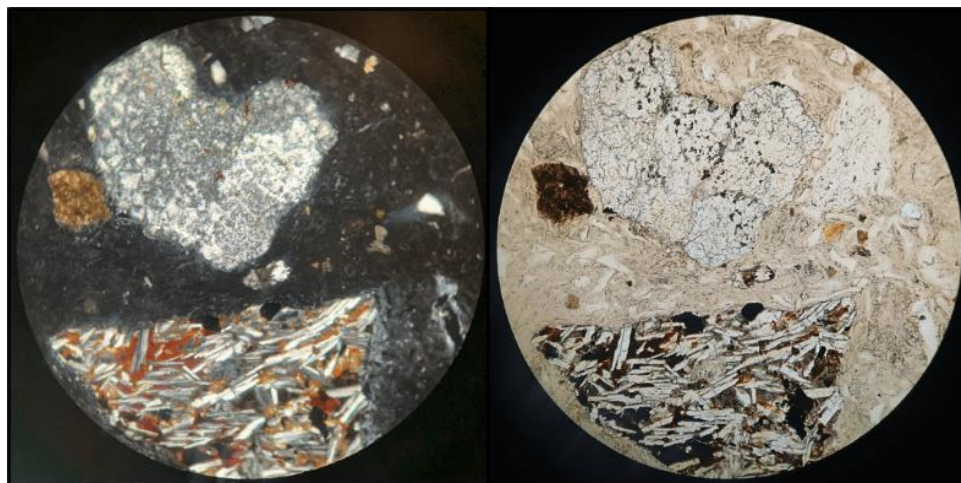


Figure 21: Image of Tdit4 sample BC19A26B. The left image is in XPL, whereas the right is in PPL, represented in 100X optical zoom.

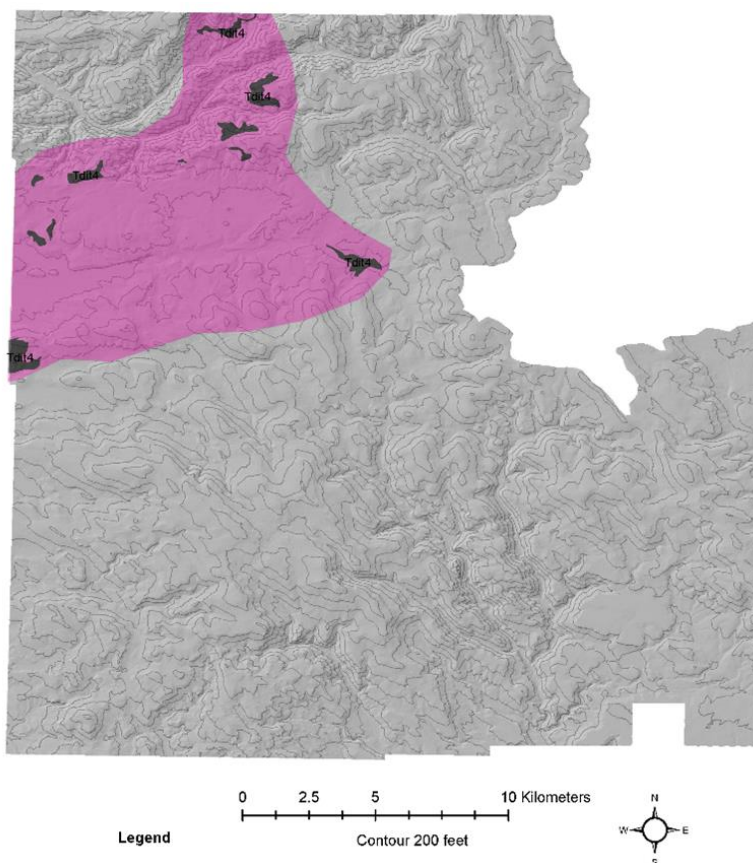


Figure 22: Distribution of the unit Tdit4 (magenta) across the entire mapping area with other units greyed out.

IV. Tdit2 – Dinner Creek Tuff, Unit 2 (15.5 Ma)

The second oldest unit of the Dinner Creek Tuff has an age of 15.5 Ma. Outcrops are poor, appearing only in the south-central region of the JOJM mapping area, mainly along the eastern flank of Long Mountain. The tuff is mostly incipiently welded. The groundmass of the tuff ranges from tan to gray in color, and small (mostly ~2 cm) gray to white pumices are common and black glassy lithic fragments. Feldspar phenocrysts make up about 5 – 10% of the rock. The tuff is less than 10 meters thick. Tdit2 roughly covers an area of ~28 km² with a minimal calculated volume of ~0.2 km³. Some sections include a partially welded zone as defined by vitrophyre grading upward into less welded tuff. The presence of large, dark-

colored, scoriaceous pumice fragments (up to 30–40 centimeters) and obsidian lithic fragments (up to 15 cm) suggest close proximity to the Dinner Creek vent. Exceptionally large pumice fragments were found at some of these outcrops.



Figure 23: On the left is a hand sample of Dinner Creek Tuff unit 2. The right image shows this unit in an outcrop.

The most abundant phenocryst in Tdit2 is plagioclase with a composition of ~ 20 An (Streck et al., 2015). Geochemically, the tuff can be distinguished from the Dinner Creek Tuff unit 1 by its lower wt. % SiO₂ (72–74) and lower Y (~ 50 ppm) but higher Sr content (>100 ppm) (Ferns et al., 2017). Dark-colored pumices are iron-rich with 5.2 wt. % FeO*. Dinner Creek Tuff unit 2 erupted from a caldera located at Ironside Mountain, about 148 km, to the northeast of the project area (Cruz, 2017).

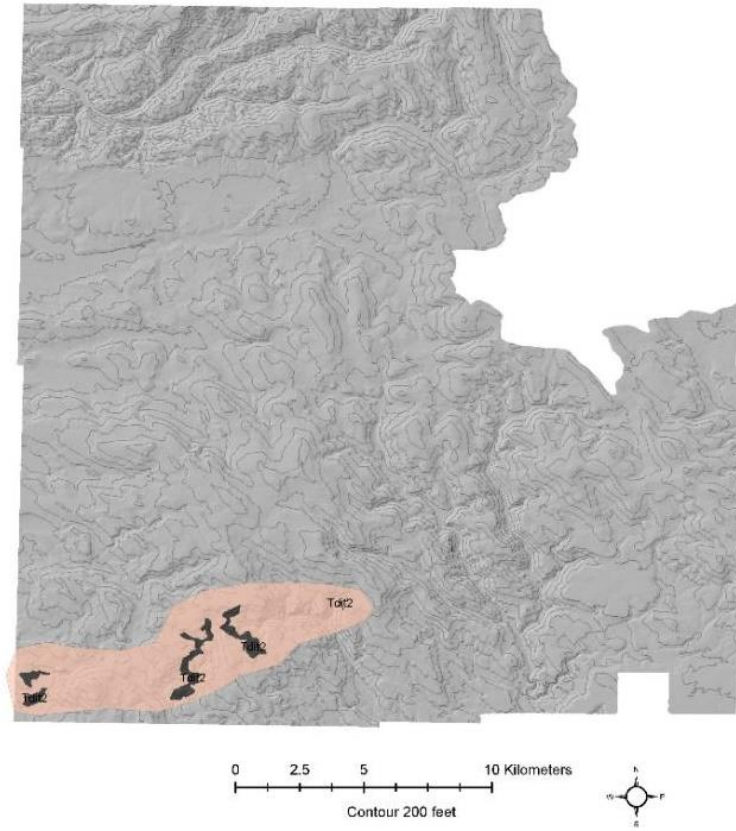


Figure 24: Distribution of the unit Tdit2 (peach) across the entire mapping area with other units greyed out.

V. Tdit1 – Dinner Creek Tuff, Unit 1 (16.1 Ma)

Outcrops of the Dinner Creek Tuff unit 1 are widely distributed across the JOJM study area with variable thickness, suggesting a variable paleo-topography at the time of the eruption., Tdit 1 is also found within the west-central portion of the BC map and in a small southern region of the MPT quad. The Dinner Creek Tuff unit 1 is the oldest, dated at 16.15 Ma, and is the most extensive of the Dinner Creek Tuff units (Hanna, 2018). Tdit1 is lithologically variable, ranging from rheomorphic to lithophysal sections, with a basal vitrophyre in outcrop or as float of glassy tuff found. In general, this unit is the thickest unit of the Dinner Creek Tuff, also in the project area, with maximal thicknesses ranging

from about 20 to 80 meters. Average outcrop thickness is between ~3m and ~30m, with some of the thickest exposures found near road cuts and drainages. Tdit1 roughly covers ~140 km² with an estimated, calculated volume of ~2.3 km³. Sections with lithophysal tuff or where the tuff is rheomorphic appear to be sections where the tuff was originally thickest.

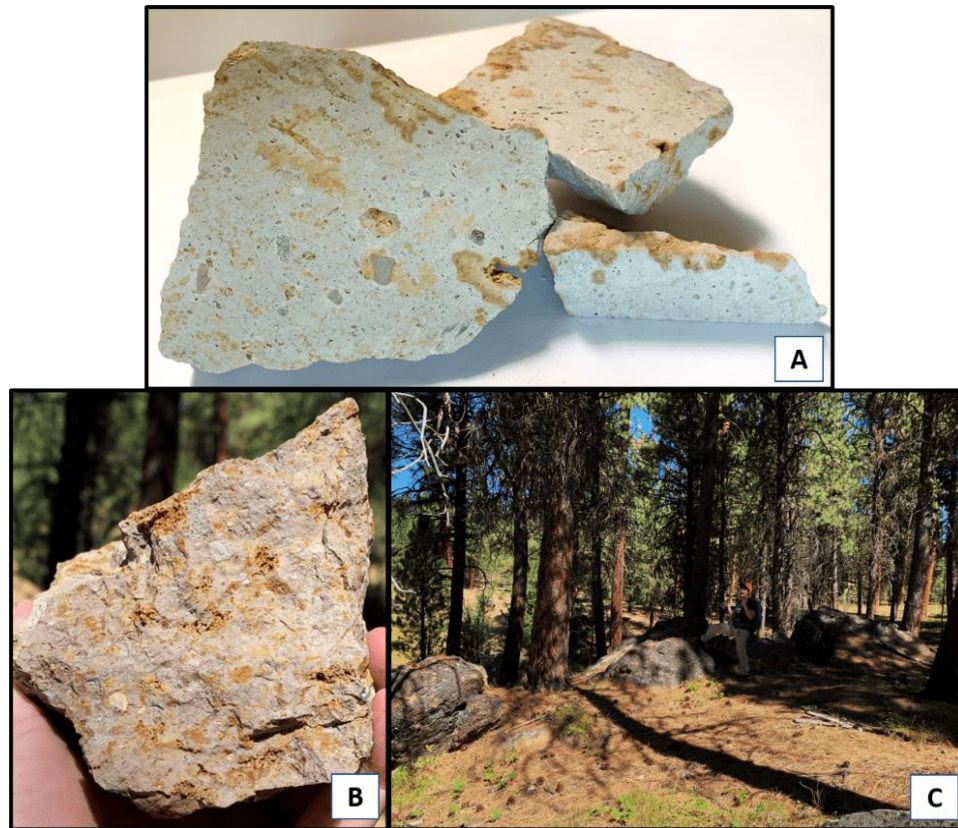


Figure 25: Dinner Creek Tuff unit 1 is found in varying shades of color and alteration, basal vitrophyre, spherulitic tuff, and devitrified. Image A is from sample BC19A61, where B and C are from sample CD1979.

In thin section, the groundmass is typically welded glass shards with about 3-5 percent, plagioclase phenocrysts showing albite twinning and altered clinopyroxene about 0.5-1

mm in length. A thin section of rheomorphic tuff exhibits about 1% phenocrysts with a devitrified pinkish groundmass.

Dinner Creek Tuff unit 1 has the highest silica content of all the Dinner Creek Tuff units, typically greater than 75 wt. % SiO₂ and has the highest Zr (>400 ppm), Nb (>20 ppm), and lowest Sr (<60 ppm) content of all the Dinner Creek Tuff units.

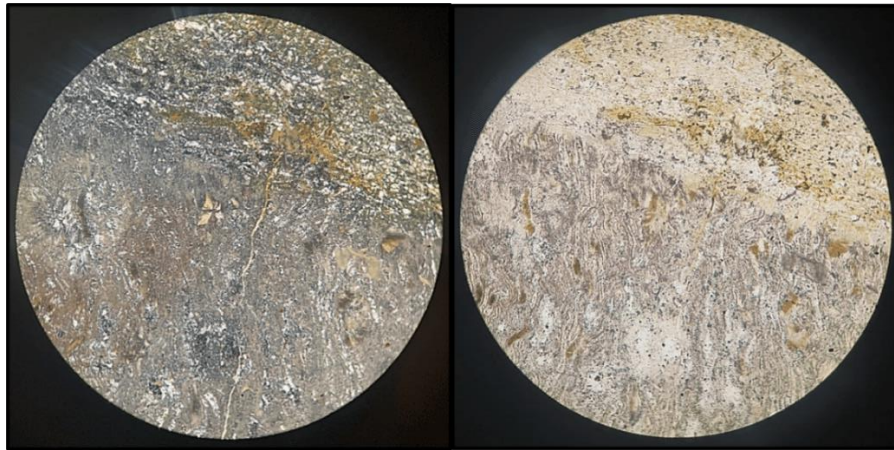


Figure 26: Thin section image of Dinner Creek unit 1 (sample BC19A61). The images display a glassy (ash) matrix. The left image is in XPL, with the right being taken in PPL. Images are in 100X optical zoom.

4.1.3 LOCAL to REGIONAL BASALTS

I. TpvD – Near Vent Pyroclastic Deposits, Basalt to Basaltic Andesite of the Strawberry Volcanics

This unit is made up of near-vent mafic pyroclastic fall and flow deposits. Vent facies of TpvD includes scattered strombolian deposits consisting of highly vesiculated lapilli to bomb-sized pyroclasts, often red or dark grey in color. Mafic bombs and spindle bombs were often abundantly found as float surrounding outcrops. Outcrops contain lithic fragments of aphyric andesite. Stratigraphically overlies the Dinner Creek Tuff units, having a maximum

age of 15.5 Ma. Exposures are typically between approximately 3-10m in height. The largest outcrop is found in the northernmost-central region of the BC quad near Juniper Springs (Figure 27 and Figure 28), with dipped beds reaching 40m thick and surrounded by the andesite of the Strawberry Volcanics.



Figure 27: Photograph looking at a sizeable basaltic-andesite outcrop in the BC map's northernmost-central region (sample BC19B07).

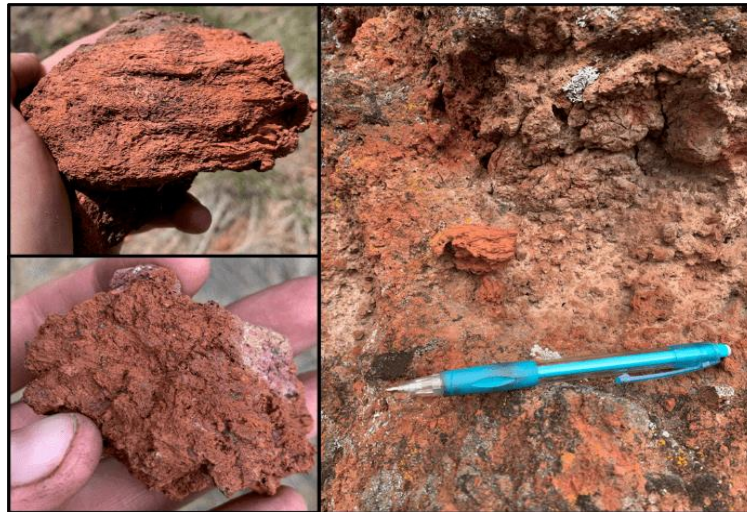


Figure 28: Close-up look at the basaltic andesite outcrop (Sample BC19B07). Highly vesiculated red basaltic andesitic scoria consisting of fine lapilli occasional coarse ash and featuring spindle bombs around and protruding out of the outcrop.

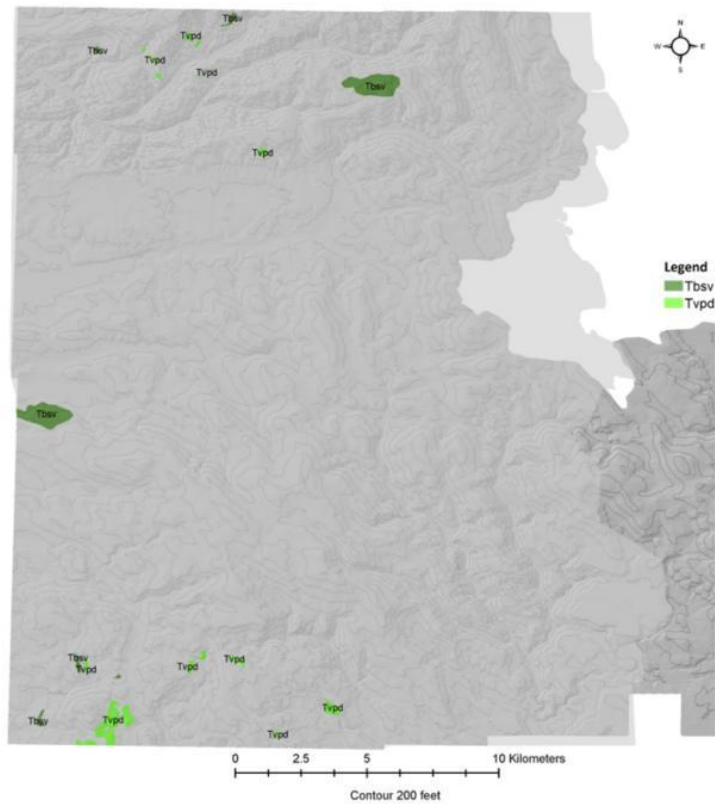


Figure 29: Distribution of the units Tvpd (light green) and Tpsv (dark green) across the entire mapping area with other units greyed out.

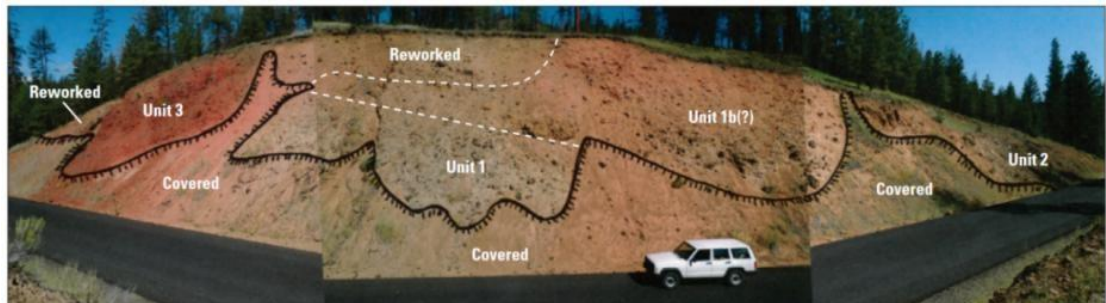


Figure 30: Photograph looking north at mafic pyroclastic flow, unit Tvpd makes up units 1 and 1b in the image. Image label unit 2 and scoria fall deposits (unit 3) make up the flow of the pahoehoe toe. “Covered” means talus conceals outcrop; the black line is the upper extent of the talus. “Reworked” means the unit is slightly modified from subsequent processes. The dashed white line is the presumed contact between units. Photograph by Martin Streck. (Ferns, et al., 2017).

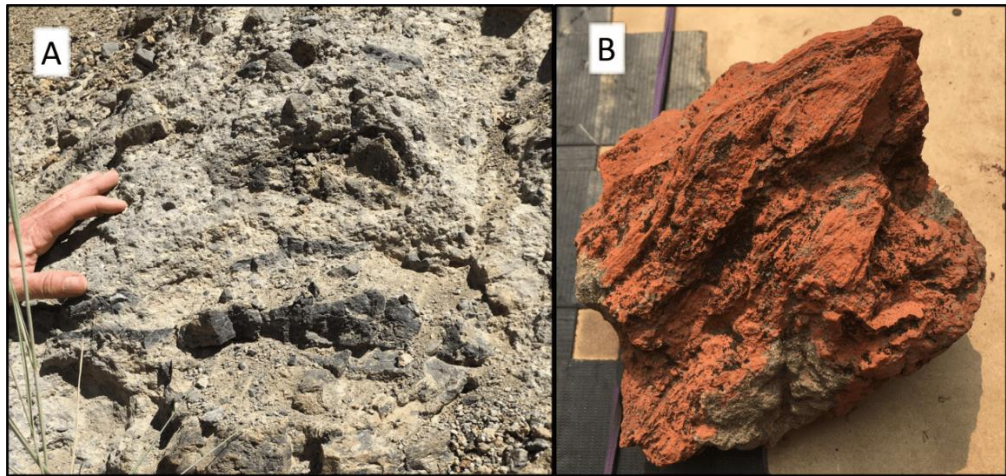


Figure 31: (A) Outcrop of Tpvd (named Tbt in JOJM quad) in roadcut along NF17, icelandite juvenile clasts are pictured. (B) Spindle bomb.

Figure 30 illustrates one roadcut exposure in the JOJM quad, where Tpvd is not only strombolian deposits but also includes what appears to be proximal flow deposits and is named Tbt in the JOJM 7.5 min mapped quadrangle from 2018. The dark scoria throughout the entire outcrop of Figure 30 is icelandite. More details of this outcrop are found in Ferns et al. (2017). Mafic pyroclastic fragments are phenocryst poor and contain less than 8% phenocryst, mainly consisting of plagioclase, minor olivine, and rare pyroxene.

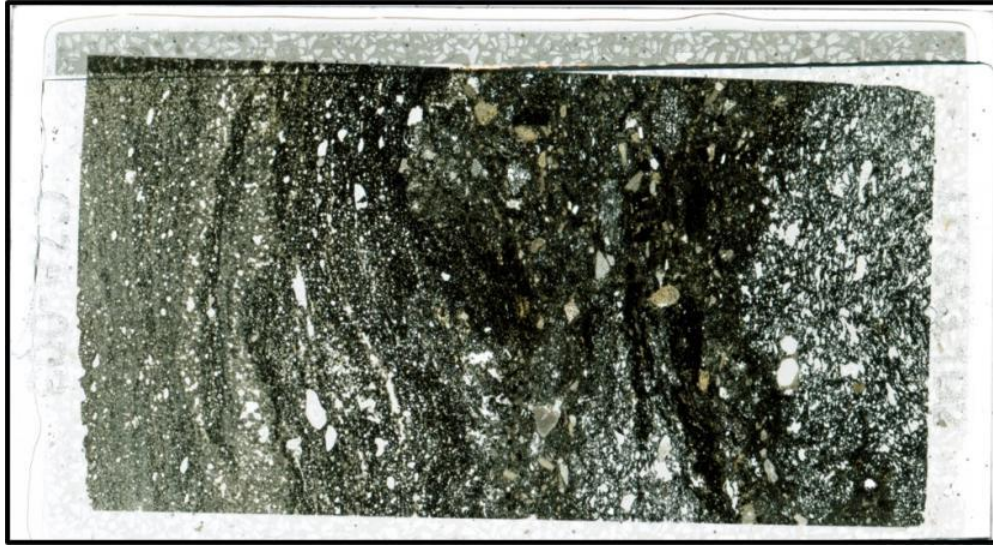


Figure 32: Pictured is a full thin section image of sample JJ18A3.1D2. The unit is abbreviated as Tbt in JOJM 7.5 min quadrangle from 2018. This thin section is in PPL and showing a glassy matrix containing lithics and is vesicle rich.

II. Tbsv – Basalt to Basaltic Andesite Lavas of Strawberry Volcanics (Miocene)

Outcrops of Tbsv are, in general, found scattered throughout the JOJM and BC quadrangles. Small outcrops are found in the far southwestern corner of JOJM. The larger outcrop of Tbsv in JOJM is in the northwestern region of the quad. The largest area of Tbsv is found in the northeast of the BC quad. There is a small exposure in the northwest section of BC that overlies sandstones of the accreted terrane. Outcrops or float are typically massive. Lavas are intercalated with Tasv and are rarely mappable. Hand samples are coarsely grained, dark-colored, and range from dense to vesiculated. The coarse-grained basalt to basaltic andesite is highly crystalline but phenocryst poor with olivine phenocrysts observable in the

hand sample and sometimes a few plagioclase phenocrysts. Observable olivine phenocrysts in hand samples were used to map lavas as basalt to basaltic andesite.



Figure 33: Basalt of the Strawberry Volcanics, sample BC19B36 in hand sample.

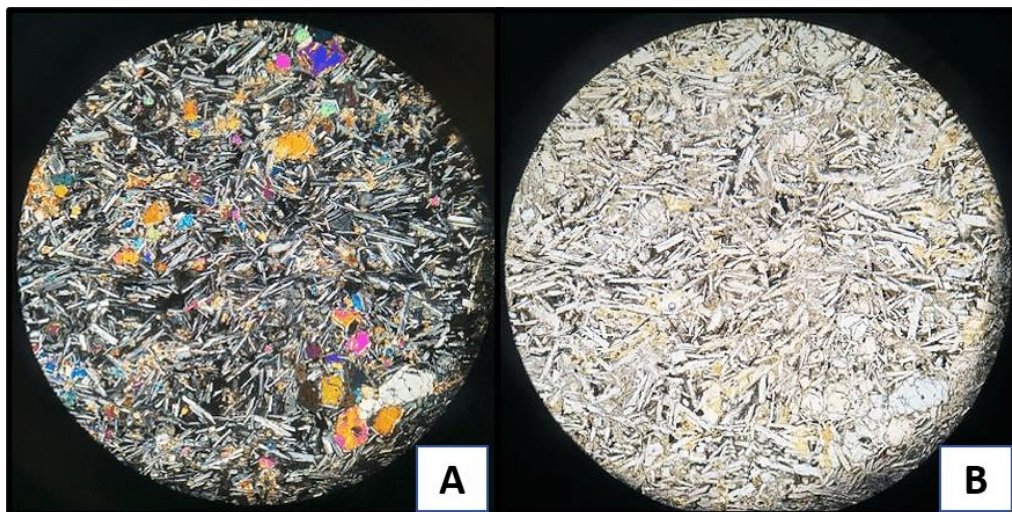


Figure 34: Basalt of the Strawberry Volcanics, sample BC19B36 in thin section. Image A is in XPL, B is in PPL, 40X optical zoom.

In thin section, olivine phenocrysts make up ~5%, and the texture is intergranular. The groundmass comprises coarse plagioclase laths with interstitial pyroxene. The coarse groundmass has no preferred alignment. Groundmass under 400X magnification and PPL conditions indicate abundant yellowish to vibrant interference colors suggesting mafic interstitial silicates are orthopyroxene and augite. One sample of basaltic andesite lava has a silica content of about 53 wt.% and a FeO* content of 9.23 wt.%. The sample contains a few large olivine phenocrysts within a microcrystalline groundmass primarily made up of plagioclase with some olivine and pyroxene (Figure 34). Hence, samples of Tbsv have a silica range of about 50 to 53 wt. % SiO₂ (Figure 35).

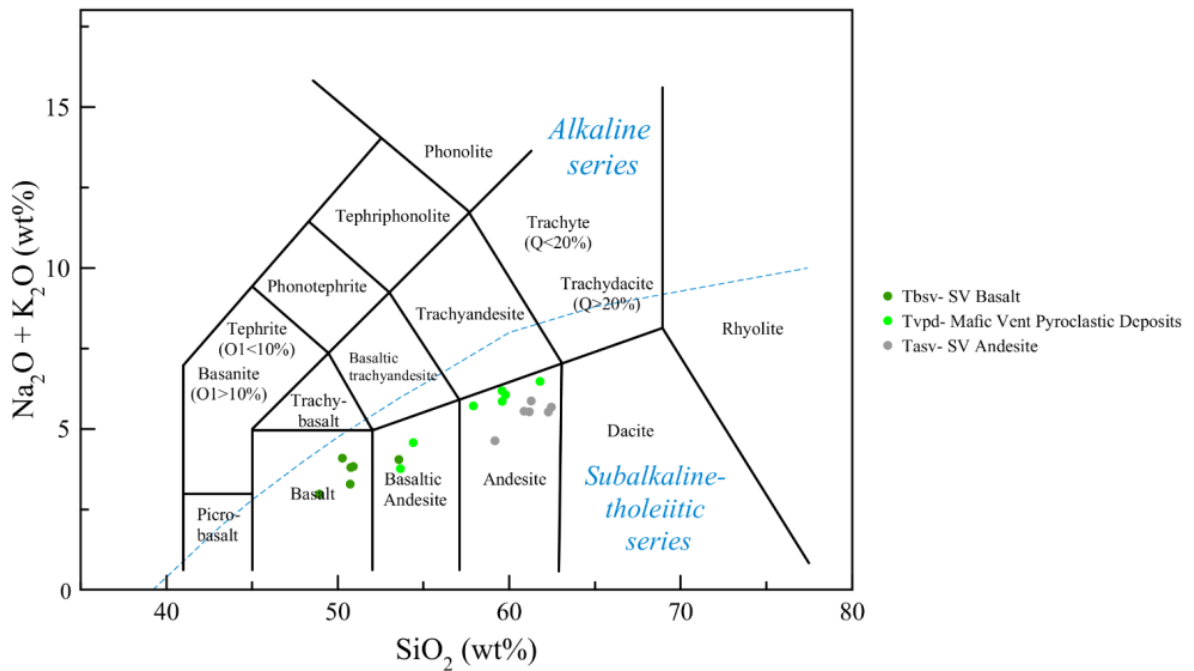


Figure 35: Total alkali-silica classification diagram displaying the samples of basaltic to andesitic compositions from this project.

4.1.4 INTERMEDIATE STRAWBERRY VOLCANICS

I. Tasv –Andesite of Strawberry Volcanics (16-12 Ma)

The andesite of the Strawberry Volcanics comprises lavas of andesitic compositions exposed throughout the entire project area. This unit includes intercalated unmappable (only sparsely distinguished or exposed in the field) basalt to basaltic andesite lavas of Tbsv. Outcrops are often platy, blocky, or smooth with conchoidal fracturing in habit with very thin plates to massive. Tasv often appears aphyric, but phenocryst content varies from aphyric to ~12%. The groundmass is defined as a very fine sugary matrix of plagioclase with little pyroxene. Plagioclase and ortho- and clinopyroxene dominate the phenocrysts in the Tasv unit. Aphyric andesite is the dominant rock lithology of Tasv of the main sequence of the southern part of the Strawberry volcanic field (Steiner and Streck, 2013). Tasv lavas occur above the oldest rhyolite of the area but are intercalated with the younger rhyolites of the Strawberry Volcanics. Analyzed samples of Tasv have a range of SiO₂ from 58 to 62 wt. % (Figure 35) and Zr content of 148 to 168 ppm. Tasv lavas are typically southward dipping at an angle of ~10 degrees, and this has been observed in the region south of Strawberry Mountain. In the northern-central region of the BC quad, an andesite dike was discovered. In the hand sample, the dike shows elongated vesicles as well as a hypabyssal texture. The andesite dike in the outcrop has near-horizontal columnar jointing and overall is about 8 m wide by 15 m long. Image A in Figure 36 is of the andesite dike outcrop located within the BC quad.



Figure 36: Photograph (A) is an andesite dike (sample BC19B45), with image B representing the dike in hand sample. Image C is from sample BC19A22 displaying a distinct lithological variant of Tasv that is fine-grained, black, and fractures conchoidally.

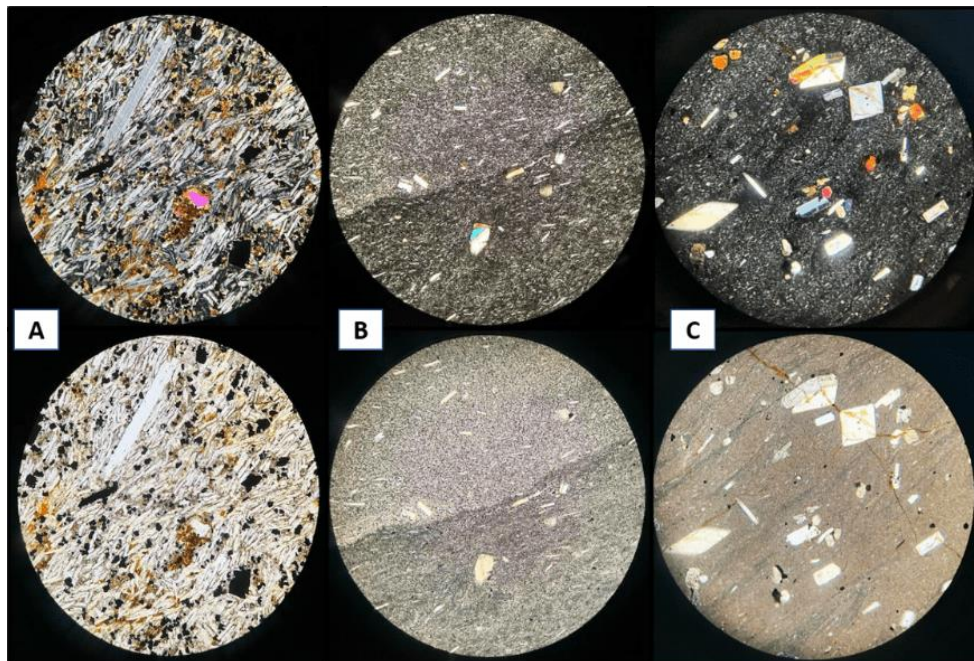


Figure 37: Sample numbers and optical zoom are as follows - (A) BC19A50 (100X), (B) BC19A22 (40X), (C) BC19C69 (40X). The top half of the photograph's thin sections are in XPL, with the bottom half in PPL.

One distinctive facies of Tasv is 'black' andesite exhibiting conchoidal fractures that make it almost appear to be glassy (image C of Figure 37). Groundmass crystals are very small and only discernible in thin sections (sample BC19A22, image B in Figure 37). The more typical Tasv (image A in Figure 37) contains <1-10% plagioclase phenocrysts with <1 mm in size set in a sugary groundmass.

II. Ttms – Tuff of Milk Spring (Mid-Miocene)

The tuff of Milk Spring is composed of different pyroclastic deposits. This unit stratigraphically overlies the rhyolite of Canyon Creek in the north-eastern region of the BC quadrangle and just below the Rhyolite of Buckhorn Spring. The unit Ttms also crops out in the southern region of JOJM and on the southwestern margin of MPT. The tuff of Milk Spring also sporadically occurs in the northwestern end of the LVW quad. The largest outcrop of the tuff of Milk Spring is located off NF909, just south of Milk Spring at the coordinates (44.034, -118.805). Overall, this unit is white to light grey in color and has a thickness range from 5 to 30 m. The depositional settings for Ttms are comprised of fallout, ash-flows, and surges, the latter of which was made up of several events. Its massive member overlies the stratified surge deposits. The observed lithics in all the lithological deposits of Ttms range from lapilli to bomb size (up to 0.5 m) and contain all the Dinner Creek Tuff units, rhyolites of the Strawberry Volcanics, obsidian, and andesite lithologies. Juvenile components of Ttms consist of glass shards, vesiculated pumice shards, and lapilli to bomb-sized pumices. The groundmass is fine-grained and non-porphyritic, and the color is light brownish gray with black to brown clasts.



Figure 38: The first image on the upper left is a finely stratified tuff of Milk Spring consisting of the surge and fallout deposits. The hand in the image measures a section of about 5cm thick. The image on the upper right is the outcrop used in the thickness model image found at the bottom of this figure. The bottom image was generated using Google Earth and knowledge of this field location in the JOJM quadrangle. Ttms outcrop in this location measures about 35 m in thickness.



Figure 39: (A)-(B) Milk Spring Tuff of the south-central region of the Jump-off Joe Mountain quadrangle. The basal surge and fallout deposits are about 1 m thick and overlain by an ignimbrite incorporating larger lithics. (C) Fallout tuff and surge deposit in a nearby section of the Milk Spring Tuff.



Figure 40: Milk Spring Tuff in hand sample BC19C56 displays lithics made up of multiple units.

The lower stratified surge deposits are thinly bedded, consisting of ash to bomb-sized pumices, smaller lithics. The surge deposits contain visible pumices and Strawberry andesite lithics in the hand sample, along with some large clasts of Dinner Creek Tuff unit 1. The estimated area for Ttms in the region is $\sim 140 \text{ km}^2$. The most evolved component of the Milk Spring Tuff is pumice clast of rhyolitic composition. However, bulk samples of the ignimbrite typically straddle the andesite/dacite transition with SiO_2 contents of ~ 61 to $64 \text{ wt.}\%$ and are iron-rich, ranging from 6.6 to $7.7 \text{ wt.}\% \text{ FeO}^*$. In the thin section, the groundmass is primarily glass with some groundmass plagioclase laths. Ttms comprises about $\sim 5\%$ plagioclase phenocrysts, glass, and seldom anhedral amphibole phenocrysts.

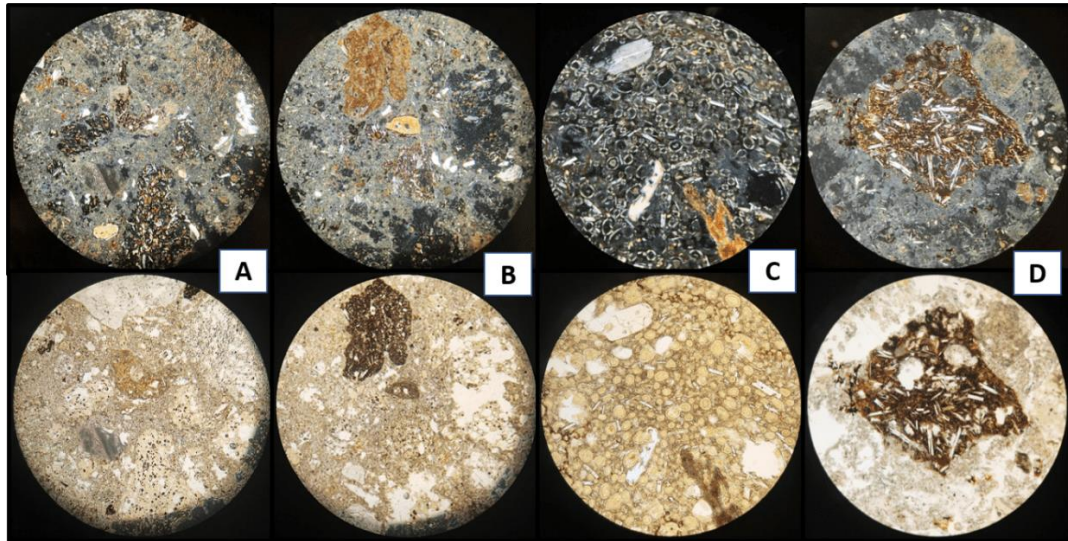


Figure 41: Milk Spring Tuff in thin section, XPL on top with PPL images on the bottom. Note prominent lithic fragments in B and C with lithologies of andesites of the Strawberry Volcanics. All images are from sample BC19C56, with A and B in 100X optical zoom. Lastly, with C and D in a 40X optical zoom.

III. Thsd – Holdout Spring Dacite (Oligocene)

Holdout Spring Dacite is found as blocks in the debris flow portion of the Mullen Spring Volcanic Clastics unit (Tmus) along NF17 in the southern region of the JOJM quad, cropping out only in small regions. This unit also crops out in the north-eastern region of LVW. One sample, MS-18-02, was geochemically analyzed and best correlated with the Oligocene dacites found in the adjacent Calamity Butte quadrangle (Cruz and Streck, 2018). Calamity Butte quad lies just south of JOJM. Holdout Spring Dacite can be greenish in color and contains large plagioclase phenocrysts up to 1 cm. The Thsd units are found in only a few outcrops confined to a small area. The estimated area for Thsd in the region is $\sim 1.4 \text{ km}^2$. In the thin section, pseudomorphs of amphibole are present, and large crystals are visibly plucked from the cut thin section. The shape of these plucked crystals that remain suggests they were likely mostly plagioclase and hornblende.

IV. Tmus – Mullen Spring Volcanic Clastics (Mid-Miocene)

Tmus crops out solely along NF17 in the southern region of the JOJM quad. This unit occurs in two depositional variants primary volcanic block and ash flow and reworked debris flow. Overall, this unit appears to be roughly the same age as the rhyolites of the Strawberry Volcanic.

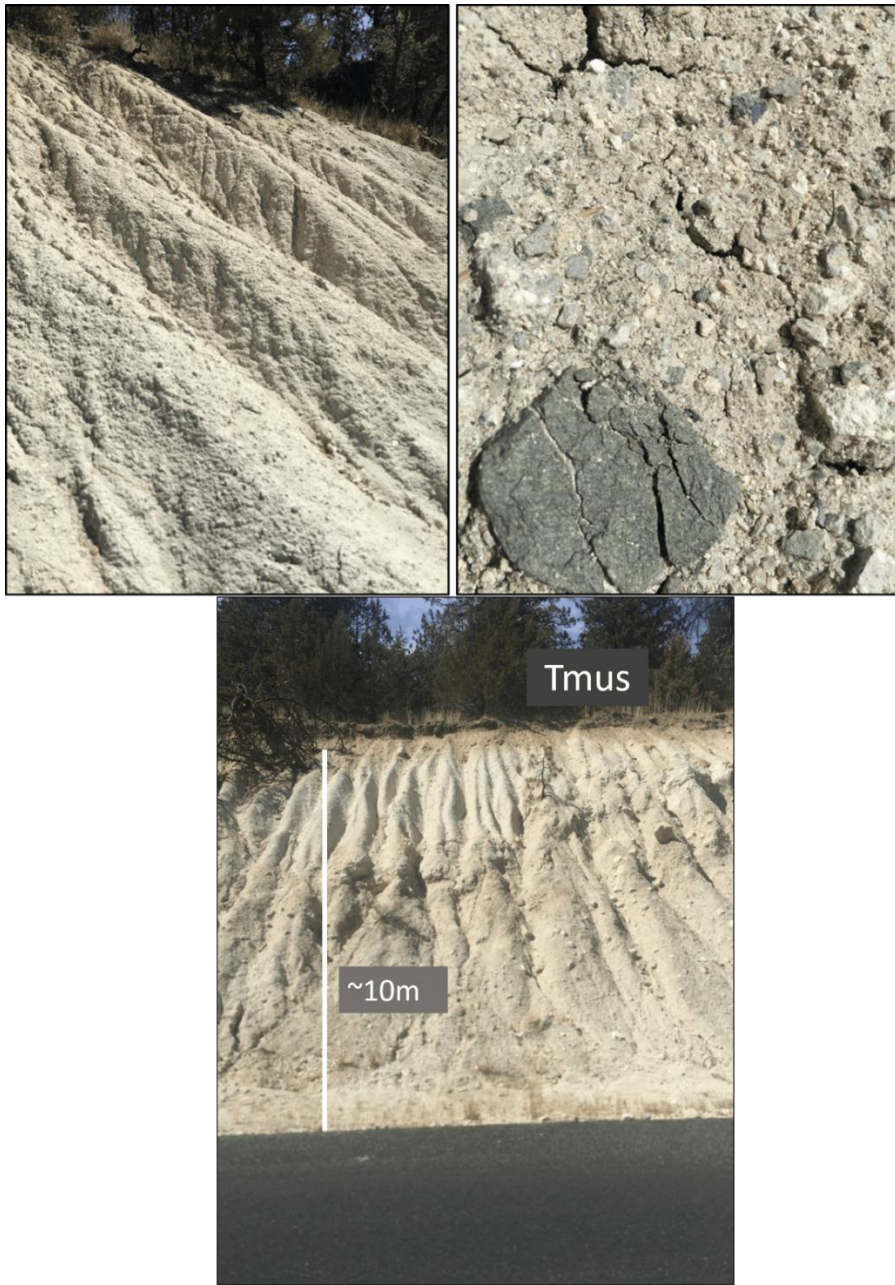


Figure 42: Left upper image is of the fine-grained epiclastic debris flow member in outcrop off NF17. The right image is a close-up image of this unit's block and ash flow member, the Mullen Spring Volcanic Clastics. The lower image is the same outcrop but detailing its unit thickness.

The block and ash flow tuff are light grey to cream in color and unconsolidated in outcrop, ranging in thickness from 8-20 m. The blocks that are within this flow unit are compositionally dacite and rhyolite. The dacite blocks are crystal-rich, containing plagioclase, where the rhyolite blocks are crystal poor. The dacite clasts belong to the unit Holdout Spring Dacite (Thsd), which is presumed to be late Oligocene in age. Charcoal chips have been identified in the block and ash flow deposit. The epiclastic debris flow member overlies the primary volcanic deposit. The estimated area for Tmus in the region is $\sim 7.5 \text{ km}^2$, producing a volume estimated at 0.1 km^3 .

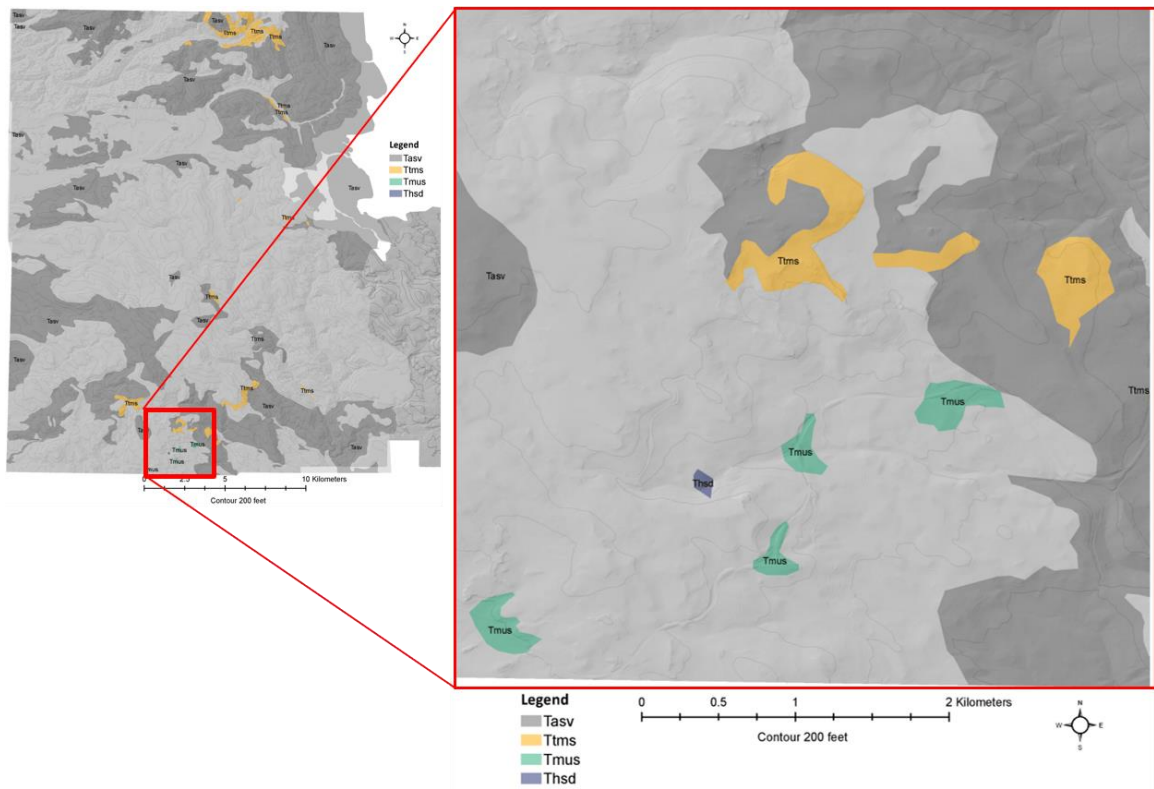


Figure 43: Geologic field map highlighting the units Tmus (pale turquoise) and the unit Thsd (purple). These units are superimposed on the entire mapped extent, with most other units greyed out, besides for Tasv and Tms for context regarding the zoomed-in image.

4.2 Lithology, Petrography, and Composition of the STRAWBERRY RHYOLITES

4.2.1 APHYRIC and PHENOCRYST POOR UNITS

I. Trtcs – Rhyolite of Three Cabin Spring (14.8 Ma)

The rhyolite of Three Cabin Spring is observed in two facies, an obsidian member and a devitrified member. These two members are often found in close proximity to one another, and both members contain virtually no phenocrysts. The devitrified portion is typically fine-grained and light grey to cream in color. The glassy member is always dense obsidian with occasional faint flow banding. The rhyolites of Three Cabin Spring in the study area were mapped and amounted to ~43 km², the second largest of all the Strawberry Rhyolite units. Whole-rock age dating by the ⁴⁰Ar/³⁹Ar method yielded a plateau age of 14.81±0.04 Ma (see Appendix).



Figure 44: Hand sample images of Three Cabin Spring rhyolite sample CD1977, on the left in devitrified facies and on the right as obsidian from the LVW quad.

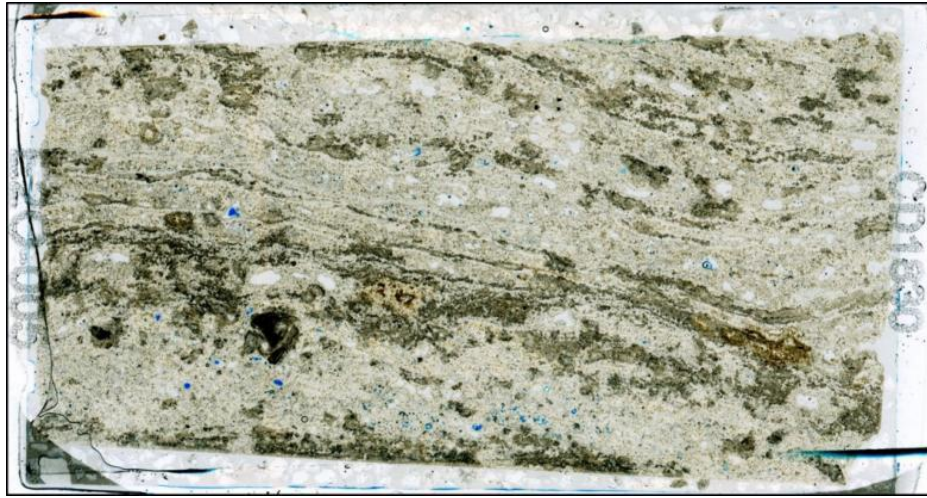


Figure 45: Thin section of a sample of devitrified Three Cabin Spring Rhyolite (Sample CD1830), with visible flow banding, in PPL.

The rhyolite of Three Cabin Spring has an average silica percentage of 77.4 wt. % SiO_2 and has an average LOI% of 0.58. Trtcs is lithologically comparable to Trcc but can be geochemically distinguished by SiO_2 , FeO^* , Y, Zr, and Sr contents. Trtcs has an average FeO^* wt.% of 0.89 and following trace element contents 26 ppm Y, 141 ppm Zr, and a Sr value of 72 ppm. Trtcs also has a distinctly high Ba value, averaging 1403 ppm, which is higher than other SR units of this study (Figure 47). Figure 48 is a plot of Nb vs. Zr and distinguishes units in this study from being I-Type or A-Type. See Figure 49 and Figure 50 for more plots of select trace elements vs. silica contents.



Figure 46: Photos are of the Rhyolite of Three Cabin Spring, the left image being from the JOJM quadrangle near Round Mountain where sample CD1875 was collected. The image on the right was generated using Google Earth and knowing where this unit crops out in the study area. This outcrop location is in the MPT quadrangle along the northwestern margin. Trtcs crops out in this location and covers the entire hillside stretching into its neighboring west quad of JOJM. Using this model, Trtcs unit thickness measures about 768m. The large size is in part a result of a fault that runs between these two locations. The fault is north-south trending and dipping to the east. A typical unit thickness will range from 40-180m.

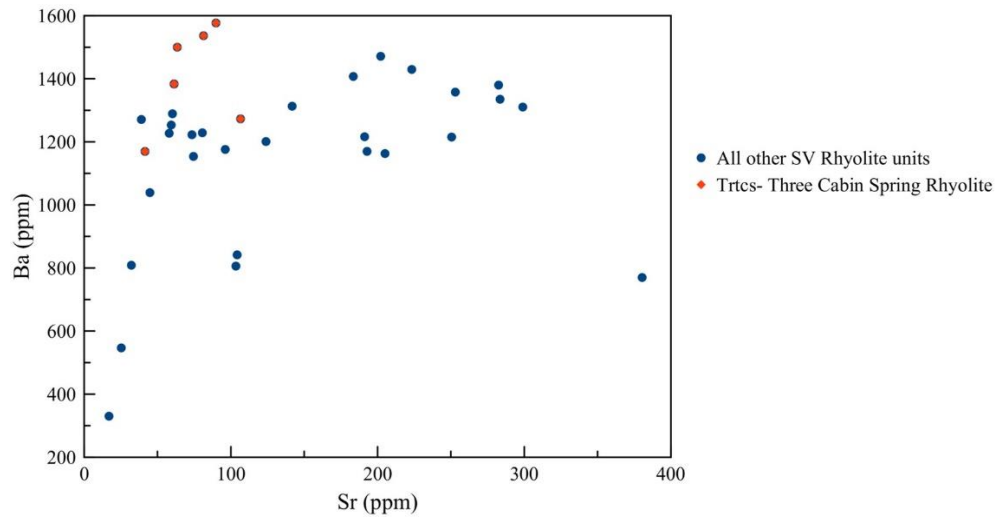


Figure 47: Ba vs. Sr variation diagram for the Strawberry Rhyolites, highlighting samples of unit Trtcs (red).

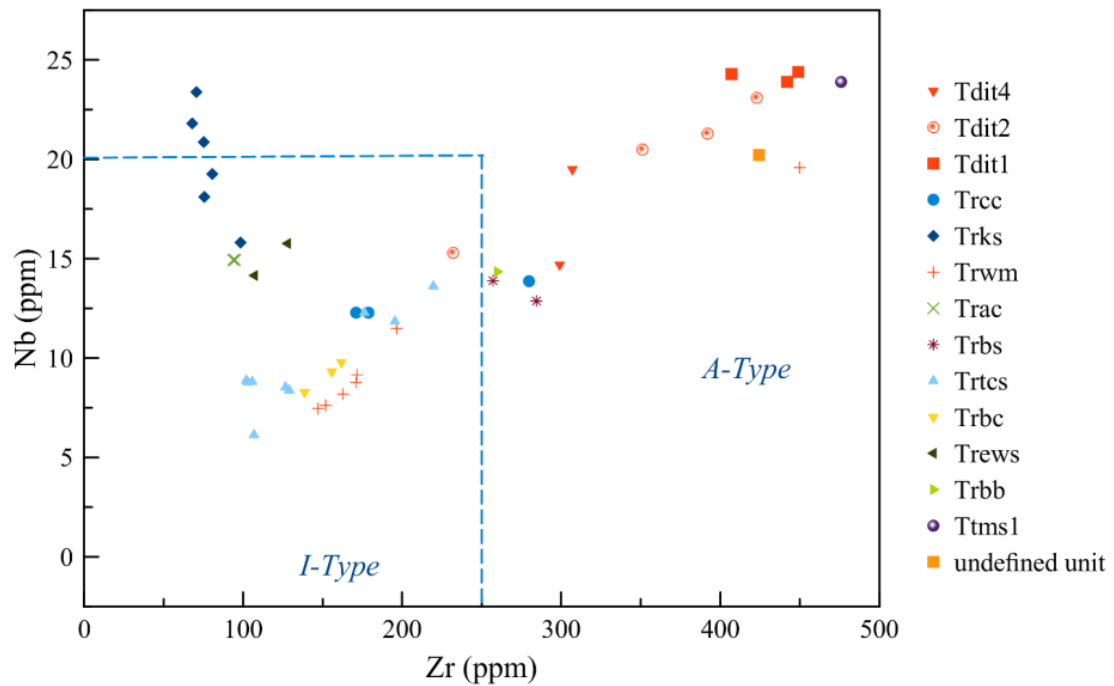


Figure 48: Nb vs. Zr variation diagram for the units found in this study. This plot classifies samples as I-type or A-type using the discrimination techniques of Whalen et al., 1987. The samples that plot outside the box have A-type affinities, and samples with Zr less than 250 ppm and Nb less than 20 ppm are classified as I-type. The coordinates of the box are X=250, Y=20. The undefined unit is regarding a (perlitic) rhyolite sample found in the MPT quadrangle. This has yet been defined as a discrete unit, as this map is still in progress by PSU graduate student Rachel Sweeten.

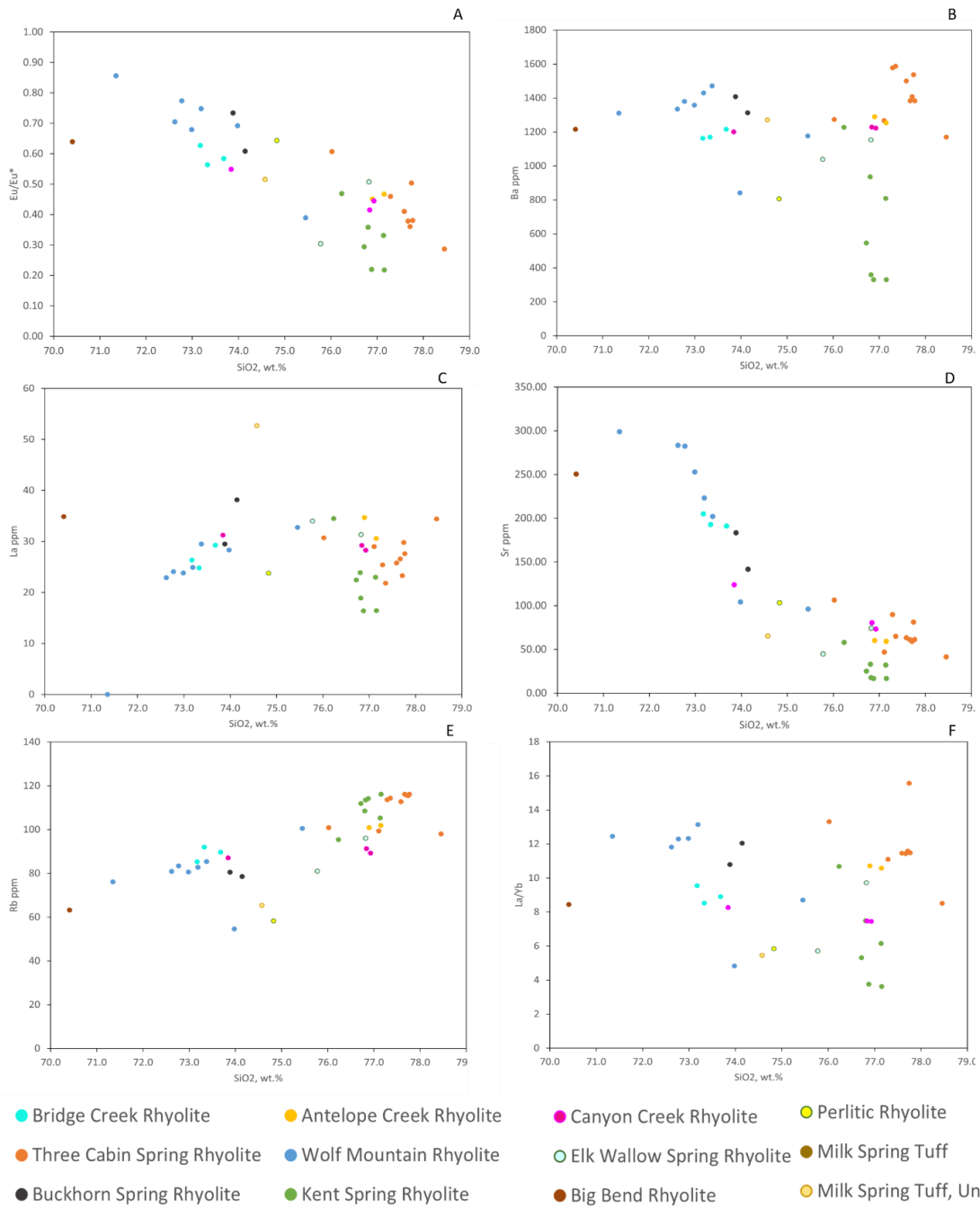


Figure 49: This figure represents plots A through F (Figure 50 with plots G through J) trace elements vs. SiO₂ wt. % plots for the SV rhyolites. Plot A: Eu/Eu* vs. SiO₂ wt. %. Plot B: Ba ppm vs. SiO₂ wt. %. Plot C: La ppm vs. SiO₂ wt. %. Plot D: Sr ppm vs. SiO₂ wt. %. Plot E: Rb ppm vs. SiO₂ wt. %. Lastly, Plot F: the ratio La/Yb ppm vs. SiO₂ wt. %.

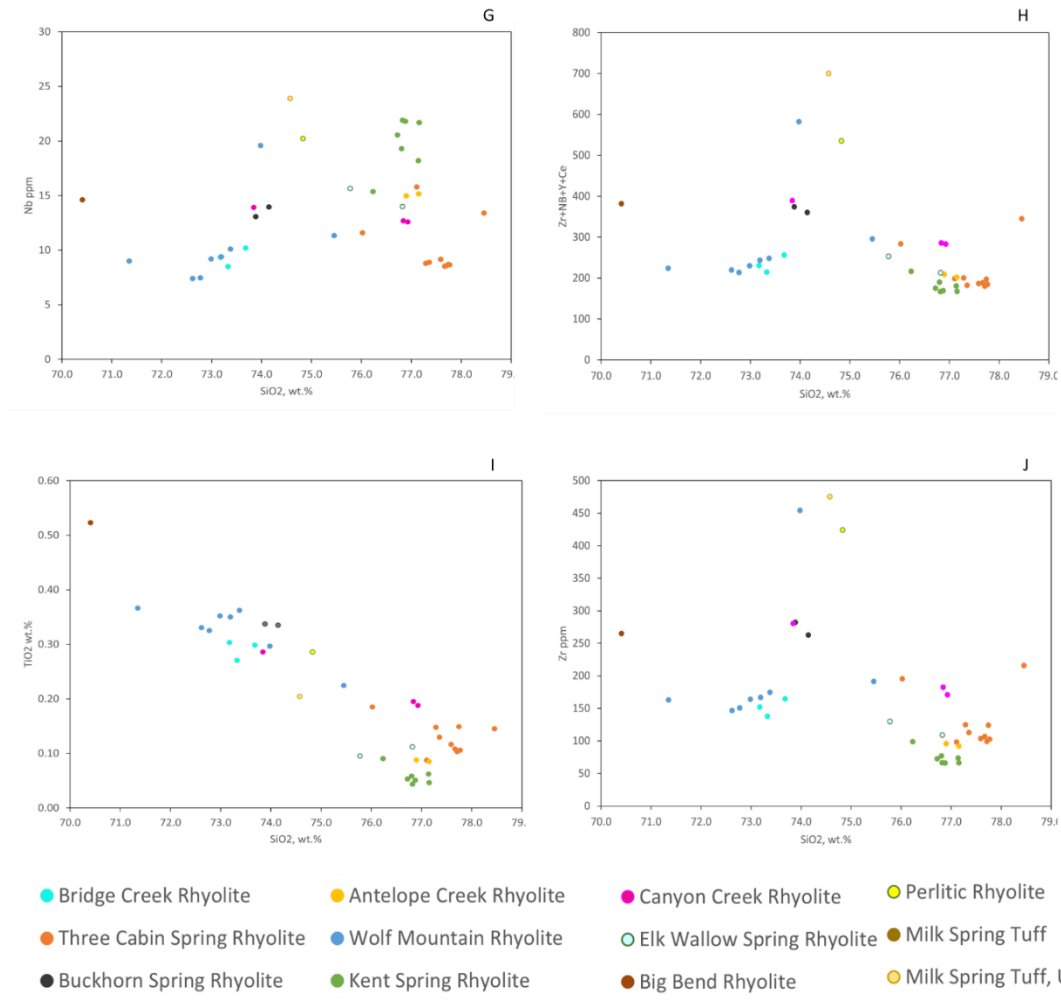


Figure 50: This figure represents G through J plots (see Figure 49 for A through F) trace elements vs. SiO₂ wt. % plots for the SV rhyolites. Plot G: Nb ppm vs. SiO₂ wt. %. Plot H: (Zr+Nb+Y+Ce) ppm vs. SiO₂ wt.%. Plot I: TiO₂ wt. % vs. SiO₂ wt. %. Lastly, Plot J: Zr ppm vs. SiO₂ wt. %.

II. Trac – Rhyolite of Antelope Creek (Mid-Miocene)

The rhyolite of Antelope Creek contains about ~4% phenocrysts. Phenocrysts consist of quartz, plagioclase, biotite, and micorphenocrysts of FeTi oxides. Samples are either devitrified and light grey in color or glassy to form obsidian. In the field, the plagioclase-

phyric obsidian that makes for a black glassy rock with white speckles is the most characteristic feature to identify this unit (Figure 51).



Figure 51: The image on the left is the obsidian member of Antelope Creek Rhyolite, and the right image is devitrified. Photos are from hand sample CD1879.

This unit crops out only sparsely in small areas along the southern border of the BC quad and the northern region of the JOJM quad. However, Trac crops out more extensively on the western side of LVW and MPT quadrangles. The devitrified member of Trac is not as abundant as its obsidian member. The area covered mapped outcrops of unit Trac is $\sim 12 \text{ km}^2$ and has a thickness of about 30-70 m. Based on two analyses of a Trac, an obsidian sample from the Jump-off Joe Mountain and the Logan Valley West quadrangles. The Antelope Creek rhyolite has a typical silica percentage of about 77% and a slightly higher Nb value of 14.9 (Figure 50).



Figure 52: Photos are from the exact outcrop location in the JOJM quadrangle where sample CD1879 was collected. The image on the left highlights the obsidian member of Trac, and the top of the hill is where its devitrified member is found. The image on the right measures from the top of the outcrop to the road, recording a thickness of 129m. Just east of this outcrop, an NW trending fault dips to the NE towards this outcrop. The fault could be accounting for some displacement thus thickness, where a typical Trac outcrop thickness ranges from 30-70m.

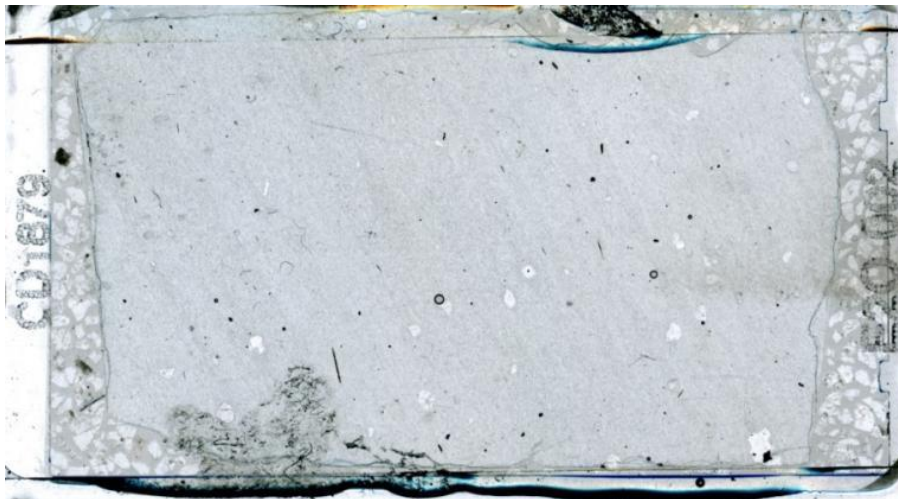


Figure 53: Obsidian of Antelope Creek rhyolite as full thin section image, showing about 4% phenocrysts, clear quartz and plagioclase, and dark shaded acicular biotite.

III. Trbs – Rhyolite of Buckhorn Spring (Mid-Miocene)

The rhyolite of Buckhorn Spring is stratigraphically one of the youngest rhyolite units of the Strawberry Volcanics and overlies the bedded fallout and ignimbrite unit of Ttms. Trbs is exclusively confined to the furthest north-eastern reaches of the BC and LVW map near its highest elevation peaks, and it reached into the quads to the north that was not mapped. Trbs is light in color. Generally, a pale pink to purple with elongated white streaks along the rocks parallel-spaced fractures and portrays faint flow bands. Hand samples are devitrified with little to no clearly visible phenocrysts. The mapped outcrop area for Trbs is $\sim 1 \text{ km}^2$ with a unit thickness of about 20-120 m.

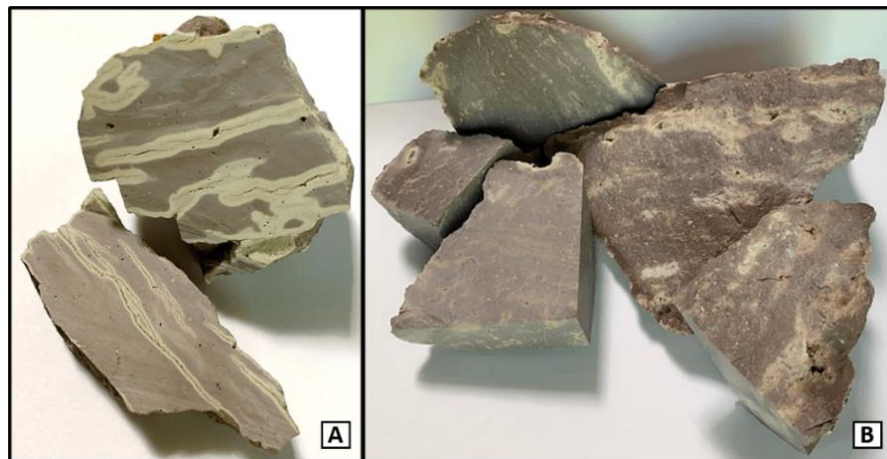


Figure 54: Hand samples of rhyolite of Buckhorn Spring unit (A) BC19C30 sample and (B) BC19C37 sample.

The sample BC19C30 was used for petrographic analysis. In thin section, the groundmass is devitrified with aligned groundmass crystals indicating flow banding. Phenocryst content is low, less than 2% consisting of plagioclase. The average silica percentage of devitrified Trbs is 74% wt. SiO_2 and has a LOI% of 1.08.



Figure 55: This image representing Trbs highlights this unit's highest peak and most exposed region in the BC quadrangle. About 1km west of this peak, a fault runs north-south for about 7km in length, dipping east. This extensional faulting and the youth of the Trbs unit itself would account for its significant cliffside exposures. Trbs typically has a thickness of about 20-120m.

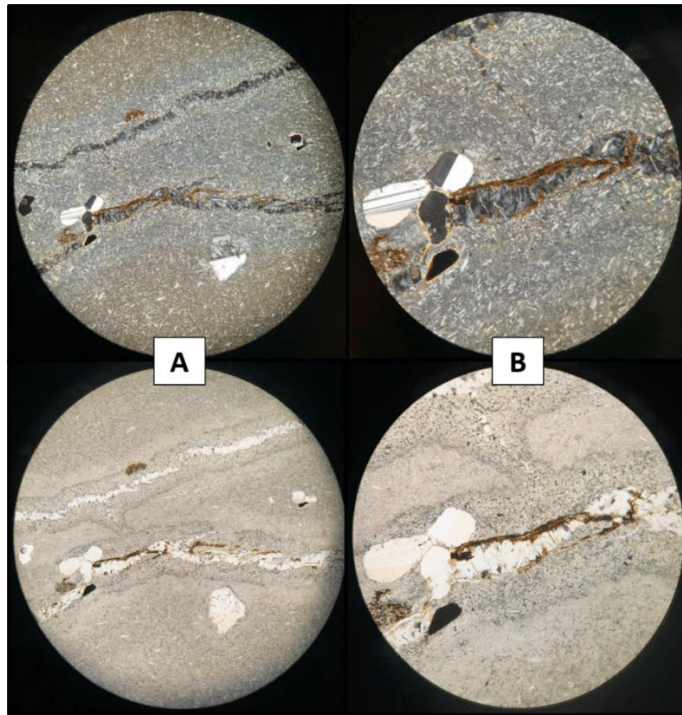


Figure 56: Images of the Rhyolite of Buckhorn Spring in thin section from sample BC19C30. The row of images on top is represented in XPL, and the bottom row is in PPL. Image (A) is in 100X optical zoom, with (B) in 40X optical zoom.

IV. Trcc – Rhyolite of Canyon Creek (Mid-Miocene)

The rhyolite of Canyon Creek crops out strictly in the northern half of the BC and LVW quadrangles and is possibly the best-exposed rhyolite unit in the region. Outcrops of this unit strike east-west, a thin layer of Trcc is found mainly as float that appears at an elevation of roughly 5000 ft in the far north-eastern region of BC quad. Trcc lies stratigraphically below the andesite and basalt to basaltic andesite of the Strawberry Volcanics (Tasv, Tbsv). Lavas of Tasv and Tbsv appear to fill a paleotopography that Trcc created, likely enhanced by erosional processes. Samples of rhyolite of Canyon Creek are light gray-purple color and devitrified, often exhibiting flow banding with some yellow secondary staining.

Rhyolite breccia can be found at the base or top of these outcrops. This is also where the glassy facies of Trcc appears either as dense obsidian or more porous, perlitic rhyolite. Devitrified and glassy samples are aphyric to extremely phenocryst poor. The thickness of Trcc can be up to ~100 m, forming large cliff faces that likely extend below the canyon bottom. The mapped outcrops for Trcc amounts to ~6 km².



Figure 57: Outcrop of rhyolite of Canyon Creek located in the map's furthest north-eastern corner (sample CD1943).

One devitrified thin section of Trcc (sample BC19A11) consists of very fine groundmass crystals. Some of these crystals are aligned, indicating flow banding. The rhyolite contains scarce mono- and polymineralic glomerocrysts. Geochemical analysis of three samples indicates an average of 75.9 SiO₂ wt.%.

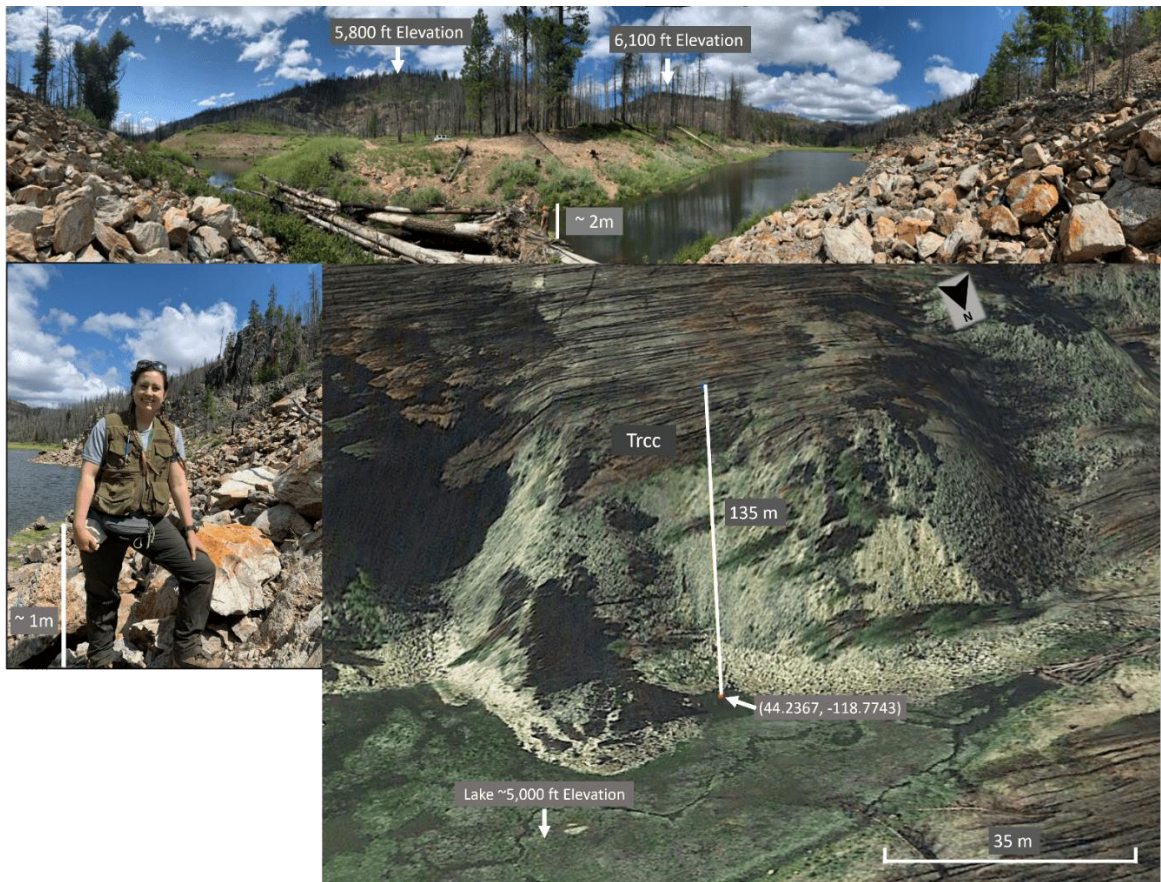


Figure 58: These images represent the rhyolite of Canyon Creek. This unit is very well exposed as it lies on a fault that runs north-south for about 7km in length and dips to the east. The east block, which incorporated the unit Trcc and its outcrop pictured, has also formed a lake in its offset. The top image shows the lake meeting Trcc in outcrop. The bottom right map was generated in Google Earth to measure the unit's exposure. The unit thickness measurement occurred from the south side of the lake to the adjoining peak. Its thickness measures 135 m, which is an accurate high range thickness value for Trcc.

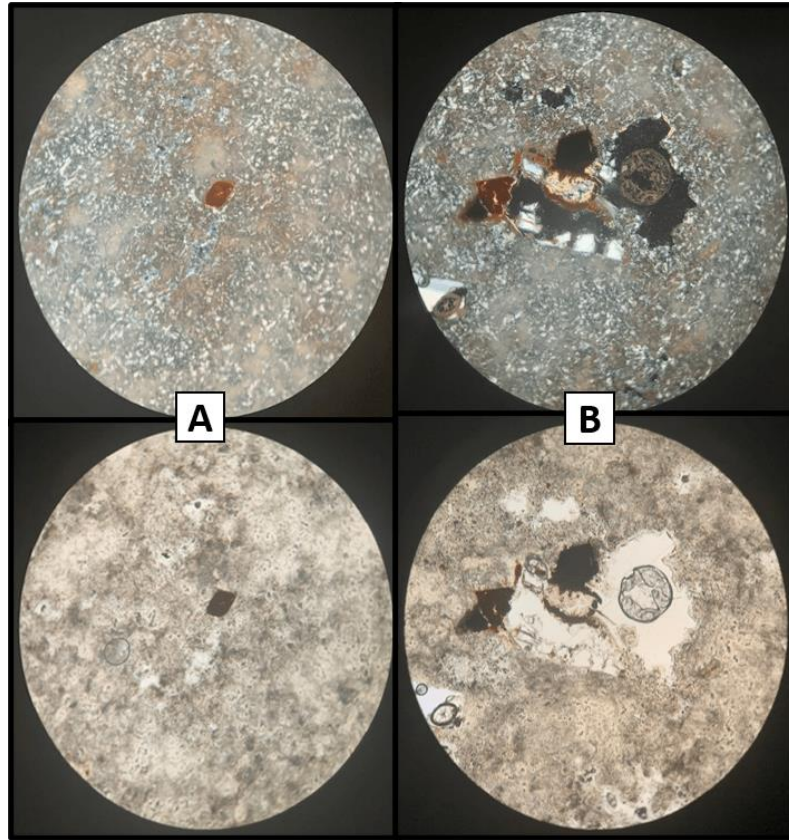


Figure 59: Thin section images of Canyon Creek rhyolite from float sample BC19A11 with images in XPL on top and PPL at the bottom (A) in 100X optical zoom and (B) in 40X optical zoom.

V. Trks – Rhyolite of Kent Spring (14.4 Ma)

Rhyolite of Kent Spring is a crystal poor rhyolite that crops out largely in the central region of the entire mapping region. This unit is only seen in this portion of the mapping area and is distinguishable by the presence of amphibole and its low phenocryst content. The outcrops mapped in the field for Trks amount to $\sim 22 \text{ km}^2$ with a unit thickness range of 40-200 m. Glassy samples are typically porous with a dull luster and have a light grey groundmass with 1% amphibole and $\sim 1\%$ plagioclase phenocrysts. The Ba ppm concentration of samples of Trks trends towards the lower concentrations with slightly increased SiO_2 (Plot B of Figure

49), suggesting that alkali feldspar just started to crystallize. Samples of this unit typically yield a silica content of ~ 77 wt. % SiO_2 . Single crystal age dating by the $^{40}\text{Ar}/^{39}\text{Ar}$ method on plagioclase from sample CD1975 yielded an age of 14.37 ± 0.02 Ma (see Appendix).



Figure 60: Kent Spring rhyolite (CD1932). Overall, the unit is crystal poor and distinguishable by the presence of amphibole.

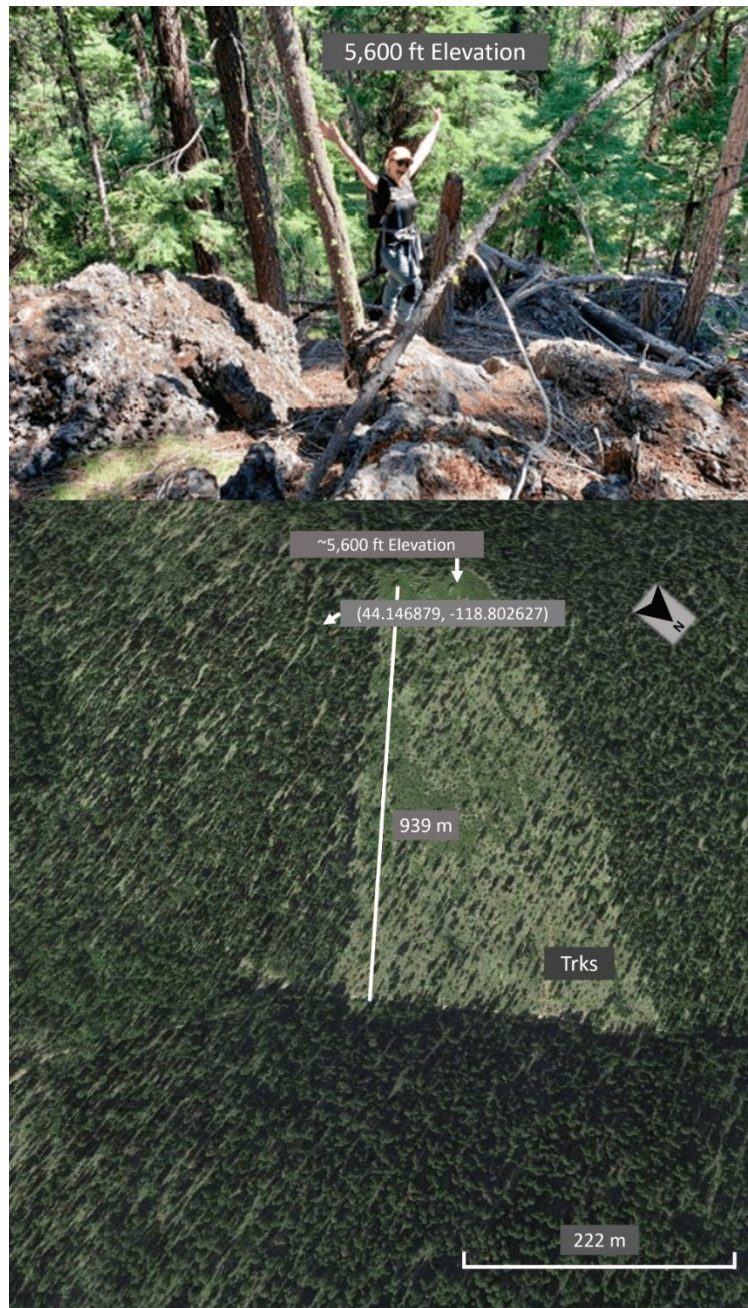


Figure 61: These images represent the rhyolite of Kent Spring and its amount of exposure due to faulting in the region. Both images are from the same outcrop, located in the far SE of the BC quadrangle. Four north-south trending faults intersect this unit in an east-dipping extensional domino effect, generating considerable exposure. With Trks remaining relatively local to this area, its typical maximum unit thickness is about 200m. The map image was produced on Google Earth along with geologic mapping knowledge of the region.

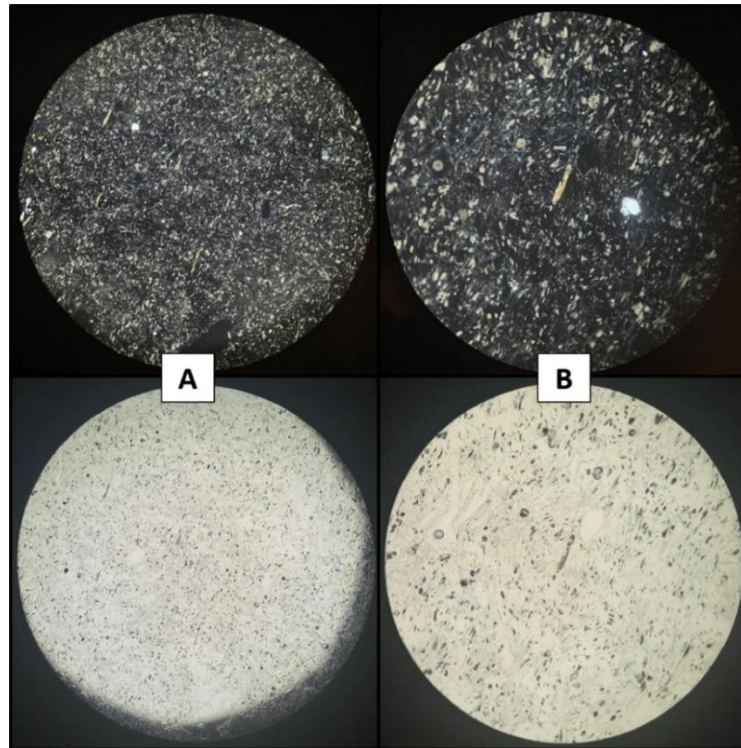


Figure 62: Thin section images of Kent Spring rhyolite sample CD1932. The top row of images is in XPL, and the bottom row is in PPL. Image (A) is in 40X optical zoom, whereas (B) is in 100X optical zoom, shown crystal poor nature with about 1% amphibole crystals.

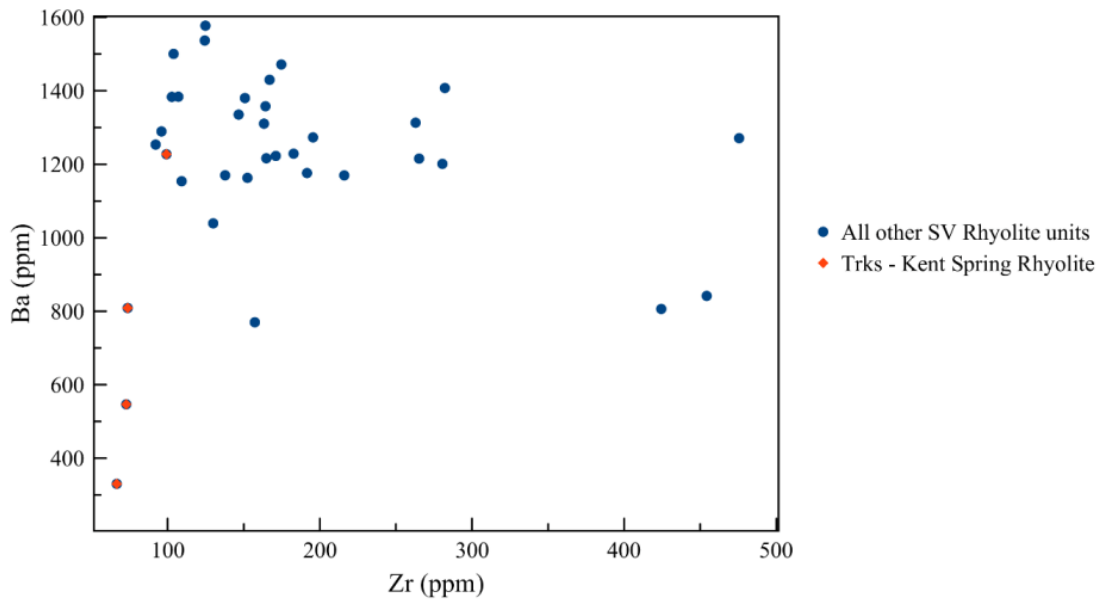


Figure 63: Ba vs. Zr variation diagram for the Strawberry Rhyolites, highlighting samples of unit Trks (red). The unit Trks has a distinctly lower Zr ppm than the other SR units.

VI. Trews – Rhyolite of Elk Wallow Spring (Mid-Miocene)

The rhyolite of Elk Wallow Spring is found in the southwestern region of LVW and primarily in the northwestern half of MPT quads. Trews is found in outcrop to be vitric to often devitrified with flow banding. The mapped outcrop area for Trews is $\sim 17 \text{ km}^2$ with a unit thickness up to 200 m.



Figure 64: The image is of the Rhyolite of Elk Wallow Spring, where the highest elevation is atop Glass Mountain in MPT and is the sample location for RS20MPT03. The map image was generated using Google Earth and used knowledge of where this unit crops out in the study area. Trews crops out in this location and covers this entire, overall wedged between Trtcs and Trac. Using this model, Trews unit thickness measures about 488m. The measurement of the unit may have a deviation as many faults that trend north-south just to the east of this location, crossing into neighboring quads of JOJM and BC. The faults are dipping to the east, generating domino extensional features. A typical unit thickness will range from 40-200m, making sense for this unit's location in the study area.

This rhyolite contains about 2-4% phenocrysts. Phenocrysts include plagioclase, quartz, amphibole, and lesser biotite. Amphibole can be quite large, 1-4mm euhedral to sub-euhedral grains (Figure 66). The biotite phenocrysts occasionally contain zircon inclusions. Outcrops of Trews are typically massive to slaty and fissile, with a tendency to be white to dark gray in color. A sample of this unit typically yields a silica content of around 76 wt. % SiO₂. This unit differs from that of Trbc by its strontium and zirconium concentrations (Figure 67). With Trews averaging about 59 ppm of Sr and 118 ppm of Zr, where Trbc is more than three times that amount for Sr at about 196 ppm and has a value of 152 ppm of Zr.



Figure 65: Hand sample of the rhyolite of Elk Wallow Spring. This sample is from the top of Glass Mountain in the Magpie Table quadrangle (RS20MPT03).

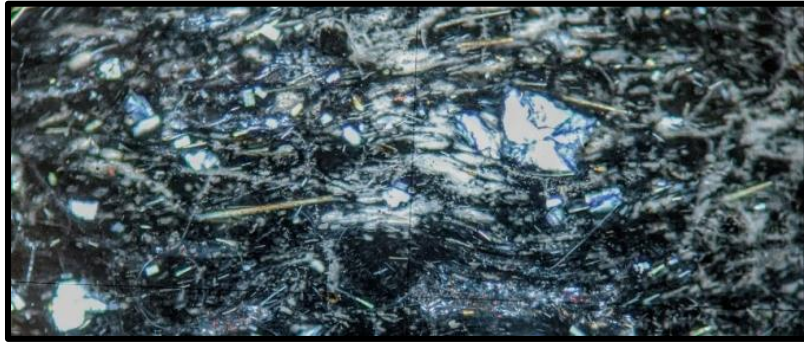


Figure 66: Petrographic thin section of Trews from the MPT quadrangle. Flow banded, with prominent acicular phenocrysts of hornblende and plagioclase phenocrysts in a glassy, flow banded groundmass.

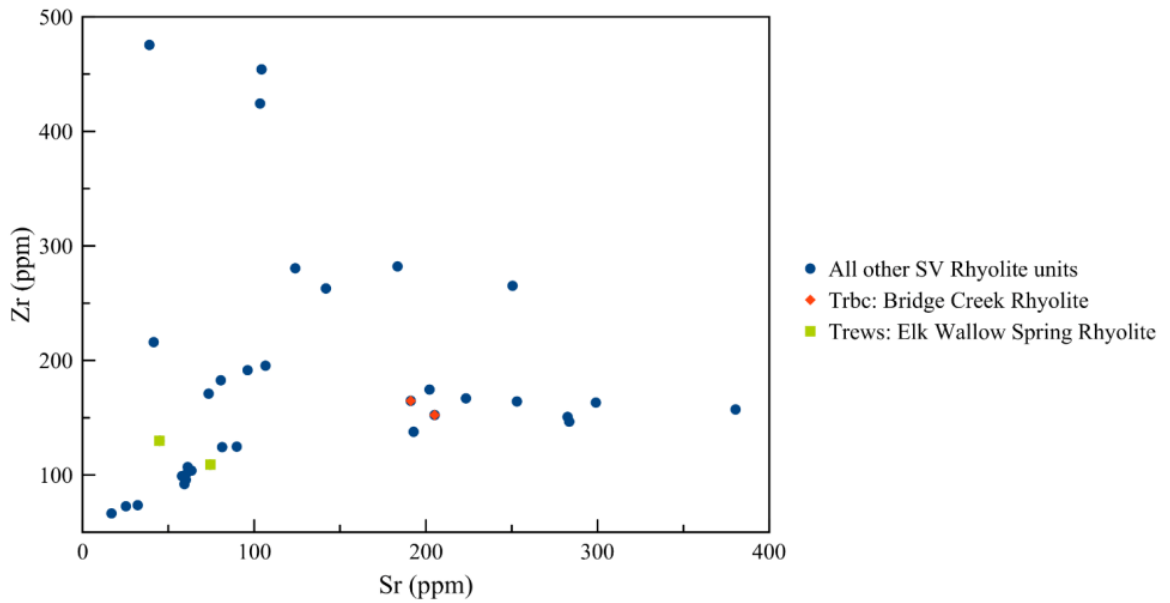


Figure 67: Zr vs. Sr variation diagram for the Strawberry Rhyolites, highlighting unit Trews (green) and Trbc (red) samples. The unit Trews and Trbc are lithologically similar but can be differentiated by their trace elements. Specifically, Zr and Sr, where the unit Trews has an overall lower Zr and Sr trace element concentration than the unit Trbc.

VII. Trbb – Rhyolite of Big Bend (Mid-Miocene)

The rhyolite of Big Bend is only found in a small region in the southwestern region of the LVW quadrangle near the Big Bend drainage area, where it clearly overlies Tasv andesitic lavas and thus appears to be one of the younger rhyolites. In outcrop, this rhyolite was most often found to be highly weathered. Outcrops varied between massive and platy and often appeared to have spherulites covering the surface. This unit is typically light gray in color with occasional elongated vesicles indicative of flow. The field mapped outcrops for Trbb amount to $\sim 0.9 \text{ km}^2$ and has a thickness range of 20-40 m. Distinct from Trtcs and Trbs, this unit contains about 4% of large (2-3 mm) plagioclase phenocrysts and pseudomorphs after pyroxene within a fine-grained groundmass (Figure 68 and Figure 69). Geochemical analysis of this unit, sample LVW-N2-2, has a silica content of 70.4 wt.% SiO_2 .

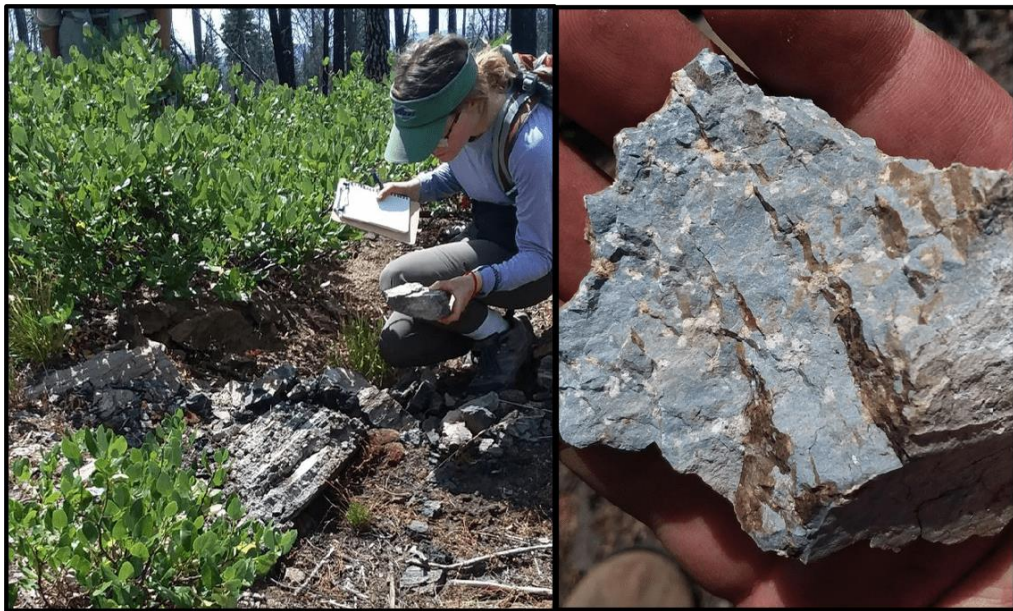


Figure 68: The image on the left is a typical outcrop of Trbb. The image on the right is a classic representation of this units' phenocrysts percentage.



Figure 69: Image is of the Rhyolite of Big Bend; the map image was generated using Google Earth and by using knowledge of where this unit crops out in the study area. Trbb crops out in this location and overall only in a small portion throughout the entire map, ~1km². Using this model, Trbb unit thickness measures about 1,039m at maximum. This area is in close proximity to Bear Creek. Large alluvium-filled meadow and creek. Directly to the west, in the quadrangle BC, there are a couple of outlier faults that trend from east to south, where all other faults in the region tend to be normal faults. I suspect that this potentially active faulting is the cause of this rather large unit thickness. Especially regarding Trbb is one of the younger, if not youngest SR unit.

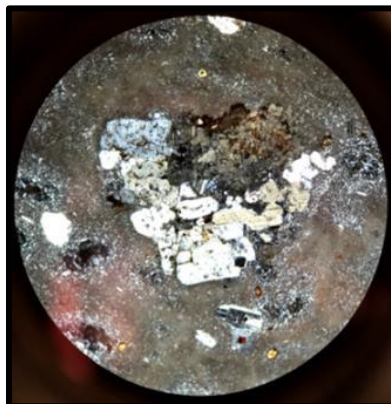


Figure 70: Thin section image of unit Trbb in XPL from sample LVW-N-19. The thin section image features a very fine-grained matrix encompassing glomerocrysts.

4.2.2 PHENOCRYST RICH UNITS

I. Trbc – Rhyolite of Bridge Creek (14.7- 14.3 Ma)

The rhyolite unit of Bridge Creek was observed primarily along the western margins of the JOJM quadrangle. Outcrops are typically large and blocky (Figure 71). They range in color from pinkish to medium gray, depending on the amount of devitrification. When Trbc is found in outcrop as glassy, samples are light and porous and do not form an obsidian member. The actual mapped outcrop area from the field for Trbc is $\sim 20 \text{ km}^2$ with a thickness up to 100 m.



Figure 70: (A) Hand sample of Trbc, devitrified with amphibole and biotite, clearly visible. (B) Vitric hand sample of Trbc, outcrop just south of Che Spring in JOJM. (C) A smaller outcrop of the Bridge Creek Rhyolite is consistently found amongst a sizeable blocky and more extensive outcrop.

Samples of Trbc contain about 10-20% phenocrysts. The most abundant phase is complexly zoned plagioclase 8-15% plagioclase, about subequal amounts of biotite and amphibole make up about 3-5% and lesser orthopyroxene and FeTi oxides. When devitrified, there are only pseudomorphs after pyroxene. In addition, there are rare phenocryst-size quartz crystals (< 5 per thin section). Trbc has an average silica content of 73.4 wt. % SiO₂. Figure 67 shows the trace elements of Zr ppm plotted vs. Sr ppm. This trace element plot differentiates Trbc from unit Trews with biotite and amphibole phenocrysts as found in Trbc (Figure 71).

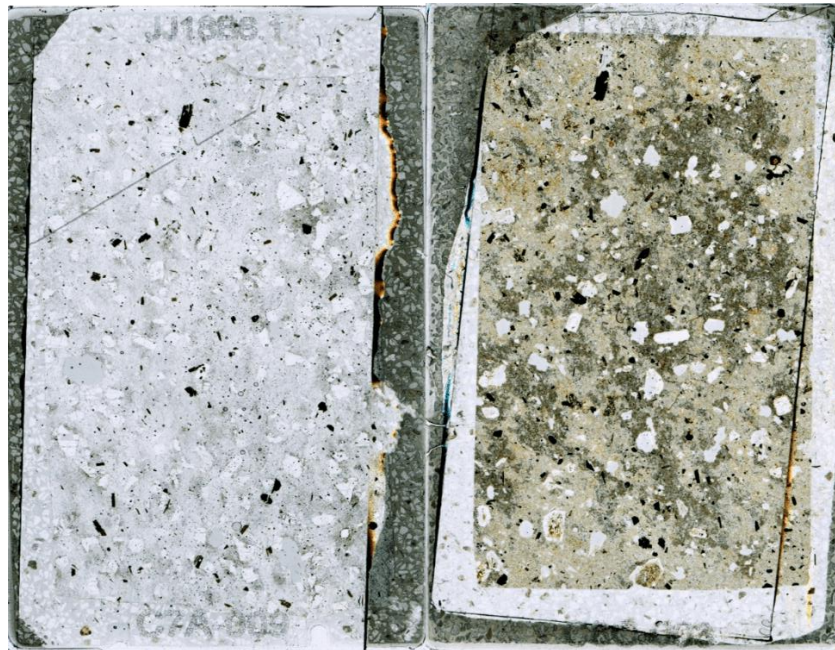


Figure 72: Thin section of the Rhyolite of Bridge Creek. Full slide images, the left is in PPL, and the right image is in XPL, from sample JJ18A257. The thin section highlights the abundance of clearly visible biotite and amphibole crystals, making up about 3%, with about 8% plagioclase.



Figure 73: Photos are of the Rhyolite of Bridge Creek (formerly known as the unit Tsvr in the 2019 JOJM map). The left image is from the JOJM quadrangle, NW of Bond Spring. The image on the right was generated using Google Earth and subsequent knowledge of this unit within the study area. The majority of Trbc crops out in this location covering the entire hill, continuously reaching the NE and SW, covering a stretch of ~7km. Using this model and a prominent location of a continuous outcrop of Trbc, its unit thickness measures about 785m. The sizeable unit thickness estimate is likely due to the extensional faulting throughout the region, exposing a substantial face of Trbc. Thus, a typical unit thickness will range from 40-100m.

II. Trwm – Rhyolite of Wolf Mountain (16.1–15 Ma)

Rhyolite of Wolf Mountain is found extensively in the eastern half of the JOJM and the western margin of MPT quadrangles. Trwm is also found in a relatively small area within the BC map, and its plagioclase phenocrysts tend to remain relatively small in size but abundant in quantity. This rhyolite is distinct in how crystal-rich it is, ranging from 20-30% plagioclase. Flow banding is also prevalent, with bands consisting of pink to grey colors (Figure 74). Hand samples of Wolf Mountain rhyolite are dark to light grey when glassy or devitrified or

are exclusively pinkish in color when devitrified. The outcrops mapped in the field for Trwm amount to $\sim 59 \text{ km}^2$, being the largest rhyolite in the project area and has a unit thickness up to 200 m.



Figure 74: Wolf Mountain rhyolite in outcrop and as hand sample (CD1921).

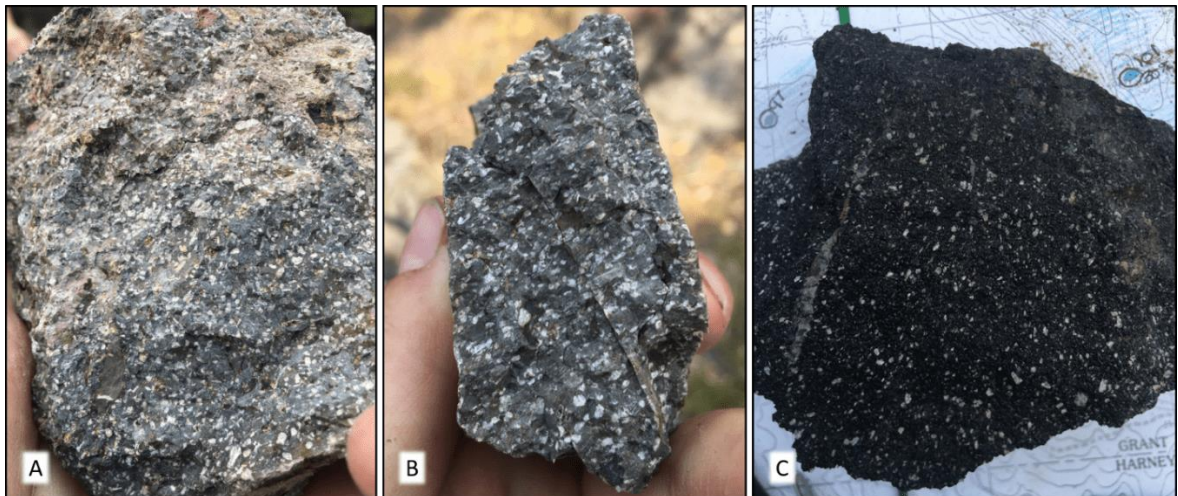


Figure 75: Wolf Mountain rhyolite in hand sample. From (A) to (C), the samples go from non-glassy to glassy. Each variety is of the 30% phenocryst-rich variety found in the Jump-off Joe Mountain quadrangle.

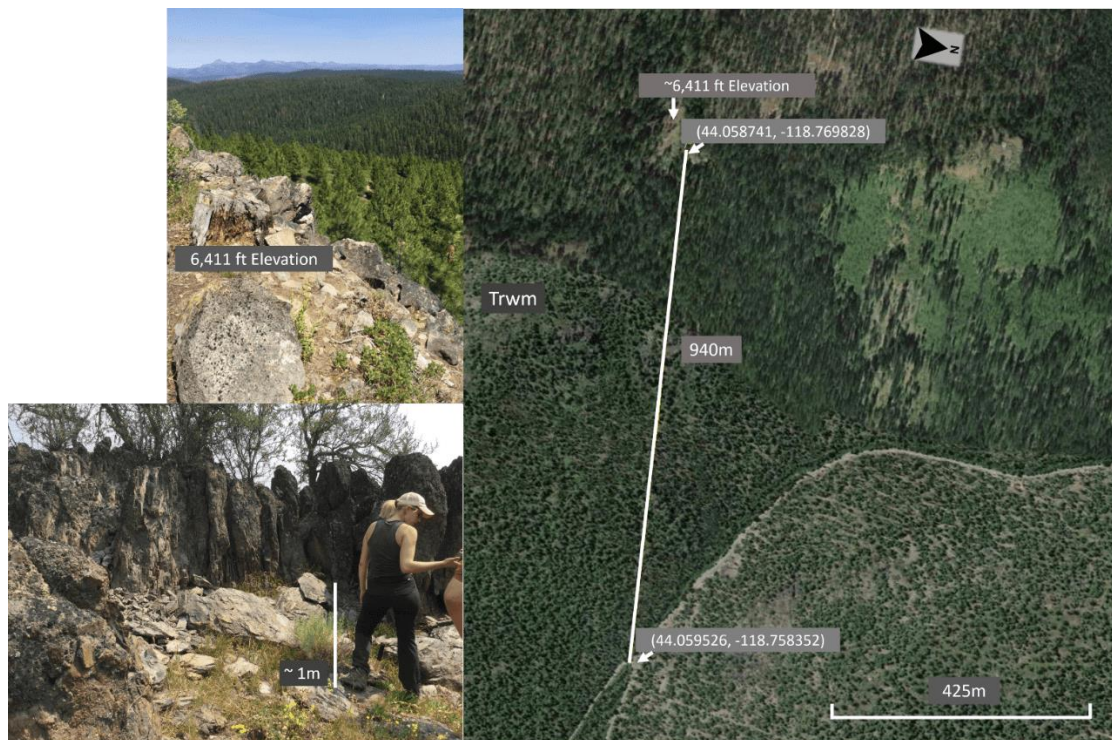


Figure 76: Photos are all from the Rhyolite of Wolf Mountain and are indeed from the south-eastern side of Wolf Mountain in the JOJM quadrangle. The image on the right was generated using Google Earth using knowledge of this unit in the study area. The majority of Trwm crops out to the South in JOJM and the east in MPT quads. By using this model, the unit Trwm thickness measures about 940m. The sizeable, estimated thickness is partly due to the north-south trending fault that dips east and runs directly through this section. In addition, the exposed Trwm is exceptional due to the extensional faulting, exposing a prominent face of Trbc. A typical unit outcrop thickness, however, remains rather large, ranging from 50-200m.

In the thin section (Figure 77), flow banding is visible in the groundmass. Phenocrysts consisted of large plagioclase (clearly seen in the hand sample) and some altered pyroxene. Pyroxene crystals are fresh in glassy samples. The groundmass can be glassy or devitrified. This unit does not contain amphibole, which distinguishes it from unit Trbc. In the north of JOJM, very glassy Trwm crops out. In thin section, the sample CD1883 exhibits fresh pyroxene and perlitic cracks. Trwm has a silica content of 73 wt. % SiO₂, and the highest

overall Sr contents are yielding an average of ~ 284 ppm Sr (represented in Plot D of Figure 49), inferring that Trwm is the least fractionated SR unit.

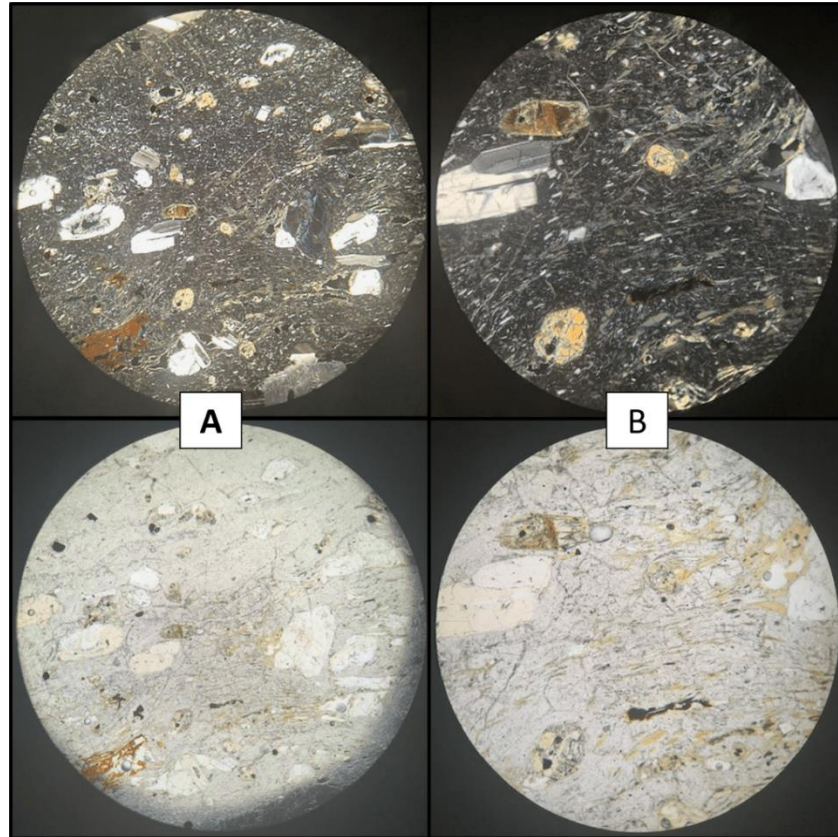



Figure 77: Thin section images from sample CD1964. The top row exhibits XPL, while the bottom row is in PPL. Image (A) is in 40X optical zoom, with (B) in 100X optical zoom.

4.3 DISTRIBUTION of RHYOLITES

The Strawberry Rhyolites of this study cover a field-mapped area with a total sum of about 182 km^2 . However, the mapped areas likely do not capture the full original distribution. In Figure 78 and Table 1, I present the estimated original distribution area for each rhyolite unit. These estimated areas sum up to a total of 386 km^2 . Using these estimated areas from Table 1, the largest rhyolite unit is Wolf Mountain (Trwm), covering about 170 km^2 , followed

by the rhyolite of Three Cabin Spring (Trtcs) at $\sim 158 \text{ km}^2$. The smallest estimated area is from the rhyolite of Big Bend (Trbb), covering an area of about 8 km^2 . Trwm and Trtcs remain in close proximity to one another and make up the large central portion of the mapped region. The tuff of Milk Spring (Ttms) follows in the third-largest estimated area, at a value of about 140 km^2 . Ttms is widely distributed throughout the entire project area, yielding a relatively large overall area.

Table 1: Calculated distribution area, from largest to smallest of Strawberry rhyolitic units. The area in this table is based on the estimated size of each unit (Figure 78) and the geometry of the polygons generated in ArcMap from the final map produced from fieldwork in this study.

Unit Name		Rhyolite Area Distribution (Km2)		
Trwm	Wolf Mountain Rhyolite	170	Largest Area	
Trtcs	Three Canyon Spring Rhyolite	157		
Ttms	Milk Spring Tuff	139		
Trews	Elk Wallow Spring Rhyolite	73		
Trac	Antelope Creek Rhyolite	69		
Trcc	Canyon Creek Rhyolite	58		
Trbc	Bridge Creek Rhyolite	54		
Trks	Kent Spring Rhyolite	51		
Trbs	Buckhorn Spring Rhyolite	9.9		
Trbb	Big Bend Rhyolite	7.6		Smallest Area

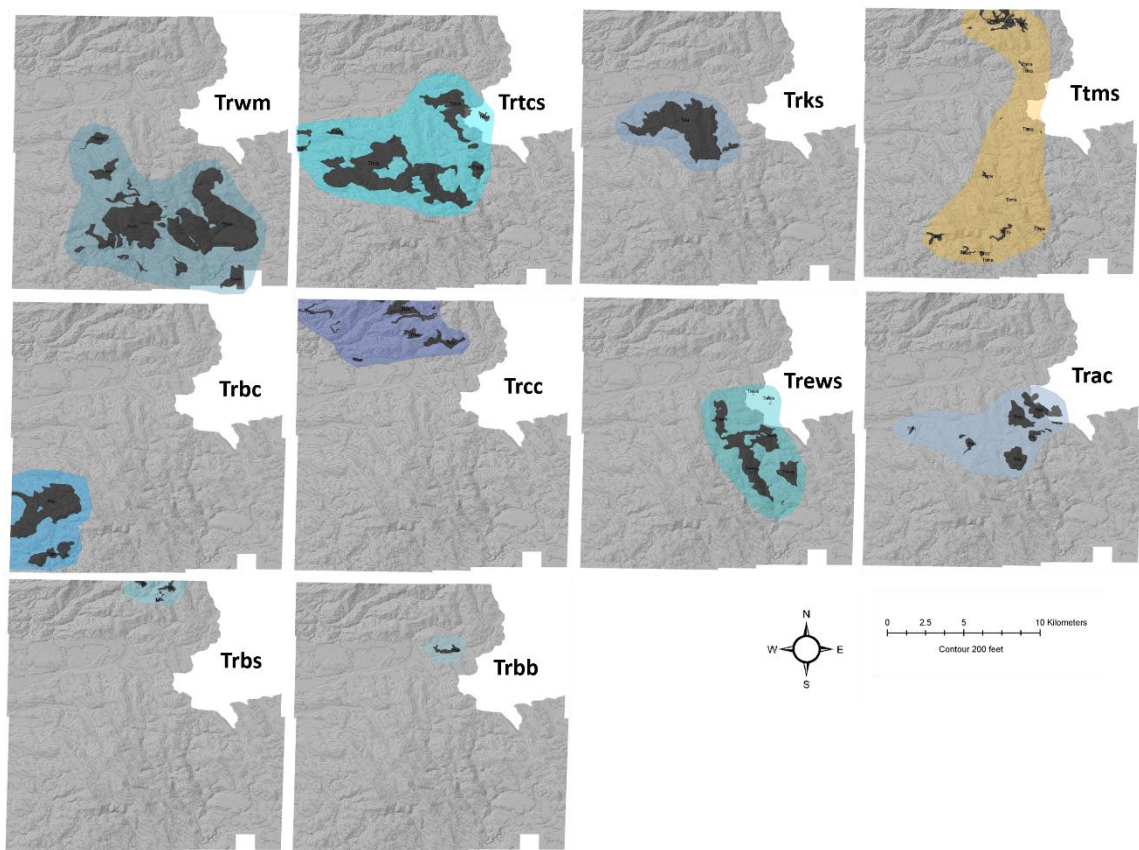


Figure 78: This study's estimated original coverage of each Strawberry rhyolite unit (in color) superimposed on the mapped extent (black).

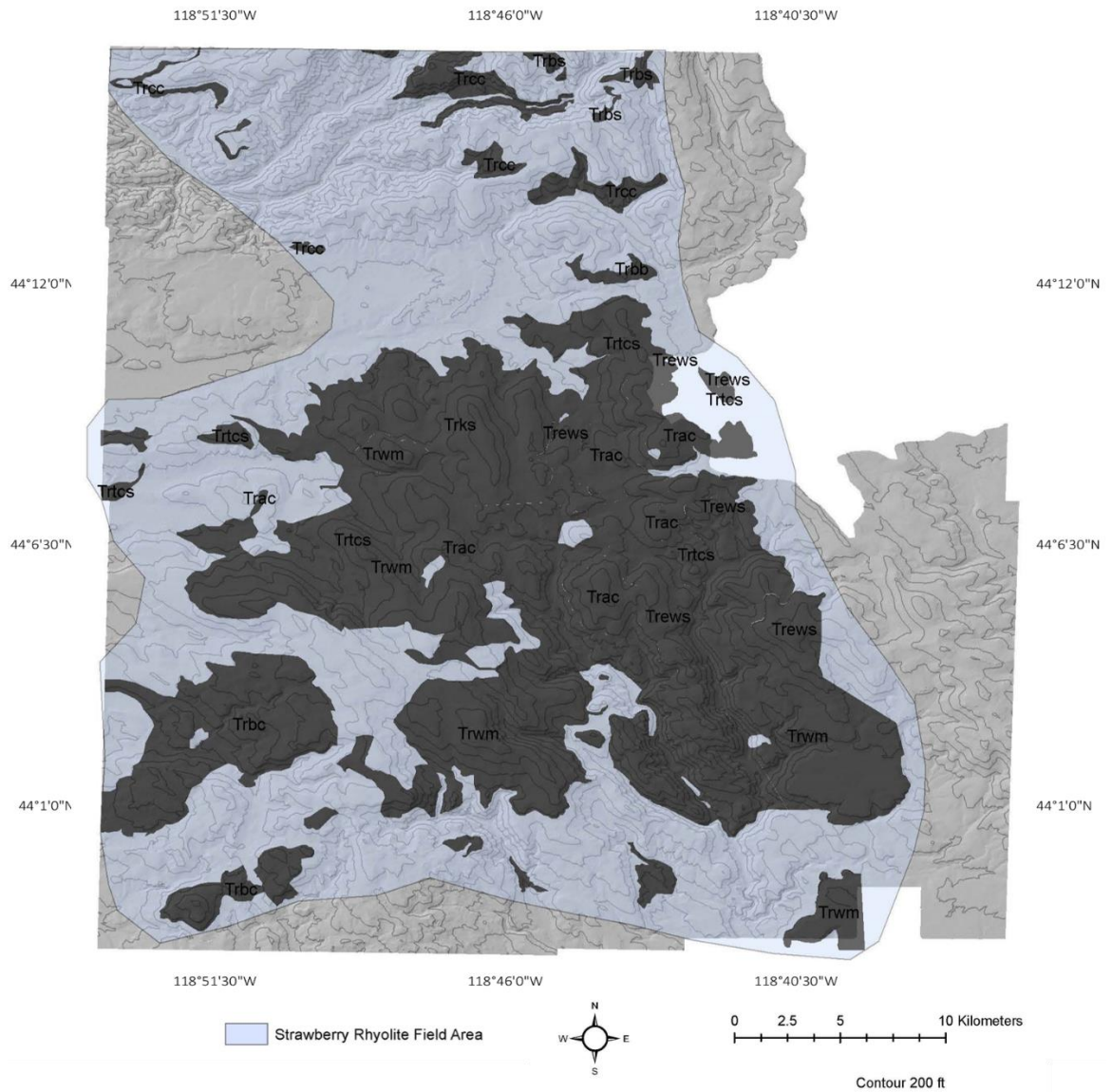


Figure 79: Geologic map showing rhyolite outcrops in dark gray and estimated original coverage of all rhyolite units of this study (in color). Dvorak conducted the mapping of the quadrangles Big Canyon and Jump-off Joe Mountain, and current PSU graduate student Rachel Sweeten mapped the Logan Valley West and Magpie Table quadrangles.

Table 2: This area and volume table is produced by compiling all the field mappings of each Strawberry rhyolite unit, generating an estimated area polygon surrounding all those units, and calculating its overall geometry in ArcMap; the area is outlined in red. Then using this geometry with field compiled data, an estimated volume is produced.

	<u>Area Sum</u> (Km ²)	<u>Estimated Unit Thickness (m)</u>		<u>Estimated Volume (Km³)</u>		<u>Average</u> <u>Volume (Km³)</u>
		<u>Minimum</u>	<u>Maximum</u>	<u>Minimum</u>	<u>Maximum</u>	
<u>All SV Rhyolite</u> <u>Units</u> (Using the Area Polygon Estimate)	386.387	32.09	129.09	12.399	48.879	31.139

4.4 AGE of STRAWBERRY RHYOLITES

Age dates generated through this study and previously acquired (Steiner & Streck 2013) are used in combination with stratigraphic field control to place rhyolite units into an eruptive sequence (Table 3). The rhyolite of Wolf Mountain is the oldest, dating to 16.16 ± 0.17 Ma, and currently, the youngest age acquired is for the rhyolite of Kent Spring at the age of 14.37 ± 0.02 Ma (Table 4). However, some rhyolites are clearly intercalated with andesite lavas of the Strawberry Volcanics, and these are the rhyolite of Buckhorn Spring and the rhyolite of Big Bend. Thus, these units are likely to be slightly younger than our youngest radiometric age. Also, some radiometric ages of different units overlap, which means that the eruptive sequence is unresolvable with available ages or that rhyolite is partially co-erupted. In general, however, the eruptive activity of the Strawberry Rhyolites is currently constrained to span a period of about 2 million years, ranging from around 16 to 14 Ma.

Table 3: Compilation of $^{40}\text{Ar}/^{39}\text{Ar}$ age dates of Strawberry rhyolite units found in this project mapped region. Unit abbreviations are elaborated by unit names in Table 1, or the legend of the project map found in the appendix.

Quad Location	Sample ID	Unit Abbreviation	Unit Name	Age (Ma)	Latitude	Longitude	Methods	Reference
Jump-Off Joe Mountain	SV-151	Trwm	Wolf Mountain Rhyolite	16.16 ± 0.17	44° 3'32.90"	118°45'14.00"	Plateau	Steiner & Streck, 2013
Jump-Off Joe Mountain	SV-144	Trwm	Wolf Mountain Rhyolite	15.34 ± 0.52	44° 4'42.80"	118°45'12.99"	Plateau	Steiner & Streck, 2013
Jump-Off Joe Mountain	MS-17-05	Trwm	Wolf Mountain Rhyolite	15.002 ± 0.047	44.065	-118.793	Single Crystal	This Study
Jump-Off Joe Mountain	JJ-17-8	Trbc	Bridge Creek Rhyolite	14.386 ± 0.032	44.016	-118.855	Single Crystal	This Study
Southwest of JOJM	SV-173	Trbc	Bridge Creek Rhyolite	14.7 ± 0.13	44° 3'46.80"	118°51'51.80"	Plateau	Steiner & Streck, 2013
Big Canyon	CD1975	Trks	Kent Spring Rhyolite	14.37 ± 0.02	44.1639	-118.79323	Single Crystal	This Study
Big Canyon	MS-14-23	Trtcs	Three Cabin Spring Rhyolite	14.81 ± 0.04	44.1734	-118.7539	Plateau	This Study
Big Canyon	SV-179	Trcc	Canyon Creek Rhyolite	15.30 ± 0.10	44°14'15.30"	118°46'43.10"	Plateau	Steiner & Streck, 2013
Big Canyon	SV-190	Trcc	Canyon Creek Rhyolite	14.79 ± 0.17	44°13'25.40"	118°46'8.10"	Plateau	Steiner & Streck, 2013

Table 4: The Strawberry Rhyolite units are listed according to age, from oldest to youngest. Unit abbreviations are elaborated by unit names in Table 1, or the legend of the project map found in the appendix.

	Unit Abbreviation	Age
Oldest	Trwm	16.16 ± 0.17
	Trwm	15.34 ± 0.52
	Trcc	15.30 ± 0.10
	Trwm	15.002 ± 0.047
	Trtcs	14.81 ± 0.04
	Trcc	14.79 ± 0.17
	Trbc	14.7 ± 0.13
	Trbc	14.386 ± 0.032
	Trks	14.37 ± 0.02
	Youngest	

5.0 DISCUSSION

5.1 VOLUME ESTIMATES

To calculate the volume of each SR unit, the thickness of each respective unit is required. Unit thicknesses were discerned in the field; however, there are considerable uncertainties. Sometimes a whole mountain, e.g., Bridge Creek Rhyolite in Figure 73, comprises one rhyolite unit. In other cases, actual outcrops are not thicker than a few meters. Given these observations, first, I chose a minimum and maximum thickness for each unit based on notes taken in the field and outcrop images with scale, also, through using the measuring tool on Google Earth to get a range of outcrop exposure along with using in-depth knowledge of the field region throughout the years of mapping the area and choosing site-specific areas with precise one unit exposure. Once the range is discerned, the field evidence is combined with thicknesses in the literature of other youthful (Pliocene and younger) rhyolite lavas and dome complexes. The estimated area for each rhyolite unit (Figure 78) is multiplied by the minimum and maximum thicknesses, which yields volume estimates for each unit. In Table 5, units are listed according to their estimated distribution from largest to smallest based on the above methods. The values obtained were found using the average of the minimum and maximum unit thicknesses multiplied by their respective calculated estimated areas (Table 6). By clearly defining a volume for each unit gives a better representation closer to their actual distributions. The largest volume is obtained for the rhyolite of Wolf Mountain (Trwm), with a value of $\sim 21 \text{ km}^3$. Trtcs follows Trwm with an average volume of $\sim 17 \text{ km}^3$, both units undoubtedly producing the largest volume out of all the Strawberry rhyolites found in this study. The smallest volume average produced is from the rhyolite of Buckhorn Spring at a value of about 0.7 km^3 . More interpretations have been conducted regarding unit age dates

and their volume relationship in understanding each of the Strawberry rhyolite unit's estimated volume.

Table 5: Calculated volume of Strawberry rhyolitic units, from largest to smallest. The volumes are calculated using each unit thickness multiplied by their respective area.

	Unit Name	Estimated Volume Average (Km ³)	
Trwm	Wolf Mountain Rhyolite	21.251	<p>Largest Volume</p> <p>Smallest Volume</p>
Trtcs	Three Canyon Spring Rhyolite	16.001	
Trews	Elk Wallow Spring Rhyolite	8.797	
Trks	Kent Spring Rhyolite	6.203	
Trcc	Canyon Creek Rhyolite	4.523	
Trbc	Bridge Creek Rhyolite	3.839	
Trac	Antelope Creek Rhyolite	3.466	
Ttms	Milk Spring Tuff	2.445	
Trbb	Big Bend Rhyolite	0.908	
Trbs	Buckhorn Spring Rhyolite	0.696	

Table 6: Calculated volumes of each SR unit based on the estimated area (see Table 1) and their respective unit maximum and minimum thicknesses that were discerned from fieldwork components and observations from well-preserved rhyolite lavas.

	Unit Name	Area Sum (Km ²)	Estimated Unit Thickness (m)		Estimated Volume (Km ³)		Average Volume (Km ³)
			Minimum	Maximum	Minimum	Maximum	
Ttms	Milk Spring Tuff	139.729	5	30	0.699	4.192	2.445
Trbs	Buckhorn Spring Rhyolite	9.937	20	120	0.199	1.192	0.696
Trbb	Big Bend Rhyolite	7.567	40	200	0.151	0.303	0.908
Trbc	Bridge Creek Rhyolite	54.839	40	100	2.194	5.484	3.839
Trews	Elk Wallow Spring Rhyolite	73.311	40	200	2.932	14.662	8.797
Trks	Kent Spring Rhyolite	51.692	40	200	2.068	10.338	6.203
Trac	Antelope Creek Rhyolite	69.313	30	70	2.079	4.852	3.466
Trcc	Canyon Creek Rhyolite	64.618	40	100	2.585	6.462	4.523
Trtcs	Three Canyon Spring Rhyolite	145.468	40	180	5.819	26.184	16.001
Trwm	Wolf Mountain Rhyolite	170.007	50	200	8.500	34.001	21.251
Tmus	Mullen Spring Volcanic Clastics	7.460	8	20	0.060	0.149	0.104
						Volume Sum (Maximum)	Volume Sum (Average)
						109.031	68.234

5.2 TEMPORAL CHANGES in MINERALOGY and COMPOSITION of RHYOLITES

The spectrum of Strawberry Rhyolites erupted from crystal-rich to aphyric, from pyroxene as the only mafic phase to having units containing only biotite or amphibole. With some units ranging from containing only plagioclase to those with plagioclase and quartz. The Strawberry Rhyolite units have been divided into two groups based on their lithology, petrography, and composition. With nine specific units making up the Strawberry Rhyolites, seven results in the aphyric and phenocryst poor unit group. The last two rhyolite units make up the second group category, which is the phenocryst rich units. The primary criteria for the units to fall into the aphyric and phenocryst poor category is having a phenocryst percentage range from aphyric to 4%. These units also fall within a silica content range of 70.4 – 77.4 wt.—% SiO₂. For a unit to be categorized as a phenocryst-rich unit, its plagioclase phenocryst percentage will range from 10– 30%, with other phenocrysts ranging from 1-5%. The following other phenocryst types are most commonly found to be biotite, amphibole, pyroxene (mostly orthopyroxene). The silica content for this rhyolite category has been found to remain a steady 73 wt.—% SiO₂.

Compositions range from low silica rhyolite (~71 wt.% SiO₂) to high silica rhyolites (up to a max value of 77.7 wt. SiO₂, (cf. Hildreth, 1981). Values above 77.7 wt.% are likely an artifact of a slight SiO₂ gain during devitrification. This range from low- to high-silica rhyolites clearly preserves a record of being progressively more differentiated (evolved) as elements that are compatible with crystallizing mineral assemblage generally decrease with increased silica, to clearly define the Strawberry Rhyolites temporal changes and the understanding of their

trace elements and how they affect the petrogenetic process. Examples for this are seen in the variation plots; Fe, Ti, Sr, and Eu (or better Eu/Eu*).

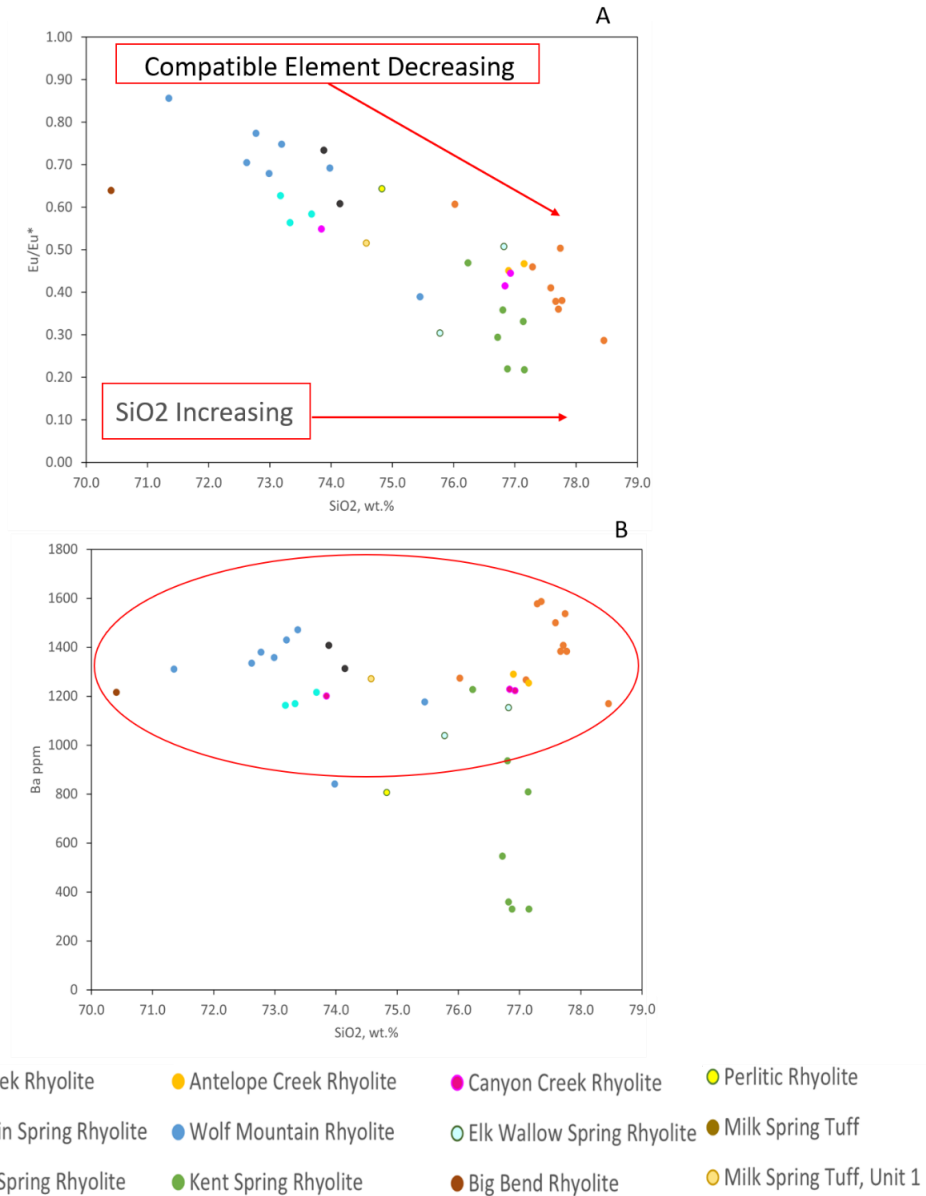


Figure 80: Plot (A) is a variation diagram for Eu/Eu* vs. SiO₂ wt.% for the Strawberry Rhyolites, highlighting the trend of as silica increases the compatible element (Eu) decrease. Plot (B) is also a variation diagram, highlighting the trace element Ba versus silica content. Circled in red, most of the units have a high Ba value (exception of Trks). This high concentration indicates how compatible they are—the higher the Ba, the stronger the compatibility in alkali feldspar.

The Eu/Eu* vs. SiO₂ wt. % variation plot (plot A in Figure 80) demonstrates a trend in that as the silica content increases, the compatible trace element europium decreases. Using plot A, Eu/Eu*, the quantitative expression for the Eu anomaly is portrayed in rare earth element diagrams. The Eu anomaly is predominantly controlled by feldspars, as europium is a compatible trace element in plagioclase and alkali feldspar. To calculate the Eu/Eu* ratio correctly, the chondrite normalized values are required for the elements Eu, Sm, and Gd. Eu* is calculated by example in Equation 1 below.

$$Eu^* = \sqrt{(Sm \times Gd)}$$

Equation 1

The Eu* expression represents where the original value would sit if no depletion has occurred. By dividing the chondrite normalized value for Eu by the found Eu* value, a value should equal a number between zero and one. Values that are closer to the number one represent the smaller the Eu anomaly. However, if values fall more towards zero, then the greater the Eu anomaly. This interpretation is represented in the Strawberry Rhyolite phenocryst rich units (Trbc and Trwm), plotting high (closer to one) Eu/Eu* values. Having a high value means these units are less evolved. Therefore, the phenocryst-rich units did not experience significant feldspar fractionation for the appropriate elements to be removed from the melt, determining how they affect the rhyolitic petrogenetic process.

Crystal-rich units such as Trwm and Trbc contain plagioclase that is often complexly zoned, a noteworthy observation as plagioclase phenocrysts in crystal poor units are much more straightforward. Complexly zoned plagioclase phenocrysts may be a result of partial melting. Based on their regional geologic history, they are more likely a product of partial

melting, recycled from older rocks that underwent a partial melting process to produce the rhyolites. So, the temporal change appears to indicate the starting up of a rhyolite field by erupting crystal-rich units which are transitioning to a mature stage where units are more crystal poor either or the complex plagioclase has been completely resorbed, or the rhyolite magma is no longer in contact with the source or country rocks containing such plagioclase. Interestingly, in plot B in Figure 80, the trace element barium values stay high, indicating that indeed alkali feldspar has not begun crystallizing (Ba is strongly compatible with alkali feldspar), except for the rhyolite of Kent Spring. Trks indicate decreasing barium, suggesting that this unit experienced more feldspar fractionation, as barium substitutes for potassium in potassium feldspar, hornblende, and biotite.

To further understand these implications of the temporal changes in the Strawberry Rhyolites, the Nb vs. Zr variation diagram (Figure 48) is used to classify samples as I-type or A-type using the discrimination techniques of Whalen et al., 1987. By applying the parameters that distinguish A- from I-type rhyolites (e.g., Whalen et al., 1987; Streck, 2014), and using the variation diagrams that involve the elements Nb, Zr, the La/Yb ratio, and the sum of Zr+Nb+Y+Ce, indicate variations amongst the Strawberry Rhyolites (as seen in plots E and F in Figure 49, along with J and H in Figure 50). Similar variations have been observed at other single Miocene rhyolite centers elsewhere in Oregon (e.g., Large, 2016; Brown, 2017; Young 2020). In general, lower silica, crystal-rich units such as Trwm and Trbc erupted early, while the more crystal poor and silica-rich units were more prevalent later. Units that indicate a slight trend towards A-type compositions, such as Trbs, Trks, and the rhyolitic portion of Ttms, erupted the latest. The development of the rhyolites with slightly more of an A-type composition follow this sequence, which is compatible with the interaction of basalt intruding

into crust, thus initiating partial melting. The production of these A-type rhyolites, combined with ramping up the heat input from basalt, supports near-liquidus rhyolite liquids. Interaction of basalts with rhyolites culminates in the production of A-type like rhyolites, supporting the association with hot spot activity. Evidence for this stage also comes from the commingling of mafic and rhyolitic magmas to produce the tuff of Milk Spring. Because we now have an understanding of the Strawberry Rhyolite units' temporal change in terms of their mineralogy and composition, we can use this to interpret petrographic relationships.

The Strawberry rhyolite field is significant as it covers an approximate area of 386 km² with an averaged overall volume of about 67 km³ and spanning a constrained period of 2 million years. Figure 81 relates volume versus age for the Strawberry Rhyolites. The trend depicted is that as the rhyolites younger, the smaller the volume they produce. This age and volume relationship may be a precursor in better determining stratigraphy of rhyolitic volcanic units, which aid in closing geologic time gaps throughout history.

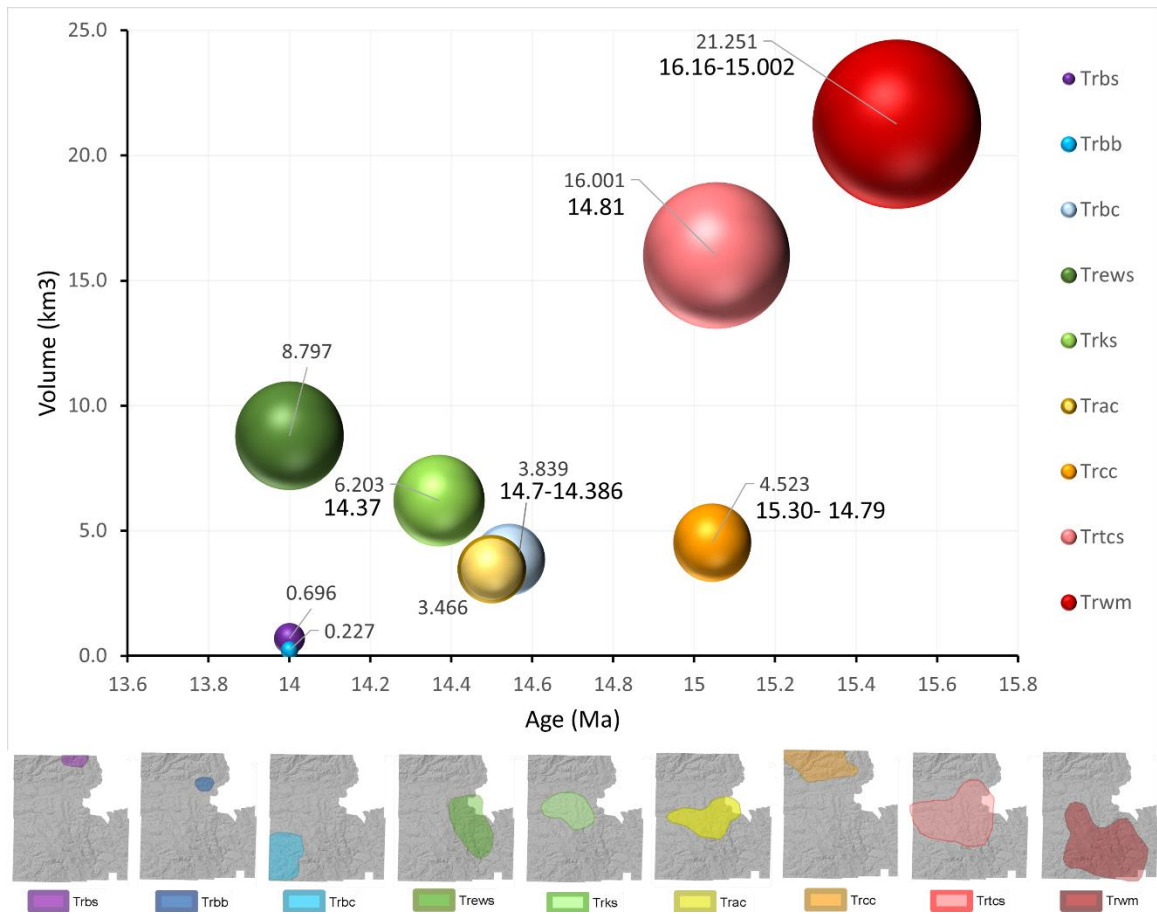


Figure 81: Estimated volume versus age plot of the Strawberry Rhyolites. This plot highlights how as the rhyolite units go from older to younger, they also trend towards larger to smaller regarding volume in size. The larger bold numbers on the plot are the age dates acquired, with the smaller numbers being their estimated volume. The map images below the graph highlight each specific unit's estimated area based on maps produced in the field area.

5.3 COMPARING the STRAWBERRY RHYOLITE FIELD with OTHER MIOCENE and YOUNGER RHYOLITE FLOWS and FIELDS

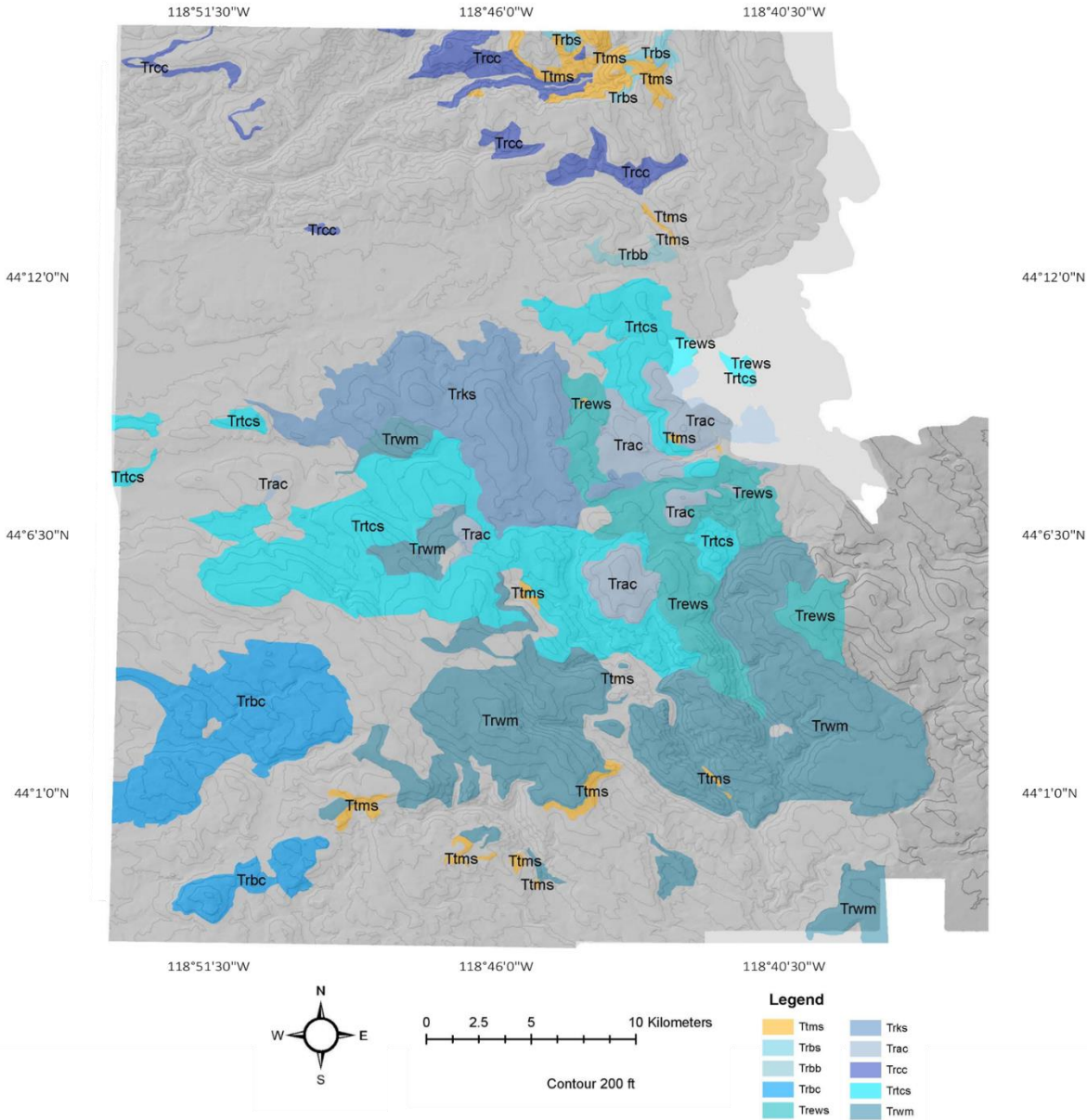


Figure 82: Map image incorporates all the rhyolite units or units with a rhyolite component (Ttms)) mapped in this project; all units that are not locally sourced rhyolites are greyed out. This map shows that the presence of rhyolite is more varied and extensive than previously mapped.

This study demonstrates that the Strawberry Rhyolites constitute a significant rhyolite field that is among the largest in Oregon. Aerial coverage of approximately 386 km² (Figure 79) and an overall estimated volume of ~67 km³ using a median thickness for each unit. On the other hand, the total volume could be greater than 100 km³ if greater thicknesses apply. I want to highlight this by comparing the Strawberry rhyolite field to well-known rhyolite lava flows and fields.

The Big Obsidian Flow generated from the Newberry Volcano is a prominent single rhyolite lava flow that erupted about 2500 years ago (Sherrod et al., 1997). The Big Obsidian flow extends over less than 8 km² (Newberry Volcano, 2021). This flow extended about 1.8 km long and is locally thicker than ~20m (Sherrod et al., 1997). The Glass Mountain rhyolites from the Medicine Lake Volcano cover an area of about 68 km² with a volume of 1.0 km³ (Donnelly, 1990). Glass Buttes is a series of late Miocene rhyolite dome complexes of the central High Lava Plains of Oregon (Walker, 2006). The Glass Buttes cover an estimated area of 140 km² (Stueber et al., 2015). According to Richard Roche's 1987 thesis, the exact volume is unknown, so we need to compile some data to get an idea. The flow nearest Musser Draw, south of Glass Butte, has a length ~1 km, a width of 0.25 km, and a thickness of 15 m. Then, little Glass Butte exposure area ranges from 5-8 km². Lastly, the largest volume is said to belong to the high-silica rhyolite sequence of the Glass Buttes Complex, having a thickness of up to 600 m (Roche, 1987). I use the 15m value from the Musser Draw flow to calculate the average volume of the little glass butte exposure by assuming similar thicknesses, yield ~ 0.1 km³. Then by averaging the two calculated areas (Musser Draw and Little Glass Butte), a calculated volume estimate for the high-silica rhyolite sequence yields 2.9 km³. Lastly, averaging all three flow areas and volumes, they amount to ~5km² and ~1km³.

The size of the Strawberry Rhyolite field discussed in this project is close to that of the Coso Volcanic Field in Inyo County, CA, in relative size. The area of this field is about 316 km²—each unit from the Coso rhyolite field range in volume from 0.0003 to 0.3 km³. There are seven distinct rhyolite domes and flows (Bacon et al., 1981). The sum of each volume of these seven domes and flows amounts to about 1.58 km³. Volumes for individual units come from Bacon et al. (1981, Table 2. Figure 83 below shows a visual representation of these fields in comparison.

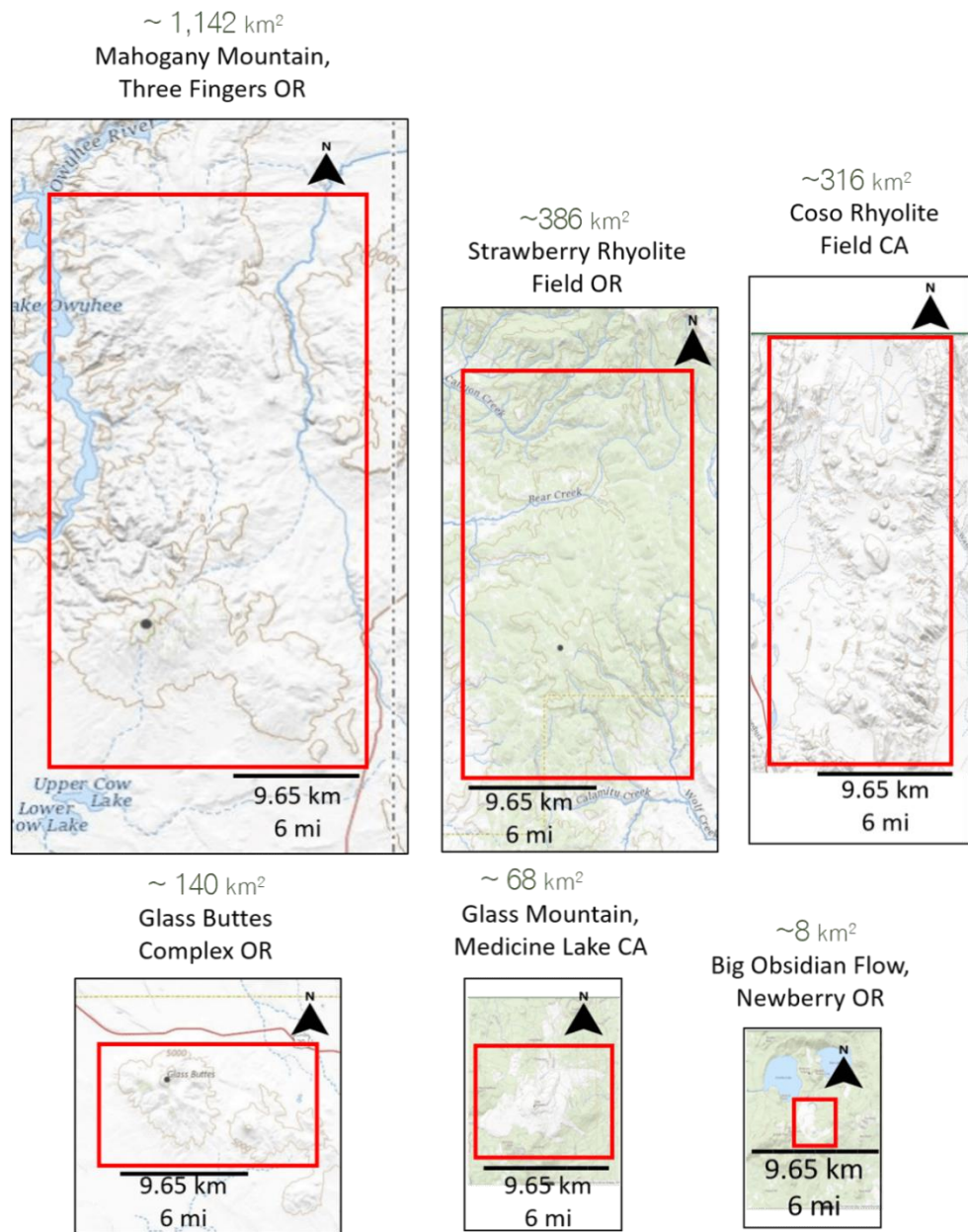


Figure 83: Figure representing a size comparison to the project area and other rhyolite fields. Each volcanic field is on the same scale to highlight its size differences.

6.0 CONCLUSION

This study centered on a largely unknown mid-Miocene rhyolite field in the greater area of the Strawberry Mountains of eastern Oregon near the town of John Day. The existence of mid-Miocene rhyolites as part of the Strawberry Volcanics in this area was initially recorded by Robyn (1977). Still, little work was done to detail distribution and differentiated units based on age, composition, and mineralogy. Steiner (2016) provided more detail on stratigraphic position, composition, and overall distribution of the rhyolites but still leaving many unanswered questions. In the context of three USGS Edmap mapping projects, this study has revealed the actual areal distribution of rhyolite units of this field, volumetric estimates, and their stratigraphic, compositional, mineralogical makeup. A minimum of 9 distinct effusive rhyolite units erupted over a 2-million-year period in addition to one (possibly two) mixed, rhyolite-andesite pyroclastic deposit from ~16.2 to 14.3 Ma. These collectively make up the Strawberry Rhyolites. The estimated cumulative area of the rhyolites is 386 km² with an estimated maximum volume of 111 km³. Rhyolites range from low-silica to high-silica composition and from phenocryst rich containing >20% phenocryst to those that are aphyric. Most units display glassy-to-devitrified lithologies. Mineral assemblages are dominated by plagioclase and mafic silicates, often containing amphibole, biotite, or both. Some units carry orthopyroxene in addition to or instead of biotite and amphibole. Strawberry rhyolites are intercalated with regional tuffs of the Dinner Creek Tuff. Although the youngest rhyolites co-erupted with basalts and andesites, they typically underlie basalt to andesites lavas of the Strawberry Volcanics. All lavas of the Strawberry Volcanics overlie pre-Cenozoic basement consisting of clastic sedimentary rocks regionally belonging to the Izee terrane and ultramafic rocks

belonging to the Baker terrane. The mid-Miocene volcanic stratigraphy is capped by the widespread late Miocene Devine Canyon and Rattlesnake Tuff erupting from the Harney Basin to the south. Faulting was likely instrumental in forming numerous N-S trending valleys that dot this part of the Blue Mountains province. Quaternary fluvial processes incised canyons and caused several deep-seated landslides, resulting in this part of the Strawberry Mountains' present topography.

Strawberry Rhyolites are now recognized to belong to the rhyolite flare-up associated with the main pulse of the CRBG volcanism, with rhyolite centers occurring near the Oregon-Nevada state border in the south to Baker City in the north and as far northwest as the Strawberry Rhyolites. Thus, adding Strawberry Rhyolites to this rhyolite flare-up increased the footprint of this province towards the northwest.

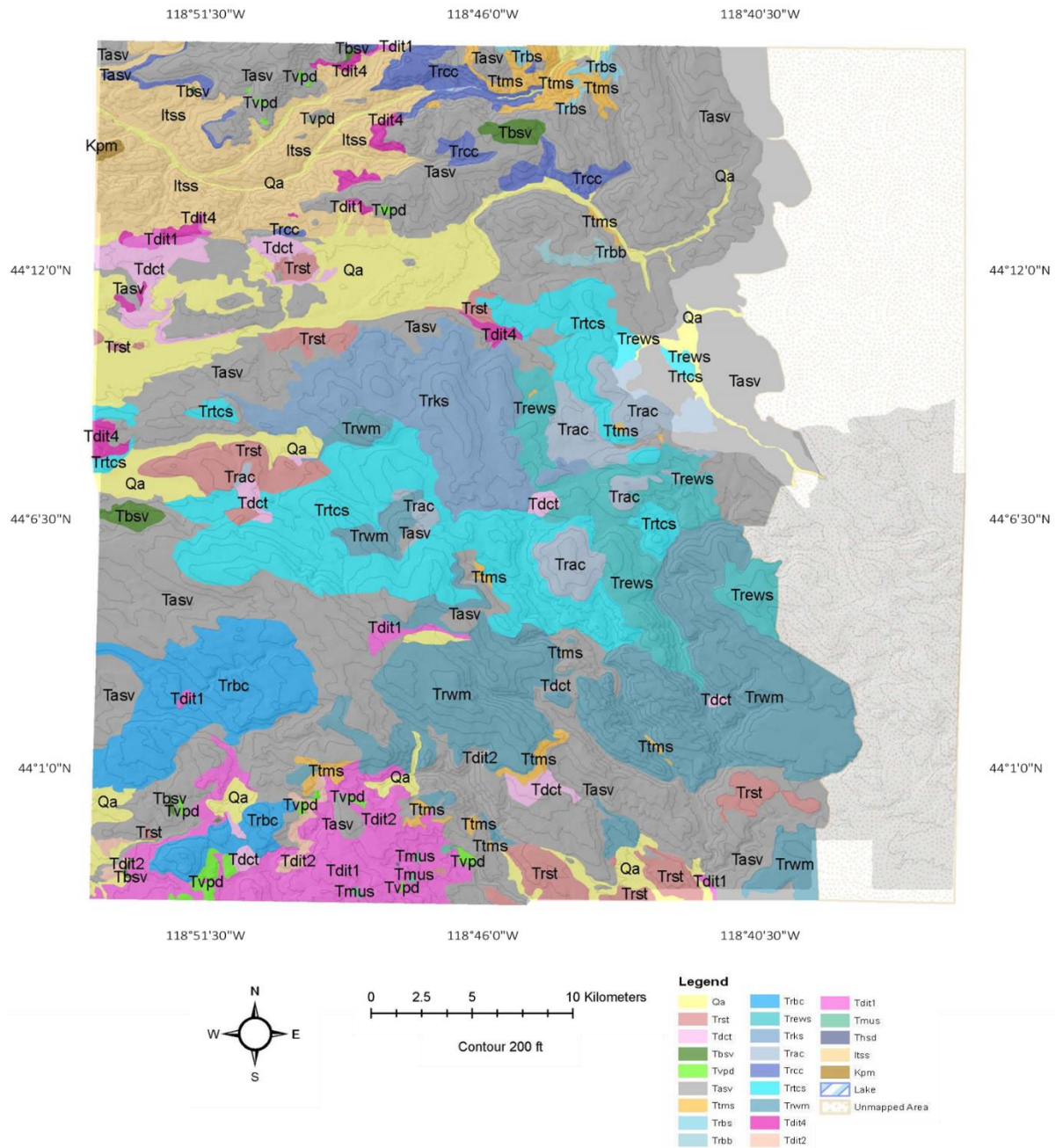


Figure 84: Geologic map produced through this study incorporates the geology of Jump-off Joe Mountain, Big Canyon, Logan Valley West, and Magpie Table quadrangles, depicting how various the area's units genuinely are.

7.0 REFERENCES

- Ambroz, Jessica A, Glascock, Michael D, & Skinner, Craig E. (2001). Chemical Differentiation of Obsidian within the Glass Buttes Complex, Oregon. *Journal of Archaeological Science*, 28(7), 741–746. <https://doi.org/10.1006/jasc.2000.0593>
- Bacon, Charles R, Macdonald, Ray, Smith, Robert L, & Baedeker, Philip A. (1981). Pleistocene high-silica rhyolites of the Coso Volcanic Field, Inyo County, California. *Journal of Geophysical Research: Solid Earth*, 86(B11), 10223–10241. <https://doi.org/10.1029/JB086iB11p10223>
- Baksi, AK, 1989, Reevaluation of the Timing and Duration of Extrusion of the Imnaha, Picture Gorge, and Grande Ronde Basalts, Columbia River Basalt Group, Geological Society of America Special Paper 239, p. 105 – 112
- Barry, T., Kelley, S., Reidel, S., Camp, V., Self, S., Jarboe, N., . . . Renne, P. (2013, August 01). Eruption chronology of the Columbia River Basalt Group. Retrieved November 19, 2020, from <https://pubs.geoscienceworld.org/books/book/661/chapter/3807104/Eruption-chronology-of-the-Columbia-River-Basalt>
- Benson, T.R. and Mahood, G.A., 2016, Geology of the Mid-Miocene Rooster Comb Caldera and Lake Owyhee Volcanic Field, eastern Oregon: Silicic volcanism associated with Grande Ronde flood basalt, *Journal of Volcanology and Geothermal Research*, v. 309, p. 96–117, doi:10.1016/j.jvolgeores.2015.11.011
- Bestland, E. A., and G. J. Retallack (1994a), Geology and paleoenvironments of the Clarno Unit, John Day Fossil Beds National Monument, Oregon, U. S. Natl. Park Syst. Open File Rep., 160-211 pp.
- Brooks, H. C., McIntyre, J. R., & Walker, G. W. (1976). Geology of the Oregon part of the Baker 1° by 2° quadrangle: Oregon Department of Geology and Mineral Industries Geologic Map: Series Map GMS-7, scale 1:250,000. Retrieved 2019, from <https://www.oregongeology.org/pubs/gms/GMS-007.pdf>
- Brown, C.E., and Thayer, T.P., 1966, Geologic map of the Canyon City quadrangle, north-eastern Oregon: US Geological Survey, Miscellaneous Geologic Investigations Map I-447, scale 1:250,000.
- Brown, E. A. (2017). Rhyolite Petrogenesis at Tower Mountain Caldera, OR (Order No.10285151). Available from Dissertations & Theses @ Portland State University; ProQuest Dissertations & Theses Global. (1949311147). <http://stats.lib.pdx.edu/proxy.php?url=http://search.proquest.com.proxy.lib.pdx.edu/dissertations-theses/rhyolite-petrogenesis-at-tower-mountaincaldera/docview/1949311147/se-2?accountid=13265>
- Cahoon, E.B., Streck, M.J., 2017, Picture Gorge Basalt, eastern Oregon: extended distribution And petrogenetic connections to Steens Basalt and Strawberry Volcanics. *Geological Society of America Abstracts with Programs*. Vol. 49, No. 6 doi: 10.1130/abs/2017AM-304582
- Cahoon, Emily B, Streck, Martin J, Koppers, Anthony A. P, & Miggins, Daniel P. (2020). Reshuffling the Columbia River Basalt chronology; Picture Gorge Basalt, the earliest and longest-erupting formation. *Geology (Boulder)*, 48(4), 348–352. <https://doi.org/10.1130/G47122.1>

- Camp, V. (2021, February 1). The Yellowstone hotspot—the source of heat that powers Yellowstone’s vast volcanic system—has long been thought to have initiated about 17 million years ago. A growing volume of evidence, however, suggests that it has been around much longer. Lecture presented at Just how long has the Yellowstone Hotspot been around? in CA, San Diego State University, San Diego.
- Camp, V.E., Ross, M.E., Hanson, W.E., 2003, Genesis of Flood Basalts and Basin and Range Volcanic Rocks from Steens Mountain to the Malheur River Gorge, Oregon, GSA Bulletin, January 2003; v. 115; no. 1; p. 105–128.
- Camp, VE, and Hanan, B.B., 2008, A Plume Triggered Delamination Origin for the Columbia River Basalt Group, Geosphere, v. 4, no. 3, p. 480–495.
- Coble, M.A., and Mahood, G.A., 2016, Geology of the High Rock caldera complex, northwest Nevada, and implications for intense rhyolitic volcanism associated with flood basalt magmatism and the initiation of the Snake River Plain–Yellowstone trend, Geosphere, vol. 12, no. 1, 58–113, doi: 10.1130/GES01162.1
- Cruz, M., and Streck, M.J., 2017, Geologic Map of the Calamity Butte Quadrangle, Oregon, unpublished USGS EdMap project.
- Cruz, M., 2018, Field Mapping Investigation and Geochemical Analysis of Volcanic Units within the Dinner Creek Tuff Eruptive Center, Malheur County, Eastern Oregon. Dissertations and Theses. Paper 3837.http://pdxscholar.library.pdx.edu/open_access_etds/383710.15760/etd.3468
- Dickinson, W., 1979, Mesozoic Forearc Basin in Central Oregon, Geology, vol. 7, p. 166 – 170
- Donnelly-Nolan, Julie M, Champion, Duane E, Miller, C. Dan, Grove, Timothy L, & Trimble, Deborah A. (1990). Post-11,000-year volcanism at Medicine Lake Volcano, Cascade Range, northern California. *Journal of Geophysical Research: Solid Earth*, 95(B12),19693–19704. <https://doi.org/10.1029/JB095iB12p19693>
- Dorsey, R.J., and LaMaskin, T.A., 2007, Stratigraphic record of Triassic-Jurassic collisional tectonics in the Blue Mountains Province, Northeastern Oregon: *American Journal of Science*, v. 307, p. 1167-1193. 41
- Dorsey, R.J., and LaMaskin, T.A., 2008, Mesozoic collision and accretion of oceanic terranes in the Blue Mountains province of north-eastern Oregon: new insights from the stratigraphic record. In Spencer, J. E., and Titley, S. R., eds. ‘Circum-Pacific Tectonics, Geologic Evolution, and Ore deposits’. Tucson, AZ, Arizona Geol. Soc. Dig. 22.
- Dorsey, R. J., & LaMaskin, T. A. (2007). Stratigraphic record of Triassic-Jurassic collisional tectonics in the Blue Mountains province, north-eastern Oregon. Retrieved November 18, 2020, from <https://www-ajsonline-org.proxy.lib.pdx.edu/content/307/10/1167.short>
- Dvorak, C.L. and Streck, M.J., 2018, Geologic Map of the Jump-Off Joe Mountain Quadrangle, Oregon, unpublished USGS EdMap project.
- Dvorak, C.L. and Streck, M.J., 2019, Geologic Map of the Big Canyon Quadrangle, Oregon, unpublished USGS EdMap project.
- Enlows, H.E., and Parker, D.J., 1972, Geochronology of the Clarno Igneous Activity in the Mitchell Quadrangle, Wheeler County, Oregon, *Ore Bin*, vol. 34, p. 104 - 110
- Ferns, Mark L., Streck, M.J, McCloughry, J.D (2017) “Field-Trip Guide to Columbia River Flood Basalts, Associated Rhyolites, and Diverse Post-Plume Volcanism in Eastern

- Oregon.” Scientific Investigations Report, USGS Publications Warehouse, 9 Aug. 2017, pubs.er.usgs.gov/publication/sir20175022O.
- Ford, M.T., Grunder, A.L., Duncan, R.A., 2013, Bimodal Volcanism of the High Lava Plains and Northwestern Basin and Range of Oregon: Distribution and Tectonic Implications of Age-Progressive Rhyolites, *Geochemistry Geophysics Geosystems*, vol. 14, no. 8, p. 2836 –2857, doi: 10.1002/ggge.20175
- Greene, R.C., 1973, Petrology of the Welded Tuff of Devine Canyon, Southeastern Oregon: USGS Professional Paper, v. 797.
- Haddock, G. (1967). The Dinner Creek welded ash-flow tuff of the Malheur Gorge area, Malheur County, Oregon. University of Oregon.
- Hanna, T. R. (2018). Areal Extent and Volumes of the Dinner Creek Tuff Units, Eastern Oregon Based on Lithology, Bulk Rock Composition and Feldspar Mineralogy (Order No. 10686814). Available from Dissertations & Theses @ Portland State University; ProQuest Dissertations & Theses Global. (2042936533). <http://stats.lib.pdx.edu/proxy.php?url=http://search.proquest.com.proxy.lib.pdx.edu/dissertations-theses/areal-extent-volumes-dinner-creek-tuff-units/docview/2042936533/se-2?accountid=13265>
- Henry, C.D., Castor, S.B., Starkel, W.A., Ellis, B.S., Wolff, J.A., Laravie, J.A., McIntosh, W.C., Heizler, M.T., 2017, Geology and Evolution of the McDermitt Caldera, Northern Nevada and Southeastern Oregon, Western USA, *Geosphere*, vol. 13, no. 4, p. 1066 – 1112, doi: 10.1130/GES01454.1
- Isom, S.I. and Streck, M.J., 2016, Geologic Map of the Telephone Butte Quadrangle, Oregon, unpublished USGS EdMap project
- Isom, S. L. (2017). Compositional and Physical Gradients in the Magmas of the Devine Canyon Tuff, Eastern Oregon: Constraints for Evolution Models of Voluminous High-silica Rhyolites (Order No. 10606618). Available from Dissertations & Theses @ PortlandState University; ProQuest Dissertations & Theses Global; Publicly Available Content Database. (1964913942). <http://stats.lib.pdx.edu/proxy.php?url=http://search.proquest.com.proxy.lib.pdx.edu/dissertations-theses/compositional-physical-gradients-magmas-devine/docview/1964913942/se-2?accountid=13265>
- Jordan, B.T., Grunder, A.L., Duncan, R.A., Deino, A., 2004, Geochronology of Age Progressive Volcanism of the Oregon High Lava Plains: Implications for the Plume Interpretation of Yellowstone, *Journal of Geophysical Research*, vol. 109, B10202, doi: 10.1029/2003JB002776
- Jordan, B.T., Grunder, A.L., Duncan, R.A., Deino, A.L., 2004. Geochronology of age progressive Volcanism of the Oregon High Lava Plains: Implications for the plume interpretation of Yellowstone: *J Geophys. Res.* 109, B10202, doi: 10.1029/2003JB002776.
- LaMaskin, T.A., Vervoort, J.D., Dorsey, R.J., Wright, J.E., 2011, Early Mesozoic Paleogeography, and Tectonic Evolution of the Western United States: Insights from Detrital Zircon U-Pb Geochronology, Blue Mountains Province, Northeastern Oregon, *Geological Society of America Bulletin*, vol. 123, p. 1939 - 1965
- Large, A. M. (2016). Silicic Volcanism at the Northern and Western Extent of the Columbia River Basalt Rhyolite Flare-up: Rhyolites of Buchanan Volcanic Complex and

- Dooley Mountain volcanic Complex, Oregon (Order No. 10158745). Available from Dissertations & Theses @ Portland State University; ProQuest Dissertations & Theses Global. (1839240247).
<http://stats.lib.pdx.edu/proxy.php?url=http://search.proquest.com.proxy.lib.pdx.edu/dissertations-theses/silicic-volcanism-at-northern-western-extent/docview/1839240247/se-2?accountid=13265>
- Long, Maureen D, Gao, Haiying, Klaus, Amanda, Wagner, Lara S, Fouch, Matthew J, James, David E, & Humphreys, Eugene. (2009). Shear wave splitting and the pattern of mantle flow beneath eastern Oregon. *Earth and Planetary Science Letters*, 288(3), 359–369. <https://doi.org/10.1016/j.epsl.2009.09.039> Manchester, SR, 1981, Fossil Plants of the Eocene Clarno Nut Beds, *Oregon Geology*, vol. 43, p.75 - 81
- McCloughry, J.D., Ferns, M.L., Streck, M.J., Patridge, K.A., Gordon, C.L., 2009, Paleogene Calderas of Central and Eastern Oregon: Eruptive Sources of Widespread Tuffs in the John Day and Clarno Formations, in ‘Volcanoes to Vineyards: Geologic Field Trips Through the Dynamic Landscape of the Pacific Northwest.’ *Geological Society of America Field Guide*, vol. 15, eds. J.E. O’Connor, R.J. Dorsey, and IP Madin, p. 407 - 434
- McKee, T.M., 1970, Preliminary Report on Fossil Fruits and Seeds from the Mammal Quarry of The Clarno Formation, Oregon, *Ore Bin*, vol. 32, p. 117 – 132
- Milliard, Justin B. Two-stage Opening of the Northwestern Basin and Range in Eastern Oregon: Evidence from the Miocene Crane Basin. Oregon State U, 2010. Web.
- Newberry volcano: Big Obsidian Flow. (n.d.). Retrieved May 1, 2021, from <https://www.usgs.gov/volcanoes/newberry/big-obsidian-flow>
- Reidel, S.P., Camp, V.E., Tolan, T.L., Martin, B.S., 2013, The Columbia River Flood Basalt Province: Stratigraphy, Areal Extent, Volume, and Physical Volcanology, in ‘The Columbia River Flood Basalt Province’ eds S.P. Reidel, V.E. Camp, M.E. Ross, J.A. Wolff, BS. Martin, T.L. Tolan, and R.E. Wells, *Geological Society of America Special Paper* 497, p. 1 - 43
- Retallack, G.J., Bestland, E.A., Fremd, T.J., 2000, Eocene and Oligocene Paleosols of Central Oregon, *Geological Society of America Special Paper* 344, 192 p.
- Robinson, P.T., Brem, G.F., McKee, E.H., 1984, John Day Formation of Oregon: a Distal Record of Early Cascade Volcanism, *Geology*, vol. 12, p. 229 – 232, doi: 10.1130/00917613(1984)12<229:JDFOOA>2.0.CO;2
- Robyn, T. L., 1977, Geology and petrology of the Strawberry Mountain volcanic series, Central Oregon. University of Oregon, Unpublished Ph.D. thesis, 189 p.
- Robyn, T. L., 1979, Miocene volcanism in eastern Oregon—An example of calc-alkaline Volcanism unrelated to subduction. *Journal of Volcanology and Geothermal Research*, 5, 149-161.
- Rogers, J.W., and Novitsky-Evans, J.M., 1977, The Clarno Formation of Central Oregon, USA, Volcanism on a Thin Continental Margin, *Earth and Planetary Science Letters*, vol. 34, p. 56 – 66, doi:10.1016/0012-821X(77)90105-4
- Roche, Richard Louis, "Stratigraphic and geochemical evolution of the Glass Buttes complex, Oregon" (1987). Dissertations and Theses. Paper 3748.
<https://doi.org/10.15760/etd.5632>
- Rytuba, JJ, and Vander Meulen, DB, 1991, Hot-spring precious-metal systems in the Lake

- Owyhee volcanic field, Oregon-Idaho: in Raines, G.L., Lisle, R.E., Schafer, R.W., Wilkinson, W.H., eds., 'Geology and ore deposits of the Great Basin', Reno, Geological Society of Nevada, Symposium Proceedings, April 1 - 5, 1990, v. 2, p. 1085 – 1096.
- Rytuba, J.J., Vander Meulen, DB, Barlock, V.E., Ferns, M.L., 1991, Hot spring gold deposits in the Lake Owyhee volcanic field, eastern Oregon, field trip 10 of Buffa, R.H., Coyner, A.R., eds., The geology and ore deposits of the Great Basin—Field trip guidebook compendium: Great Basin symposium on geology and ore deposits of the Great Basin, Reno, Nev., March 28–April 1, 1990, Reno, Nev., Geological Society of Nevada, p. 633–712.
- Schwartz, J.J., Snoke, A.W., Frost, C.D., Barnes, C.G., Gromet, LP, 2010, Analysis of the Wallowa- Baker Terrane Boundary: Implications for Tectonic Accretion in the Blue Mountains Province, Northeastern Oregon, Geological Society of America Bulletin 122, p. 517 – 536 44
- Schwartz, J. J, Snoke, A. W, Cordey, F, Johnson, K, Frost, C. D, Barnes, C. G, LaMaskin, T. A, & Wooden, J. L. (2011). Late Jurassic magmatism, metamorphism, and deformation in the Blue Mountains Province, northeast Oregon. Geological Society of America Bulletin, 123(9-10), 2083–2111. <https://doi.org/10.1130/B30327.1>
- Sherrod, D. R., Mastin, L. G., Scott, W. E., & Schilling, S. P. (1997). Volcano Hazards at Newberry Volcano, Oregon (Rep. No. 97-513). U.S. Department of the Interior U.S.G.S.
- Steiner, A. R. (2016). Field Geology and Petrologic Investigation of the Strawberry Volcanics, Northeast Oregon (Order No. 10061476). Available from Dissertations & Theses @ Portland State University; ProQuest Dissertations & Theses Global. (1776488436).
<http://stats.lib.pdx.edu/proxy.php?url=http://search.proquest.com.proxy.lib.pdx.edu/dissertations-theses/field-geology-petrologic-investigation-strawberry/docview/1776488436/se-2?accountid=132652712>.
http://pdxscholar.library.pdx.edu/open_access_etds/271210.15760/etd.2708
- Steiner, Arron & Streck, Martin. (2013). The Strawberry Volcanics: Generation of 'orogenic' andesites from tholeiite within an intra-continental volcanic suite centered on the Columbia River flood basalt province, USA. Geological Society, London, Special Publications. 385. 281-302. 10.1144/SP385.12.
- Steiner, A., & Streck, M. J. (2018). Voluminous and compositionally diverse, middle Miocene Strawberry Volcanics of NE Oregon: Magmatism cogenetic with flood basalts of the Columbia River Basalt Group. Field Volcanology: A Tribute to the Distinguished Career of Don Swanson: Geological Society of America Special Paper, 538, 41-62.
- Streck, M.J., 2014, Evaluation of crystal mush extraction models to explain crystal-poor rhyolites: Journal of Volcanology and Geothermal Research, v. 284, p. 74–94.
- Streck, M.J., and Grunder, A.L., 1995, Crystallization and welding variations in a widespread ignimbrite sheet; the Rattlesnake Tuff, eastern Oregon, USA: Bulletin of Volcanology, v. 57, p. 151–169, doi: 10.1007/BF00265035.
- Streck, M.J., and Grunder, A.L., 1997, Compositional gradients and gaps in high-silica rhyolites of the Rattlesnake Tuff, Oregon: Journal of Petrology, v. 38, p. 133–163,

- doi: 10.1093/petrology/38.1.133.
- Streck, M.J., and Grunder, A.L., 1999, Enrichment of basalt and mixing of dacite in the rootzone of a large rhyolite chamber: Inclusions and pumices from the Rattlesnake Tuff, Oregon: *Contributions to Mineralogy and Petrology*, v. 136, p. 193–212, doi: 10.1007/s004100050532.
- Streck, M.J., and Ferns, M.L., 2012, The Rhyolite flare-up of the Columbia River basalt province and its bearing on plume vs. non-plume models [abs.]: *American Geophysical Union Abstract*, no. DI53A–2372.
- Streck, M.J., and Grunder, A.L., 2012, Temporal and crustal effects on differentiation of tholeiite to calc-alkaline and ferro-trachytic suites, High Lava Plains, Oregon, USA: *American Geophysical Union Geochemistry, Geophysics, Geosystems*, v. 13, no. 11, 24 p. [Also available at <http://dx.doi.org/10.1029/2012GC004237>.]
- Streck, M., Ferns, M., & McIntosh, W., 2015, Large, persistent rhyolitic magma reservoirs above Columbia River Basalt storage sites: The Dinner Creek Tuff Eruptive Center, eastern Oregon. Retrieved November 19, 2020, from <https://pubs.geoscienceworld.org/gsa/geosphere/article/11/2/226/132195/Large-persistent-rhyolitic-magma-reservoirs-above>
- Stueber, D. O. (n.d.). Chapter 12: Glass Buttes, Oregon: 14,000 Years of Continuous Use. In 1391598585 1015764808 C. E. Skinner (Ed.), *Toolstone Geography of the Pacific Northwest* (2015 ed., pp. 193-207). Archaeology Press, Simon Fraser University.
- Swanson, D.A., 1969, Reconnaissance Geologic Map of the East Half of the Bend Quadrangle, Crook, Wheeler, Jefferson, Wasco, and Deschutes Counties, Oregon, US Geological Survey Miscellaneous Investigations Map I-568, scale 1:250,000
- Thayer, T.P., 1957, Some relations of later Tertiary volcanology and structure in eastern Oregon, v. 1 of *Volcanology of the Cenozoic: 20th International Geological Congress*, sec. 1, Mexico City, Mexico, 1956, sec. 1, p. 231–245.
- Thayer, T.P., Brown, C.E., and Hay, R.I., 1967, Preliminary geologic map of the Prairie City quadrangle, Grant County, Oregon: US Geological Survey Open-File Map, scale 1:62,500.
- Vallier, T.L., 1995, Petrology of Pre-Tertiary Igneous Rocks in the Blue Mountains Region of Oregon, Idaho, and Washington: Implications for the Geologic Evolution of a Complex Island Arc, in ‘*Geology of the Blue Mountains Region of Oregon, Idaho, and Washington: Petrology and Tectonic Evolution of Pre-Tertiary Blue Mountains Province*, eds. T.L. Vallier and H.C. Brooks, USGS Professional Paper 1438, p. 125 – 209
- Vallier, T. L., Brooks, Howard C., & Geological Survey, issuing body. (1986). *Geologic implications of Paleozoic and Mesozoic paleontology and biostratigraphy, Blue Mountains province, Oregon, and Idaho*. United States Government Printing Office.
- Wacaster, S., Streck, M.J., Belkin, H.H., and Bodnar, R.J., 2011, Compositional zoning of the Devine Canyon tuff, Oregon [abs.]: *American Geophysical Union Abstract*, no. V21C–2517.
- Walker, G. W., & Nolf, B. (2006). USGS: Geological Survey circular 838 (HIGH LAVA plains, brothers fault zone To Harney Basin, Oregon). Retrieved May 2021, from https://www.nps.gov/parkhistory/online_books/geology/publications/circ/838/sec5.htm

- Walker G. W., 1979, Revisions to the Cenozoic stratigraphy of Harney basin, southeastern Oregon, USGS Bulletin 1475, 35 p.45
- Ware, B.D., 2013, Age, Provenance, and Structure of the Weathersby Formation, Eastern Izee Sub-basin, Blue Mountains Province, Oregon and Idaho, Boise State University, MS thesis, 265 p.
- Watkins, N.D., and Baksi, AK, 1974, Magnetostratigraphy and oroclinal folding of the Columbia River, Steens, and Owyhee basalts, Oregon, Washington, and Idaho: *American Journal of Science*, v. 274, no. 2, p. 148–189. DOI: <https://doi.org/10.2475/ajs.274.2.148>
- Whalen, J. B, Currie, K. L, & Chappel, B. W. (1987). A-type granites: geochemical characteristics, discrimination and petrogenesis. *Contributions to Mineralogy and Petrology*, 95(4), 407–419. <https://doi.org/10.1007/BF00402202>
- Weaver, B., Tarney, J. Empirical approach to estimating the composition of the continental crust. *Nature* 310, 575–577 (1984).
<https://doi.org.proxy.lib.pdx.edu/10.1038/310575a0>
- Wolff, J.A., Ramos, F.C., Hart, G.I., Patterson, J.D., Brandon, A.D., 2008, Columbia River Flood Basalts from a Centralized Crustal Magmatic System, *Nature Geoscience*, vol. 1, p. 177 – 180
- Wolff, J.A., and Ramos, F.C., 2013, Source materials for the main phase of the Columbia River Basalt Group: Geochemical evidence and implications for magma storage and transport, in Reidel, S.P., Wood, JD, 1976, *The Geology of the Castle Rock Area, Grant, Harney, and Malheur Counties, Oregon*, Portland State University, MS thesis, 89 p.
- Webb, B. M. (2017). *The Littlefield Rhyolite, Eastern Oregon: Distinct Flow Units and Their Constraints on Age and Storage Sites of Grande Ronde Basalt Magmas* (Order No. 10286664). Available from Dissertations & Theses @ Portland State University; ProQuest Dissertations & Theses Global. (1951944191).
<http://stats.lib.pdx.edu/proxy.php?url=http://search.proquest.com.proxy.lib.pdx.edu/dissertations-theses/littlefield-rhyolite-eastern-oregon-distinct-flow/docview/1951944191/se-2?accountid=13265>
- Westby, E. G. (2014). *The Geology and Petrology of Enigmatic Rhyolites at Graveyard and Gordon Buttes, Mount Hood Quadrangle, Oregon* (Order No. 1571681). Available from Dissertations & Theses @ Portland State University; ProQuest Dissertations & Theses Global. (1648169512).
<http://stats.lib.pdx.edu/proxy.php?url=http://search.proquest.com.proxy.lib.pdx.edu/dissertations-theses/geology-petrology-enigmatic-rhyolites-at/docview/1648169512/se2?accountid=13265>
- Young, B. C. (2020). *Testing the Correlation of Trace Element Characteristics with the Petrology and Temperature of Eruption of Mid-Miocene Rhyolites in Eastern Oregon* (Order No. 27836528). Available from Dissertations & Theses @ Portland State University; ProQuest Dissertations & Theses Global. (2445560669).
<http://stats.lib.pdx.edu/proxy.php?url=http://search.proquest.com.proxy.lib.pdx.edu/dissertations-theses/testing-correlation-trace-element-characteristics/docview/2445560669/se-2?accountid=13265>

APPENDIX A:

Whole Rock Geochemical Data

A spreadsheet of the Strawberry Rhyolite Units that have more than one geochemical sample and their averages calculated. Multiple geochemical spreadsheets with their respective unit names have been broken down to categorize the Strawberry Rhyolites. Along with multiple more spreadsheets of all the non-Strawberry Rhyolite units found in the study area.

Strawberry Volcanic Rhyolite unit averages

*9 of the 12 units have more than one geochemical sample to generate an average.

Unit Name	Canyon Creek Rhyolite	Kent Spring Rhyolite	Wolf Mountain Rhyolite	Antelope Creek Rhyolite	Buckhorn Spring Rhyolite	Three Cabin Spring Rhyolite
Unit Abbreviation	Trcc	Trks	Trwm	Trac	Trbs	Trtcs
Amount of Samples in Average	4	7	8	2	2	9
XRF	Normalized Major Elements (Weight %):					
SiO2	76.52	76.82	73.22	77.02	74.01	77.36
TiO2	0.20	0.06	0.33	0.09	0.34	0.13
Al2O3	12.92	13.30	14.71	12.98	14.35	12.82
FeO*	1.15	0.82	2.27	0.91	1.83	0.92
MnO	0.03	0.04	0.05	0.04	0.02	0.02
MgO	0.13	0.04	0.24	0.07	0.16	0.09
CaO	0.82	0.56	1.92	0.69	1.34	0.72
Na2O	4.11	3.61	3.63	3.87	4.19	3.61
K2O	4.09	4.74	3.59	4.32	3.71	4.31
P2O5	0.03	0.01	0.06	0.01	0.04	0.02
*Pre Normalized Sum	98.11	96.83	96.54	99.26	98.56	98.87
LOI %	1.64	3.04	3.03	0.27	1.08	0.58
	Unnormalized Trace Elements (ppm):					
Ni	2.52	2.74	3.45	2.87	1.97	2.24
Cr	3.27	3.26	4.85	3.11	3.19	3.25
Sc	5.49	4.89	6.34	3.49	6.42	3.83
V	5.93	1.57	24.21	3.31	12.38	5.02
Ba	1205.55	648.14	1287.85	1271.39	1360.37	1435.20
Rb	91.39	109.27	80.55	101.38	79.57	111.61
Sr	79.79	28.49	217.97	59.70	162.60	70.53
Zr	212.55	74.53	201.49	93.92	272.52	118.71
Y	38.84	41.10	25.03	31.17	28.98	22.83
Nb	13.16	19.83	10.44	15.06	13.51	9.86
Ga	15.22	16.95	15.84	15.93	16.67	13.90
Cu	1.68	1.29	5.24	1.62	3.29	2.36
Zn	37.19	37.10	49.53	33.19	55.12	25.12
Pb	14.47	15.84	13.96	14.94	14.18	16.63
La	30.79	22.22	23.28	32.64	33.83	26.66
Ce	61.50	45.60	45.33	65.82	52.39	49.06
Th	8.24	10.23	7.02	10.23	6.52	9.62
Nd	27.45	21.58	20.26	27.14	28.51	19.47
U	3.95	4.34	3.70	4.08	3.13	3.91

Strawberry Volcanic Rhyolite Unit Averages

*9 of the 12 units have more than one geochemical sample to generate an average.

Unit Name	Canyon Creek Rhyolite	Kent Spring Rhyolite	Wolf Mountain Rhyolite	Antelope Creek Rhyolite	Buckhorn Spring Rhyolite	Three Cabin Spring Rhyolite
Unit Abbreviation	Trcc	Trks	Trwm	Trac	Trbs	Trtcs
ICP-MS						
La ppm	31.85	24.11	25.89	34.73	34.56	28.20
Ce ppm	63.13	49.87	47.25	68.19	56.38	52.43
Pr ppm	7.63	6.05	5.82	7.74	8.09	5.78
Nd ppm	28.34	22.90	21.66	28.05	29.47	20.22
Sm ppm	6.02	5.50	4.49	5.37	5.83	3.90
Eu ppm	0.80	0.57	0.94	0.77	1.19	0.53
Gd ppm	5.73	5.63	4.15	4.88	5.07	3.47
Tb ppm	1.01	1.06	0.71	0.86	0.85	0.60
Dy ppm	6.46	6.83	4.40	5.25	5.12	3.74
Ho ppm	1.36	1.42	0.92	1.08	1.06	0.78
Er ppm	3.95	4.05	2.65	3.08	2.91	2.24
Tm ppm	0.62	0.63	0.42	0.49	0.46	0.35
Yb ppm	4.01	4.11	2.76	3.26	3.02	2.32
Lu ppm	0.64	0.65	0.44	0.51	0.46	0.37
Ba ppm	1232.17	720.10	1306.88	1318.22	1396.44	1483.11
Th ppm	8.41	10.60	7.38	10.77	7.23	10.10
Nb ppm	13.02	19.88	10.33	14.94	13.38	8.77
Y ppm	37.61	39.79	25.60	31.11	28.07	22.04
Hf ppm	6.10	3.58	5.47	3.66	6.80	4.07
Ta ppm	1.01	1.86	0.84	1.43	0.98	0.84
U ppm	3.57	4.48	3.43	4.21	2.96	4.39
Pb ppm	13.70	14.98	13.35	14.37	13.71	15.86
Rb ppm	91.41	110.46	80.99	102.19	78.95	114.63
Cs ppm	3.69	4.42	3.89	4.23	1.98	5.06
Sr ppm	80.29	31.01	218.48	59.26	158.81	75.13
Sc ppm	5.25	4.79	6.43	4.22	6.24	3.99
Zr ppm	212.28	78.03	207.23	94.28	270.75	124.03

Strawberry Volcanic Rhyolite unit averages

*9 of the 12 units have more than one geochemical sample to generate an average.

Unit Name Unit Abbreviation	Bridge Creek Rhyolite Trbc	Elk Wallow Spring Rhyolite Trews	Milk Spring Tuff Tms
Amount of Samples in Average	3	2	2
XRF	Normalized Major Elements (Weight %):		
SiO ₂	73.39	76.30	59.60
TiO ₂	0.29	0.10	1.16
Al ₂ O ₃	14.20	13.67	16.42
FeO*	2.23	1.15	8.29
MnO	0.05	0.04	0.14
MgO	0.47	0.10	4.22
CaO	2.17	0.77	6.26
Na ₂ O	3.30	3.44	2.32
K ₂ O	3.83	4.41	1.29
P ₂ O ₅	0.08	0.02	0.31
*Pre Normalized Sum	97.33	95.82	92.19
LOI %	2.21	3.69	2.72
	Unnormalized Trace Elements (ppm):		
Ni	5.39	2.76	49.76
Cr	6.19	2.61	103.50
Sc	6.80	4.68	19.59
V	27.48	3.49	136.33
Ba	1183.04	1096.44	652.55
Rb	89.00	88.48	23.21
Sr	196.34	59.58	396.28
Zr	151.59	119.46	149.12
Y	29.33	43.27	24.88
Nb	9.35	14.83	9.52
Ga	15.81	16.44	16.47
Cu	7.47	4.32	31.04
Zn	49.93	42.34	90.72
Pb	14.14	14.78	5.88
La	26.81	32.68	19.93
Ce	43.78	55.58	40.62
Th	7.80	8.45	2.77
Nd	23.97	31.29	21.50
U	5.05	4.30	0.80

Strawberry Volcanic Rhyolite unit averages

*9 of the 12 units have more than one geochemical sample to generate an average.

Unit Name Unit Abbreviation	Bridge Creek Rhyolite Trbc	Elk Wallow Spring Rhyolite Trews	Milk Spring Tuff Ttms
ICP-MS			
La ppm	26.50	33.20	19.76
Ce ppm	44.82	57.48	40.79
Pr ppm	6.34	8.18	5.20
Nd ppm	24.24	31.56	21.10
Sm ppm	5.26	6.73	4.62
Eu ppm	0.98	0.82	1.37
Gd ppm	4.86	6.52	4.53
Tb ppm	0.82	1.15	0.73
Dy ppm	5.11	7.08	4.32
Ho ppm	1.05	1.47	0.89
Er ppm	2.98	4.30	2.43
Tm ppm	0.46	0.71	0.35
Yb ppm	2.95	4.69	2.25
Lu ppm	0.48	0.75	0.35
Ba ppm	1216.88	1122.74	655.66
Th ppm	8.38	9.29	2.39
Nb ppm	9.13	14.96	9.67
Y ppm	28.78	42.82	23.47
Hf ppm	4.35	4.40	3.57
Ta ppm	0.89	1.37	0.60
U ppm	4.46	4.21	0.81
Pb ppm	13.45	14.55	6.16
Rb ppm	87.86	88.34	22.60
Cs ppm	4.11	3.84	0.89
Sr ppm	195.80	58.65	388.22
Sc ppm	6.69	4.47	20.01
Zr ppm	152.03	117.56	145.38

Rhyolite of Buckhorn Spring (Trbs)

Sample ID	BC19C30	LVW-N-MS53
Quadrangle Unit	BC	LVW
Abbreviation	Trbs	Trbs
Latitude	44.2446	44.24516
Longitude	-118.75257	-118.72201
Thin Section Available	Yes	Yes
Age Date		
XRF	Normalized Major Elements (Weight %):	
SiO ₂	73.882	74.14
TiO ₂	0.337	0.34
Al ₂ O ₃	14.558	14.14
FeO*	1.299	2.37
MnO	0.011	0.03
MgO	0.154	0.16
CaO	1.537	1.15
Na ₂ O	4.458	3.93
K ₂ O	3.712	3.70
P ₂ O ₅	0.051	0.04
*Pre Normalized Sum	98.608	98.50
LOI %	1.077	1.07
Unnormalized Trace Elements (ppm):		
Ni	2	2
Cr	3	3
Sc	6	7
V	10	14
Ba	1408	1313
Rb	81	79
Sr	183	142
Zr	282	263
Y	28	30
Nb	13.1	14.0
Ga	17	17
Cu	3	4
Zn	60	50
Pb	14	14
La	30	38
Ce	51	54
Th	6	7
Nd	23	34
U	3	3

Rhyolite of Buckhorn Spring (Trbs)

ICP-MS

Sample ID	BC19C30	LVW-N-MS53
La ppm	30.84	38.28
Ce ppm	55.95	56.81
Pr ppm	6.93	9.25
Nd ppm	25.16	33.78
Sm ppm	5.27	6.39
Eu ppm	1.21	1.17
Gd ppm	4.80	5.33
Tb ppm	0.81	0.89
Dy ppm	5.03	5.20
Ho ppm	1.06	1.06
Er ppm	2.85	2.96
Tm ppm	0.44	0.49
Yb ppm	2.86	3.18
Lu ppm	0.45	0.48
Ba ppm	1452	1341
Th ppm	7.18	7.28
Nb ppm	12.87	13.90
Y ppm	27.33	28.81
Hf ppm	6.89	6.70
Ta ppm	0.93	1.02
U ppm	3.24	2.67
Pb ppm	13.69	13.73
Rb ppm	80.3	77.6
Cs ppm	2.20	1.75
Sr ppm	181	137
Sc ppm	5.9	6.5
Zr ppm	284	257

Rhyolite of Big Bend (Trbb)

Sample ID	LVW-N2-2
Quadrangle Unit	LVW
Abbreviation	Trbb
Latitude	44.1913706
Longitude	-118.747144
Thin Section Available	Yes
Age Date	

XRF	Normalized Major Elements (Weight %):
SiO2	70.41
TiO2	0.52
Al2O3	14.59
FeO*	3.69
MnO	0.09
MgO	0.58
CaO	2.34
Na2O	3.94
K2O	3.71
P2O5	0.13
*Pre Normalized Sum	98.43
LOI %	1.17

Unnormalized Trace Elements (ppm):	
Ni	2
Cr	2
Sc	10
V	15
Ba	1215
Rb	63
Sr	250
Zr	265
Y	41
Nb	14.6
Ga	18
Cu	2
Zn	84
Pb	11
La	35
Ce	61
Th	6
Nd	31
U	2

Rhyolite of Big Bend (Trbb)

ICP-MS

Sample ID	LVW-N2-2
La ppm	33.72
Ce ppm	62.67
Pr ppm	8.40
Nd ppm	32.73
Sm ppm	6.68
Eu ppm	1.39
Gd ppm	6.53
Tb ppm	1.08
Dy ppm	6.45
Ho ppm	1.39
Er ppm	3.96
Tm ppm	0.63
Yb ppm	4.00
Lu ppm	0.63
Ba ppm	1237
Th ppm	5.92
Nb ppm	14.35
Y ppm	39.86
Hf ppm	6.62
Ta ppm	0.97
U ppm	2.28
Pb ppm	11.66
Rb ppm	62.1
Cs ppm	2.01
Sr ppm	238
Sc ppm	9.0
Zr ppm	260

Rhyolite of Bridge Creek (Trbc)

Sample ID	JJ-17-05	JJ-17-8	AS-SV-173
Quadrangle Unit	JOJM	JOJM	Just South Southwest of JOJM Trbc
Abbreviation	Trbc	Trbc	Trbc
Latitude	44.0084	44.0162	44° 3'46.80"
Longitude	-118.8531	-118.8537	118°51'51.80"
Thin Section Available	Yes		
Age Date		14.39±0.03	14.7±0.13
XRF	Normalized Major Elements (Weight %):		
SiO ₂	73.174	73.679	73.328
TiO ₂	0.304	0.298	0.270
Al ₂ O ₃	14.398	13.952	14.237
FeO*	2.380	2.288	2.015
MnO	0.051	0.036	0.050
MgO	0.467	0.359	0.570
CaO	2.250	2.064	2.211
Na ₂ O	2.845	3.780	3.278
K ₂ O	4.057	3.466	3.964
P ₂ O ₅	0.074	0.078	0.077
*Pre Normalized Sum	95.883	98.781	
LOI %	3.642	0.780	
	Unnormalized Trace Elements (ppm):		
Ni	6	6	4.5
Cr	7	5	6.7
Sc	7	7	6.5
V	26	29	27.1
Ba	1163	1216	1169.9
Rb	85	90	92
Sr	205	191	192.8
Zr	152	165	137.7
Y	29	33	25.6
Nb	9.4	10.2	8.5
Ga	16	16	15.5
Cu	8	8	6.4
Zn	49	58	42.1
Pb	14	14	14.5
La	26	29	24.8
Ce	40	49	43.1
Th	8	7	8.5
Nd	25	28	18.8
U	5	4	5.8

Rhyolite of Bridge Creek (Trbc)

ICP-MS

Sample ID	JJ-17-05	JJ-17-8	AS-SV-173
La ppm	26.56	30.66	22.27
Ce ppm	43.88	47.03	43.55
Pr ppm	6.31	7.55	5.16
Nd ppm	24.00	29.51	19.21
Sm ppm	5.17	6.27	4.32
Eu ppm	1.03	1.15	0.77
Gd ppm	4.87	5.73	3.98
Tb ppm	0.83	0.95	0.68
Dy ppm	5.15	5.90	4.28
Ho ppm	1.06	1.20	0.89
Er ppm	2.97	3.40	2.55
Tm ppm	0.45	0.52	0.39
Yb ppm	2.78	3.44	2.61
Lu ppm	0.48	0.56	0.42
Ba ppm	1212	1247	1192
Th ppm	7.97	8.43	8.74
Nb ppm	9.32	9.79	8.28
Y ppm	29.40	32.16	24.79
Hf ppm	4.40	4.66	3.99
Ta ppm	0.89	0.93	0.83
U ppm	4.19	4.48	4.70
Pb ppm	13.15	13.90	13.30
Rb ppm	84.4	87.5	91.7
Cs ppm	4.07	3.83	4.42
Sr ppm	204	186	198
Sc ppm	7.0	7.0	6.2
Zr ppm	156	162	139

Rhyolite of Elk Wallow Spring (Trews)

Sample ID	LVW-S-2	RS20MPT2
Quadrangle Unit	LVW	MPT
Abbreviation	Trews	Trews
Latitude	44.161448	44.077
Longitude	-118.717	-118.72106
Thin Section Available	Yes	
Age Date		

XRF	Normalized Major Elements (Weight %):	
SiO2	75.78	76.82
TiO2	0.10	0.11
Al2O3	14.20	13.15
FeO*	1.26	1.04
MnO	0.04	0.04
MgO	0.08	0.13
CaO	0.71	0.84
Na2O	3.35	3.53
K2O	4.48	4.33
P2O5	0.01	0.02
*Pre Normalized Sum	95.40	96.25
LOI %	4.12	3.26

Unnormalized Trace Elements (ppm):		
Ni	3	3
Cr	3	2
Sc	6	4
V	4	2
Ba	1039	1154
Rb	81	96
Sr	45	74
Zr	130	109
Y	56	31
Nb	15.7	14.0
Ga	18	15
Cu	7	2
Zn	50	34
Pb	16	14
La	34	31
Ce	52	59
Th	8	9
Nd	36	26
U	4	4

Rhyolite of Elk Wallow Spring (Trews)

ICP-MS

Sample ID	LVW-S-2	RS20MPT2
La ppm	35.39	31.00
Ce ppm	54.47	60.49
Pr ppm	9.35	7.00
Nd ppm	36.95	26.18
Sm ppm	8.33	5.12
Eu ppm	0.84	0.81
Gd ppm	8.47	4.57
Tb ppm	1.50	0.81
Dy ppm	9.32	4.84
Ho ppm	1.94	1.01
Er ppm	5.68	2.92
Tm ppm	0.93	0.49
Yb ppm	6.19	3.19
Lu ppm	0.97	0.52
Ba ppm	1073	1173
Th ppm	8.38	10.20
Nb ppm	15.77	14.16
Y ppm	55.27	30.36
Hf ppm	5.00	3.81
Ta ppm	1.41	1.33
U ppm	4.02	4.40
Pb ppm	15.33	13.77
Rb ppm	81.0	95.6
Cs ppm	3.29	4.39
Sr ppm	45	72
Sc ppm	5.3	3.7
Zr ppm	128	107

Rhyolite of Kent Spring (Trks)

Sample ID	CD1932	CD1975	CD1876	AS-SV-63
Quadrangle Unit	BC	BC	JOJM	JOJM
Abbreviation	Trks	Trks	Trks	Trks
Latitude	44.1641	44.1639	44.1014	44° 6'56.00"
Longitude	-118.78826	-118.79323	-118.7706	118°44'56.00"
Thin Section Available	Yes	Yes		
Age Date		14.37 ± 0.02		
XRF	Normalized Major Elements (Weight %):			
SiO ₂	77.154	76.719	77.139	76.80
TiO ₂	0.046	0.053	0.062	0.058
Al ₂ O ₃	13.097	13.268	13.109	13.20
FeO*	0.750	0.836	0.809	0.80
MnO	0.045	0.043	0.041	0.040
MgO	0.032	0.044	0.054	0.03
CaO	0.506	0.548	0.577	0.53
Na ₂ O	3.483	3.480	3.351	3.93
K ₂ O	4.877	4.991	4.846	4.59
P ₂ O ₅	0.010	0.019	0.014	0.014
*Pre Normalized Sum	95.976	97.757	95.504	99.51
LOI %	3.619	2.032	3.497	
	Unnormalized Trace Elements (ppm):			
Ni	3	3	6	2
Cr	3	4	3	3
Sc	5	5	5	5
V	1	2	2	1
Ba	330	546	809	936
Rb	116	112	105	109
Sr	17	25	32	33
Zr	66	73	74	77
Y	45	42	38	39
Nb	21.7	20.5	18.2	19.3
Ga	17	18	15	18
Cu	2	2	2	0
Zn	37	36	34	34
Pb	15	15	15	18
La	16	22	23	24
Ce	35	40	51	55
Th	10	10	10	11
Nd	18	22	23	27
U	5	4	4	3

Rhyolite of Kent Spring (Trks)

Sample ID	AS-SV-133	AS-SV-134	LVW-S-66
Quadrangle Unit	BC	BC	LVW
Abbreviation	Trks	Trks	Trks
Latitude	44°10'7.60"	44°10'4.40"	44.12722894
Longitude	118°47'35.30"	118°47'33.40"	-118.7399601
Thin Section Available			Yes
Age Date			
XRF	Normalized Major Elements (Weight %):		
SiO ₂	76.88	76.82	76.23
TiO ₂	0.051	0.044	0.09
Al ₂ O ₃	13.35	13.23	13.83
FeO*	0.78	0.73	1.04
MnO	0.044	0.044	0.05
MgO	0.02	0.02	0.08
CaO	0.52	0.52	0.69
Na ₂ O	3.52	3.86	3.63
K ₂ O	4.83	4.72	4.33
P ₂ O ₅	0.011	0.012	0.02
*Pre Normalized Sum	95.33	97.34	96.41
LOI %			3.01
	Unnormalized Trace Elements (ppm):		
Ni	2	2	2
Cr	3	4	3
Sc	5	6	4
V	3	0	2
Ba	330	359	1227
Rb	114	114	95
Sr	17	18	58
Zr	66	67	99
Y	47	46	31
Nb	21.8	21.9	15.4
Ga	17	18	17
Cu	0	1	2
Zn	39	39	41
Pb	17	17	15
La	16	19	35
Ce	35	33	71
Th	10	10	11
Nd	19	17	26
U	6	5	4

Rhyolite of Kent Spring (Trks)

ICP-MS

Sample ID	CD1932	CD1975	CD1876	AS-SV-63	AS-SV-133	AS-SV-134	LVW-S-66
La ppm	16.91	22.88	24.41	27.72	17.84		34.92
Ce ppm	36.98	43.79	50.57	55.33	38.55		74.01
Pr ppm	4.71	5.93	6.13	6.81	5.02		7.73
Nd ppm	18.70	22.78	23.07	25.38	19.95		27.54
Sm ppm	5.29	5.76	5.44	5.62	5.62		5.24
Eu ppm	0.40	0.57	0.59	0.66	0.42		0.77
Gd ppm	5.96	5.99	5.35	5.60	6.14		4.75
Tb ppm	1.15	1.13	1.01	1.02	1.20		0.85
Dy ppm	7.75	7.39	6.45	6.47	7.94		4.99
Ho ppm	1.59	1.53	1.37	1.35	1.66		1.03
Er ppm	4.57	4.30	3.87	3.84	4.74		2.99
Tm ppm	0.72	0.66	0.61	0.58	0.73		0.49
Yb ppm	4.67	4.31	3.97	3.70	4.74		3.27
Lu ppm	0.73	0.68	0.64	0.60	0.74		0.51
Ba ppm	341	565	823	969	349		1273
Th ppm	10.19	10.65	10.19	10.80	10.44		11.34
Nb ppm	21.81	20.87	18.11	19.27	23.39		15.82
Y ppm	45.12	42.31	37.94	36.42	45.95		31.01
Hf ppm	3.50	3.61	3.41	3.57	3.60		3.78
Ta ppm	2.06	1.97	1.70	1.79	2.15		1.50
U ppm	4.67	4.45	4.28	4.42	4.79		4.27
Pb ppm	14.93	14.68	14.54	15.50	15.42		14.82
Rb ppm	116.5	112.6	106.3	111.9	119.6		95.9
Cs ppm	4.80	4.50	4.26	3.96	4.82		4.19
Sr ppm	17	26	34	33	18		58
Sc ppm	5.0	4.7	5.4	4.4	5.3		3.9
Zr ppm	68	75	76	81	71		98

Rhyolite of Kent Spring (Trks)

ICP-MS

Sample ID	AS-SV-133	AS-SV-134	LVW-S-66
La ppm	17.84		34.92
Ce ppm	38.55		74.01
Pr ppm	5.02		7.73
Nd ppm	19.95		27.54
Sm ppm	5.62		5.24
Eu ppm	0.42		0.77
Gd ppm	6.14		4.75
Tb ppm	1.20		0.85
Dy ppm	7.94		4.99
Ho ppm	1.66		1.03
Er ppm	4.74		2.99
Tm ppm	0.73		0.49
Yb ppm	4.74		3.27
Lu ppm	0.74		0.51
Ba ppm	349		1273
Th ppm	10.44		11.34
Nb ppm	23.39		15.82
Y ppm	45.95		31.01
Hf ppm	3.60		3.78
Ta ppm	2.15		1.50
U ppm	4.79		4.27
Pb ppm	15.42		14.82
Rb ppm	119.6		95.9
Cs ppm	4.82		4.19
Sr ppm	18		58
Sc ppm	5.3		3.9
Zr ppm	71		98

Rhyolite of Antelope Creek (Trac)

Sample ID	CD1879	LVW-S-26
Quadrangle Unit	JOJM	LVW
Abbreviation	Trac	Trac
Latitude	44.1136	44.1526307
Longitude	-118.7781	-118.724092
Thin Section Available	Yes	Yes
Age Date		

XRF	Normalized Major Elements (Weight %):	
SiO2	77.149	76.90
TiO2	0.085	0.09
Al2O3	13.015	12.95
FeO*	0.909	0.91
MnO	0.036	0.04
MgO	0.051	0.09
CaO	0.684	0.70
Na2O	3.742	3.99
K2O	4.318	4.32
P2O5	0.010	0.02
*Pre Normalized Sum	98.900	99.62
LOI %	0.517	0.03

Unnormalized Trace Elements (ppm):		
Ni	4	2
Cr	3	3
Sc	3	4
V	4	2
Ba	1254	1289
Rb	102	101
Sr	59	60
Zr	92	96
Y	31	31
Nb	15.2	15.0
Ga	16	16
Cu	2	1
Zn	33	34
Pb	15	15
La	31	35
Ce	64	68
Th	10	10
Nd	26	28
U	4	4

Rhyolite of Antelope Creek (Trac)

ICP-MS

Sample ID	CD1879	LVW-S-26
La ppm	34.72	34.74
Ce ppm	68.12	68.25
Pr ppm	7.72	7.76
Nd ppm	27.93	28.16
Sm ppm	5.49	5.25
Eu ppm	0.80	0.74
Gd ppm	4.96	4.80
Tb ppm	0.88	0.83
Dy ppm	5.57	4.94
Ho ppm	1.12	1.03
Er ppm	3.17	2.99
Tm ppm	0.49	0.49
Yb ppm	3.28	3.24
Lu ppm	0.51	0.50
Ba ppm	1314	1322
Th ppm	10.64	10.90
Nb ppm	14.94	14.94
Y ppm	30.90	31.33
Hf ppm	3.69	3.63
Ta ppm	1.42	1.44
U ppm	4.21	4.22
Pb ppm	14.30	14.44
Rb ppm	104.4	100.0
Cs ppm	4.18	4.28
Sr ppm	60	59
Sc ppm	4.7	3.8
Zr ppm	95	94

Rhyolite of Canyon Creek (Trcc)

Sample ID	MS1904A	AS-SV-190	LVW-N-25	AS-SV-179
Quadrangle Unit	BC	BC	LVW	BC
Abbreviation	Trcc	Trcc	Trcc	Trtcs
Latitude	44.2501333	44°13'25.40"	44.21937453	44°14'15.30"
Longitude	-118.8023	118°46'8.10"	-118.744795	118°46'43.10"
Thin Section Available			Yes	
Age Date		14.79 ± 0.17		15.30 ± 0.10
XRF	Normalized Major Elements (Weight %):			
SiO ₂	73.842	76.926	76.84	78.454
TiO ₂	0.286	0.188	0.20	0.145
Al ₂ O ₃	14.006	12.658	12.65	12.359
FeO*	1.910	1.188	1.21	0.296
MnO	0.055	0.037	0.04	0.002
MgO	0.219	0.134	0.17	0.001
CaO	1.170	0.814	0.85	0.450
Na ₂ O	4.216	4.121	4.12	3.991
K ₂ O	4.254	3.912	3.91	4.285
P ₂ O ₅	0.041	0.023	0.03	0.016
*Pre Normalized Sum	96.466		99.76	
LOI %	3.288		0.00	
	Unnormalized Trace Elements (ppm):			
Ni	2	3	1	3.4
Cr	3	3.2	3	3.4
Sc	6	5.1	5	5.6
V	9	5.2	7	2.7
Ba	1201	1222.6	1229	1169.7
Rb	87	89.2	91	98
Sr	124	73.4	80	41.4
Zr	281	171	183	216
Y	35	37.6	37	45.8
Nb	13.9	12.6	12.7	13.4
Ga	16	14.4	15	16
Cu	2	2.7	2	0.5
Zn	56	35.2	36	21.2
Pb	14	13.7	14	16.2
La	31	28.3	29	34.4
Ce	60	61.9	54	70.1
Th	8	8.4	8	8.8
Nd	27	26.3	24	32.1
U	4	4	3	4.6

Rhyolite of Canyon Creek (Trcc)

ICP-MS

Sample ID	MS1904A	AS-SV-190	LVW-N-25	AS-SV-179
La ppm	31.73	29.51	29.24	36.91
Ce ppm	63.82	59.07	58.66	70.96
Pr ppm	7.55	7.04	7.00	8.95
Nd ppm	27.98	26.15	25.82	33.40
Sm ppm	5.93	5.67	5.37	7.12
Eu ppm	1.04	0.80	0.72	0.66
Gd ppm	5.57	5.36	5.18	6.82
Tb ppm	0.97	0.97	0.92	1.20
Dy ppm	6.18	6.22	5.71	7.73
Ho ppm	1.31	1.31	1.22	1.62
Er ppm	3.73	3.88	3.61	4.57
Tm ppm	0.57	0.60	0.60	0.69
Yb ppm	3.84	3.96	3.91	4.34
Lu ppm	0.61	0.63	0.64	0.69
Ba ppm	1240	1255	1240	1195
Th ppm	8.01	8.46	8.27	8.89
Nb ppm	13.87	12.29	12.29	13.62
Y ppm	34.91	35.96	35.69	43.88
Hf ppm	7.35	5.38	5.31	6.37
Ta ppm	1.00	1.01	1.02	1.02
U ppm	3.44	3.42	3.37	4.04
Pb ppm	14.15	13.10	13.24	14.31
Rb ppm	85.9	90.5	88.9	100.4
Cs ppm	3.87	3.32	3.31	4.27
Sr ppm	122	77	77	45
Sc ppm	6.2	5.1	4.4	5.3
Zr ppm	280	171	179	220

Rhyolite of Three Cabin Spring (Trtcs)

Sample ID	CD1922	CD1905	MS-14-23	CD1845	AS-SV-85	AS-SV-61
Quadrangle Unit	BC	BC	BC	JOJM	BC	MPT
Abbreviation	Trtcs	Trtcs	Trtcs	Trtcs	Trtcs	Trtcs
Latitude	44.1332	44.1437	44.1734	44.1036	44°10'23.80"	44° 9'2.00"
Longitude	-118.79103	-118.8362	-118.7539	-118.8283	118°44'14.20"	118°44'28.00"
Thin Section Available	Yes	Yes				
Age Date				14.81±0.04		

XRF	Normalized Major Elements (Weight %):					
SiO ₂	77.768	76.021	77.588	77.287	77.36	77.11
TiO ₂	0.106	0.185	0.117	0.148	0.130	0.088
Al ₂ O ₃	12.377	13.815	12.483	12.694	12.76	13.38
FeO*	0.854	0.774	0.914	1.036	1.39	0.95
MnO	0.031	0.008	0.031	0.034	0.020	0.023
MgO	0.089	0.143	0.109	0.145	0.06	0.05
CaO	0.677	0.924	0.705	0.917	0.63	0.51
Na ₂ O	3.732	3.964	3.698	3.558	3.29	3.50
K ₂ O	4.353	4.147	4.338	4.159	4.34	4.38
P ₂ O ₅	0.013	0.019	0.017	0.021	0.020	0.017
*Pre Normalized Sum	99.154	98.414	99.189	99.143	98.79	98.05
LOI %	0.310	1.240		0.195		

Unnormalized Trace Elements (ppm):						
Ni	3	2	0	3	3	3
Cr	4	3	4	4	2	3
Sc	4	5	3	4	4	4
V	4	9	4	6	8	3
Ba	1383	1273	1500	1577	1587	1267
Rb	116	101	113	114	114	99
Sr	61	107	63	90	65	47
Zr	103	195	104	125	113	98
Y	23	21	24	22	20	27
Nb	8.7	11.6	9.2	8.8	8.9	15.8
Ga	14	16	13	13	13	15
Cu	3	2	3	3	2	1
Zn	25	28	27	26	19	29
Pb	16	16	17	16	18	16
La	28	31	26	25	22	29
Ce	50	56	50	45	41	57
Th	9	9	9	10	9	11
Nd	20	20	20	17	17	22
U	4	4	3	4	4	4

Rhyolite of Three Cabin Spring (Trtcs)

ICP-MS

Sample ID	CD1922	CD1905	MS-14-23	CD1845	AS-SV-85	AS-SV-61
La ppm	27.62	30.65	27.48	25.50		
Ce ppm	52.17	58.77	51.27	47.96		
Pr ppm	5.73	5.91	5.72	5.30		
Nd ppm	20.24	20.13	19.73	18.70		
Sm ppm	3.97	3.85	3.90	3.71		
Eu ppm	0.47	0.72	0.50	0.53		
Gd ppm	3.54	3.37	3.55	3.35		
Tb ppm	0.60	0.59	0.62	0.61		
Dy ppm	3.87	3.70	3.82	3.73		
Ho ppm	0.81	0.76	0.81	0.76		
Er ppm	2.34	2.24	2.30	2.25		
Tm ppm	0.36	0.36	0.36	0.35		
Yb ppm	2.41	2.30	2.40	2.30		
Lu ppm	0.38	0.35	0.38	0.38		
Ba ppm	1431	1319	1550	1619		
Th ppm	10.36	9.74	10.12	9.70		
Nb ppm	8.78	11.85	6.14	8.38		
Y ppm	23.29	20.61	22.79	21.69		
Hf ppm	3.63	5.94	3.64	4.00		
Ta ppm	0.87	0.95	0.62	0.82		
U ppm	4.55	4.05	4.35	4.32		
Pb ppm	15.91	15.45	15.77	15.39		
Rb ppm	116.5	100.8	114.4	117.6		
Cs ppm	5.46	3.24	5.02	5.48		
Sr ppm	62	106	66	89		
Sc ppm	3.4	5.0	3.4	4.5		
Zr ppm	103	195	107	129		

Rhyolite of Three Cabin Spring (Trtcs)

Sample ID	AS-SV-60	CD1830	RS20MPT47
Quadrangle Unit	MPT	JOJM	MPT
Abbreviation	Trtcs	Trtcs	Trtcs
Latitude	44° 9'50.00"	44.1187	44.07220651
Longitude	118°44'47.00"	-118.8224	-118.7229364
Thin Section Available		Yes	
Age Date			
XRF	Normalized Major Elements (Weight %):		
SiO2	77.71	77.743	77.67
TiO2	0.103	0.149	0.11
Al2O3	12.40	12.998	12.44
FeO*	0.85	0.654	0.90
MnO	0.030	0.008	0.03
MgO	0.08	0.058	0.10
CaO	0.68	0.789	0.69
Na2O	3.76	3.282	3.68
K2O	4.37	4.285	4.37
P2O5	0.015	0.033	0.02
*Pre Normalized Sum	99.42	98.271	99.38
LOI %		0.966	0.17
	Unnormalized Trace Elements (ppm):		
Ni	1	3	2
Cr	4	2	3
Sc	4	3	3
V	2	5	4
Ba	1408	1537	1384
Rb	116	116	116
Sr	59	81	61
Zr	99	124	107
Y	25	20	23
Nb	8.6	8.7	8.5
Ga	14	14	13
Cu	1	2	4
Zn	25	22	26
Pb	19	17	16
La	23	30	27
Ce	48	44	50
Th	10	9	10
Nd	20	20	19
U	4	4	5

Rhyolite of Three Cabin Spring (Trtcs)

ICP-MS

Sample ID	AS-SV-60	CD1830	RS20MPT47
La ppm	28.82	29.52	27.79
Ce ppm	54.48	50.09	52.27
Pr ppm	6.04	5.97	5.78
Nd ppm	21.18	21.21	20.38
Sm ppm	4.10	4.03	3.76
Eu ppm	0.46	0.62	0.44
Gd ppm	3.64	3.44	3.40
Tb ppm	0.64	0.60	0.59
Dy ppm	3.98	3.52	3.57
Ho ppm	0.84	0.71	0.75
Er ppm	2.42	1.94	2.23
Tm ppm	0.37	0.30	0.36
Yb ppm	2.49	1.90	2.43
Lu ppm	0.41	0.29	0.39
Ba ppm	1445	1586	1431
Th ppm	10.50	9.90	10.38
Nb ppm	8.88	8.54	8.81
Y ppm	22.89	19.78	23.21
Hf ppm	3.66	4.03	3.61
Ta ppm	0.86	0.84	0.91
U ppm	4.58	4.39	4.49
Pb ppm	16.11	16.04	16.38
Rb ppm	117.1	120.1	115.8
Cs ppm	5.53	5.08	5.59
Sr ppm	58	83	62
Sc ppm	3.6	4.7	3.3
Zr ppm	102	127	106

Rhyolite of Wolf Mountain (Trwm)

Sample ID	AS-SV-139	AS-SV-144	AS-SV-151	CD1877
Quadrangle Unit	JOJM	JOJM	JOJM	JOJM
Abbreviation	Trwm	Twmr	Trwm	Trwm
Latitude	44.0704	44.0786	44.0591	44.1190
Longitude	-118.7689	-118.7536	-118.7539	-118.7834
Thin Section Available				Yes
Age Date		15.34±0.52	16.16 ± 0.17	
XRF	Normalized Major Elements (Weight %):			
SiO ₂	73.375	72.987	73.191	71.349
TiO ₂	0.362	0.352	0.350	0.367
Al ₂ O ₃	14.899	15.000	14.569	16.379
FeO*	2.346	2.289	2.235	2.463
MnO	0.034	0.037	0.053	0.039
MgO	0.115	0.254	0.230	0.224
CaO	1.658	2.027	1.993	2.496
Na ₂ O	3.719	3.530	3.861	3.092
K ₂ O	3.409	3.470	3.422	3.563
P ₂ O ₅	0.082	0.054	0.097	0.029
*Pre Normalized Sum	97.639	95.007	98.086	96.025
LOI %				3.295
	Unnormalized Trace Elements (ppm):			
Ni	3	3	3	5
Cr	5	5	5	6
Sc	7	6	6	6
V	36	25	30	29
Ba	1472	1358	1430	1311
Rb	85	81	83	76
Sr	202	253	223	299
Zr	175	164	167	163
Y	20	20	19	18
Nb	10.1	9.2	9.4	9.0
Ga	16	15	16	17
Cu	8	3	7	7
Zn	48	43	49	43
Pb	14	15	15	15
La	30	24	25	0
Ce	44	37	49	34
Th	8	7	8	7
Nd	20	16	19	16
U	3	3	4	5

Rhyolite of Wolf Mountain (Trwm)

Sample ID	CD1883	CD1964	MS-17-05	RS20MPT49
Quadrangle Unit	JOJM	BC	JOJM	MPT
Abbreviation	Trwm	Trwm	Trwm	Trwm
Latitude	44.1044	44.1378	44.0652	44.06324561
Longitude	-118.7952	-118.79169	-118.7926	-118.7166629
Thin Section Available	Yes	Yes		Yes
Age Date			~15.0	
XRF	Normalized Major Elements (Weight %):			
SiO2	72.620	72.773	75.451	73.98
TiO2	0.331	0.325	0.224	0.30
Al2O3	14.783	14.980	13.324	13.71
FeO*	2.216	2.215	1.541	2.82
MnO	0.054	0.061	0.046	0.08
MgO	0.504	0.224	0.189	0.15
CaO	2.464	2.322	1.019	1.35
Na2O	3.622	3.406	3.656	4.17
K2O	3.301	3.664	4.511	3.39
P2O5	0.103	0.030	0.037	0.05
*Pre Normalized Sum	96.394	96.842	96.197	96.10
LOI %	2.646	2.613	3.251	3.34
	Unnormalized Trace Elements (ppm):			
Ni	4	3	5	2
Cr	5	6	4	2
Sc	5	5	6	10
V	29	29	10	5
Ba	1335	1380	1176	842
Rb	81	83	101	55
Sr	284	283	96	104
Zr	147	151	192	454
Y	19	17	36	53
Nb	7.4	7.5	11.3	19.6
Ga	16	16	15	17
Cu	6	7	2	3
Zn	45	43	45	81
Pb	15	14	14	11
La	23	24	33	28
Ce	47	38	57	56
Th	6	7	9	5
Nd	18	16	27	31
U	3	4	5	3

Rhyolite of Wolf Mountain (Trwm)

ICP-MS

Sample ID	AS-SV-139	AS-SV-144	AS-SV-151	CD1877
La ppm		24.86	25.41	22.94
Ce ppm		43.51	46.23	39.35
Pr ppm		5.14	5.36	4.89
Nd ppm		18.81	19.62	17.32
Sm ppm		3.69	3.82	3.35
Eu ppm		0.77	0.88	0.87
Gd ppm		3.24	3.35	2.87
Tb ppm		0.54	0.54	0.49
Dy ppm		3.33	3.26	3.07
Ho ppm		0.68	0.67	0.62
Er ppm		1.95	1.88	1.77
Tm ppm		0.30	0.29	0.27
Yb ppm		2.02	1.93	1.84
Lu ppm		0.33	0.32	0.29
Ba ppm		1450	1485	1330
Th ppm		7.35	7.70	7.74
Nb ppm		9.16	8.78	8.20
Y ppm		19.14	17.93	16.66
Hf ppm		4.59	4.59	4.42
Ta ppm		0.74	0.74	0.73
U ppm		3.42	3.67	3.17
Pb ppm		13.68	13.91	14.33
Rb ppm		84.2	86.7	75.3
Cs ppm		4.32	4.20	3.63
Sr ppm		258	231	284
Sc ppm		6.6	5.8	6.2
Zr ppm		172	171	163

Rhyolite of Wolf Mountain (Trwm)

ICP-MS

Sample ID	CD1883	CD1964	MS-17-05	RS20MPT49
La ppm	22.65	22.98	34.22	28.18
Ce ppm	42.25	41.78	59.54	58.08
Pr ppm	4.87	4.89	7.88	7.68
Nd ppm	17.62	17.45	29.31	31.53
Sm ppm	3.63	3.46	6.15	7.34
Eu ppm	0.78	0.81	0.76	1.72
Gd ppm	3.16	2.95	5.71	7.79
Tb ppm	0.53	0.49	0.99	1.36
Dy ppm	3.27	3.10	6.25	8.51
Ho ppm	0.68	0.63	1.33	1.86
Er ppm	1.88	1.80	3.81	5.51
Tm ppm	0.29	0.28	0.60	0.87
Yb ppm	1.92	1.87	3.93	5.83
Lu ppm	0.30	0.30	0.62	0.92
Ba ppm	1367	1422	1229	865
Th ppm	7.00	7.29	8.98	5.62
Nb ppm	7.46	7.63	11.50	19.59
Y ppm	18.34	17.47	36.55	53.10
Hf ppm	3.98	4.12	5.66	10.96
Ta ppm	0.67	0.68	0.95	1.39
U ppm	3.34	3.61	4.02	2.77
Pb ppm	13.16	13.41	14.30	10.67
Rb ppm	82.5	83.6	100.0	54.6
Cs ppm	4.25	4.05	4.62	2.15
Sr ppm	278	279	96	102
Sc ppm	5.7	5.5	5.1	10.2
Zr ppm	147	152	197	450

Milk Spring Tuff (Ttms)

Sample ID	LVW-N-MS46	MS-14-20
Quadrangle Unit	LVW	JOJM
Abbreviation	Ttms	Ttms
Latitude	44.23675	44.0341
Longitude	-118.72873	-118.8053
Thin Section Available	Yes	
Age Date		
XRF	Normalized Major Elements (Weight %):	
SiO2	56.61	62.597
TiO2	1.36	0.954
Al2O3	16.07	16.765
FeO*	9.04	7.543
MnO	0.16	0.122
MgO	5.23	3.215
CaO	7.27	5.245
Na2O	2.70	1.945
K2O	1.17	1.415
P2O5	0.41	0.199
*Pre Normalized Sum	95.09	89.282
LOI %	4.33	1.114
Unnormalized Trace Elements (ppm):		
Ni	85	14
Cr	164	43
Sc	23	17
V	181	91
Ba	535	770
Rb	23	23
Sr	412	380
Zr	141	157
Y	25	24
Nb	10.6	8.5
Ga	16	17
Cu	46	16
Zn	87	94
Pb	5	6
La	21	19
Ce	42	39
Th	2	4
Nd	22	21
U	1	1

Milk Spring Tuff (Ttms)

ICP-MS

Sample ID	LVW-N-MS46	MS-14-20
La ppm	19.34	20.17
Ce ppm	41.33	40.25
Pr ppm	5.31	5.09
Nd ppm	21.90	20.30
Sm ppm	4.78	4.46
Eu ppm	1.48	1.26
Gd ppm	4.74	4.31
Tb ppm	0.77	0.69
Dy ppm	4.38	4.25
Ho ppm	0.90	0.88
Er ppm	2.47	2.39
Tm ppm	0.36	0.35
Yb ppm	2.33	2.17
Lu ppm	0.36	0.34
Ba ppm	535	777
Th ppm	1.87	2.91
Nb ppm	10.67	8.67
Y ppm	24.26	22.68
Hf ppm	3.31	3.83
Ta ppm	0.64	0.56
U ppm	0.68	0.94
Pb ppm	5.21	7.10
Rb ppm	23.1	22.1
Cs ppm	0.59	1.19
Sr ppm	398	378
Sc ppm	22.3	17.7
Zr ppm	139	152

Milk Spring Tuff, Unit 1 (Ttms1)

Sample ID	JJ18A6.7D2
Quadrangle Unit	JOJM
Abbreviation	Ttms1
Latitude	44.03869929
Longitude	-118.7907317
Thin Section Available	Yes

Age Date

XRF	Normalized Major Elements (Weight %):
SiO2	74.57
TiO2	0.20
Al2O3	14.30
FeO*	2.51
MnO	0.07
MgO	0.36
CaO	0.69
Na2O	2.72
K2O	4.56
P2O5	0.02

*Pre Normalized Sum

LOI %

Unnormalized Trace Elements (ppm):	
Ni	7
Cr	2
Sc	6
V	7
Ba	1271
Rb	65
Sr	39
Zr	476
Y	92
Nb	23.9
Ga	25
Cu	6
Zn	147
Pb	19
La	53
Ce	108
Th	8
Nd	53
U	3

Milk Spring Tuff, Unit 1 (Ttms1)

ICP-MS

Sample ID	JJ18A6.7D2
La ppm	54.81
Ce ppm	113.69
Pr ppm	14.13
Nd ppm	55.57
Sm ppm	12.68
Eu ppm	2.19
Gd ppm	13.14
Tb ppm	2.45
Dy ppm	16.29
Ho ppm	3.50
Er ppm	10.10
Tm ppm	1.57
Yb ppm	10.06
Lu ppm	1.60
Ba ppm	1298
Th ppm	8.53
Nb ppm	23.71
Y ppm	93.08
Hf ppm	12.80
Ta ppm	1.57
U ppm	3.08
Pb ppm	18.80
Rb ppm	68.8
Cs ppm	2.46
Sr ppm	40
Sc ppm	5.3
Zr ppm	483

*Unassigned Rhyolite Unit

Sample ID	RS20MPT45
Quadrangle Unit	MPT
Abbreviation	*unassigned /Perlitic Rhyolite
Latitude	44.0581531
Longitude	-118.6925051
Thin Section Available	Yes

Age Date

XRF	Normalized Major Elements (Weight %):
SiO2	74.83
TiO2	0.29
Al2O3	13.51
FeO*	2.74
MnO	0.06
MgO	0.17
CaO	1.09
Na2O	3.57
K2O	3.71
P2O5	0.05
*Pre Normalized Sum	96.02
LOI %	3.81

Unnormalized Trace Elements (ppm):

Ni	2
Cr	2
Sc	10
V	6
Ba	806
Rb	58
Sr	103
Zr	424
Y	41
Nb	20.2
Ga	17
Cu	2
Zn	76
Pb	11
La	24
Ce	50
Th	5
Nd	24
U	3

***Unassigned Rhyolite Unit**

ICP-MS

Sample ID	RS20MPT45
La ppm	24.97
Ce ppm	51.91
Pr ppm	6.51
Nd ppm	26.37
Sm ppm	5.84
Eu ppm	1.24
Gd ppm	5.94
Tb ppm	1.06
Dy ppm	6.43
Ho ppm	1.43
Er ppm	4.25
Tm ppm	0.69
Yb ppm	4.27
Lu ppm	0.75
Ba ppm	830
Th ppm	5.83
Nb ppm	19.74
Y ppm	40.32
Hf ppm	10.37
Ta ppm	1.39
U ppm	2.83
Pb ppm	10.90
Rb ppm	57.9
Cs ppm	2.19
Sr ppm	102
Sc ppm	9.6
Zr ppm	421

All other units that are not the Strawberry Rhyolites

Sample ID	MS-18-02	MS-18-05	BC19B47	MS-15-38
Quadrangle Unit	JOJ	JOJ	BC	JOJ
Abbreviation	Thsd	Tmus	Tdit1	Tdit1
Latitude	44.0132	44.0122	44.2029	44.0106
Longitude	-118.7819	-118.7907	-118.8028	-118.7819
Thin Section Available			yes	
Age Date	Oligocene, ~23 ma			
SiO2	66.671	76.147	75.211	75.456
TiO2	0.727	0.311	0.223	0.184
Al2O3	20.790	19.389	12.995	12.676
FeO*	1.761	1.334	2.089	2.446
MnO	0.012	0.014	0.049	0.058
MgO	0.423	0.323	0.043	0.154
CaO	4.652	0.267	0.346	0.664
Na2O	3.705	0.408	3.322	2.497
K2O	1.088	1.793	5.709	5.851
P2O5	0.170	0.015	0.013	0.015
*Pre Normalized Sum	94.740	90.775	95.566	94.645
LOI %	4.688	8.502	3.911	4.086
Ni	6.368	2.600	2.338	1.881
Cr	16.418	14.600	3.682	0.792
Sc	9.453	7.200	2.289	4.257
V	60.695	41.700	2.438	5.940
Ba	1315.589	436.800	1803.338	1372.239
Rb	7.118	97.020	79.755	90.684
Sr	593.717	35.600	45.024	35.343
Zr	152.414	113.643	407.244	448.700
Y	10.945	27.700	62.785	106.326
Nb	9.552	22.100	24.278	24.354
Ga	20.895	20.800	21.641	21.087
Cu	14.129	8.100	2.687	4.356
Zn	31.044	52.600	136.415	168.795
Pb	17.512	13.200	15.124	18.117
La	17.512	24.600	43.581	56.232
Ce	33.731	35.800	85.968	99.396
Th	3.582	10.200	6.070	6.831
Nd	14.428	17.000	44.377	59.499
U	2.388	3.200	4.080	4.059

All other units that are not the Strawberry Rhyolites

Sample ID	PFC1548	MS-15-21A	MS-15-21B
Quadrangle Unit	JOJ	JOJ	JOJ
Abbreviation	Tdit1	Tdit2	Tdit2
Latitude	44.0068	44.0092	44.0092
Longitude	-118.8324	-118.8238	-118.8238
Thin Section Available			
Age Date			
XRF	Normalized Major Elements (Weight %):		
SiO2	75.899	74.210	70.418
TiO2	0.171	0.215	0.529
Al2O3	12.344	12.876	13.542
FeO*	2.140	2.695	5.175
MnO	0.064	0.055	0.123
MgO	0.046	0.071	0.288
CaO	0.544	0.939	1.921
Na2O	2.816	2.963	3.904
K2O	5.965	5.962	3.964
P2O5	0.011	0.014	0.135
*Pre Normalized Sum	95.771	95.365	96.329
LOI %	2.957	3.409	2.767
Unnormalized Trace Elements (ppm):			
Ni	1.111	3.773	3.078
Cr	3.737	1.192	14.796
Sc	4.343	2.284	11.916
V	4.646	1.887	11.817
Ba	1445.108	1566.855	1415.819
Rb	81.810	84.008	70.900
Sr	28.886	93.541	168.413
Zr	441.775	391.800	350.700
Y	92.213	72.390	66.829
Nb	23.937	21.250	20.456
Ga	20.705	21.548	21.052
Cu	2.626	3.277	6.057
Zn	150.591	137.133	158.781
Pb	19.695	15.789	13.505
La	48.076	41.110	35.847
Ce	92.516	88.576	83.313
Th	7.575	7.646	6.554
Nd	47.773	43.295	40.316
U	3.535	3.277	3.575

All other units that are not the Strawberry Rhyolites

ICP-MS

Sample ID	MS-18-02	MS-18-05	BC19B47	MS-15-38
La ppm	19.984	23.561	43.916	61.463
Ce ppm	37.279	37.446	89.236	102.689
Pr ppm	4.397	5.346	11.720	15.690
Nd ppm	15.799	19.215	46.436	62.515
Sm ppm	3.054	4.065	10.589	14.401
Eu ppm	1.201	0.585	1.988	2.160
Gd ppm	2.504	3.850	10.080	15.225
Tb ppm	0.403	0.696	1.794	2.761
Dy ppm	2.286	4.483	11.648	18.597
Ho ppm	0.438	0.912	2.444	4.038
Er ppm	1.100	2.560	6.976	11.765
Tm ppm	0.157	0.394	1.062	1.814
Yb ppm	1.001	2.558	6.799	11.694
Lu ppm	0.143	0.413	1.071	1.864
Ba ppm	1340.882	446.195	1826.435	1425.876
Th ppm	4.902	10.239	7.157	8.120
Nb ppm	9.033	21.021	23.715	24.231
Y ppm	10.290	26.845	63.079	106.601
Hf ppm	3.739	3.641	10.298	12.231
Ta ppm	0.700	1.983	1.469	1.477
U ppm	1.429	3.385	3.475	3.626
Pb ppm	17.117	12.475	14.702	17.944
Rb ppm	6.854	97.363	76.314	88.897
Cs ppm	0.323	6.470	2.740	3.000
Sr ppm	566.233	35.102	44.973	37.172
Sc ppm	9.156	8.026	2.260	4.048
Zr ppm	150.494	110.557	407.138	457.901

All other units that are not the Strawberry Rhyolites

ICP-MS

Sample ID	PFC1548	MS-15-21A	MS-15-21B
La ppm	46.645	43.852	40.402
Ce ppm	95.690	90.423	85.619
Pr ppm	12.393	11.561	10.945
Nd ppm	49.743	46.364	44.443
Sm ppm	11.707	10.572	10.695
Eu ppm	1.709	2.090	2.614
Gd ppm	12.289	10.857	10.594
Tb ppm	2.320	1.980	1.900
Dy ppm	15.539	12.699	12.032
Ho ppm	3.445	2.749	2.563
Er ppm	10.215	7.905	7.343
Tm ppm	1.597	1.196	1.103
Yb ppm	10.460	7.723	7.104
Lu ppm	1.707	1.235	1.125
Ba ppm	1474.396	1632.830	1459.677
Th ppm	7.806	7.264	6.550
Nb ppm	23.504	21.402	20.949
Y ppm	90.622	71.687	66.648
Hf ppm	11.979	10.397	9.317
Ta ppm	1.441	1.395	1.329
U ppm	3.474	3.041	2.726
Pb ppm	17.106	15.690	13.712
Rb ppm	81.371	81.933	69.253
Cs ppm	2.953	3.348	3.001
Sr ppm	30.923	95.659	173.819
Sc ppm	3.297	2.894	13.003
Zr ppm	449.178	402.138	362.373

All other units that are not the Strawberry Rhyolites

Sample ID	CD1936A	SV-177A	SV-177B
Quadrangle Unit	BC		
Abbreviation	Tdit4	Tdit	Tdit
Latitude	44.2457	44° 0'33.00"	44° 0'33.00"
Longitude	-118.8027	118°49'25.80"	118°49'25.80"
Thin Section Available	yes		
Age Date			
XRF	Normalized Major Elements (Weight %):		
SiO2	71.934	74.352	71.856
TiO2	0.325	0.232	0.433
Al2O3	16.200	13.024	13.368
FeO*	2.259	2.383	4.451
MnO	0.057	0.069	0.093
MgO	1.539	0.042	0.217
CaO	1.723	1.003	1.398
Na2O	2.773	2.980	2.193
K2O	3.141	5.888	5.893
P2O5	0.050	0.027	0.097
*Pre Normalized Sum	88.379		
LOI %	11.240		
	Unnormalized Trace Elements (ppm):		
Ni	1.397	3.100	3.100
Cr	7.032	2.800	9.200
Sc	6.434	3.500	10.100
V	10.522	3.100	8.500
Ba	863.337	1618.600	1456.900
Rb	61.288	80.600	78.200
Sr	134.663	96.100	133.700
Zr	299.297	386.900	367.100
Y	42.544	73.200	66.400
Nb	14.715	21.700	20.700
Ga	16.758	22.200	21.700
Cu	2.892	4.500	5.600
Zn	66.384	145.600	143.200
Pb	14.561	16.300	16.100
La	30.470	44.500	38.400
Ce	64.000	91.700	82.900
Th	7.929	7.000	6.000
Nd	27.182	44.200	42.500
U	2.642	2.300	3.400

All other units that are not the Strawberry Rhyolites

Sample ID	MS-15-25A	CD18116	MS-19-05
Quadrangle Unit	JOJ	JOJ	BC
Abbreviation	Tdit2	Tdit2	Tdit4
Latitude	44.0049	44.0125	44.2450
Longitude	-118.8377	-118.8723	-118.8095
Thin Section Available			
Age Date			
XRF	Normalized Major Elements (Weight %):		
SiO ₂	75.597	63.155	68.913
TiO ₂	0.214	1.575	0.997
Al ₂ O ₃	13.296	15.534	14.554
FeO*	1.546	7.486	5.107
MnO	0.015	0.115	0.088
MgO	0.094	1.647	0.861
CaO	0.436	4.322	2.287
Na ₂ O	4.722	3.622	3.563
K ₂ O	4.059	1.732	3.313
P ₂ O ₅	0.022	0.811	0.316
*Pre Normalized Sum		93.858	94.884
LOI %	1.212	5.784	4.775
Unnormalized Trace Elements (ppm):			
Ni	2.383	7.900	0.743
Cr	1.986	9.700	2.574
Sc	2.681	21.100	14.801
V	5.958	101.800	58.856
Ba	1665.360	844.900	963.963
Rb	73.283	38.906	65.378
Sr	89.767	345.500	211.860
Zr	423.200	231.944	306.985
Y	49.650	47.600	48.708
Nb	23.137	15.300	19.454
Ga	22.740	20.000	20.147
Cu	1.986	12.300	3.960
Zn	113.401	155.200	133.700
Pb	14.796	10.200	13.118
La	30.783	31.900	37.917
Ce	64.049	63.600	74.547
Th	7.845	5.000	5.544
Nd	36.741	37.800	39.006
U	1.490	1.500	3.564

All other units that are not the Strawberry Rhyolites

ICP-MS

Sample ID	CD1936A	SV-177A	SV-177B
La ppm	31.240		
Ce ppm	69.789		
Pr ppm	7.467		
Nd ppm	28.127		
Sm ppm	5.945		
Eu ppm	0.986		
Gd ppm	5.812		
Tb ppm	1.038		
Dy ppm	6.789		
Ho ppm	1.453		
Er ppm	4.372		
Tm ppm	0.691		
Yb ppm	4.518		
Lu ppm	0.737		
Ba ppm	896.197		
Th ppm	8.238		
Nb ppm	14.721		
Y ppm	42.420		
Hf ppm	7.606		
Ta ppm	1.037		
U ppm	2.963		
Pb ppm	13.991		
Rb ppm	59.786		
Cs ppm	3.321		
Sr ppm	133.381		
Sc ppm	6.683		
Zr ppm	297.562		

All other units that are not the Strawberry Rhyolites

ICP-MS

Sample ID	MS-15-25A	CD18116	MS-19-05
La ppm	37.237	30.486	36.807
Ce ppm	67.450	65.332	76.465
Pr ppm	9.816	8.740	9.852
Nd ppm	39.288	37.257	40.233
Sm ppm	8.959	8.601	9.150
Eu ppm	2.156	2.481	2.126
Gd ppm	8.410	8.604	9.016
Tb ppm	1.493	1.456	1.523
Dy ppm	9.450	8.981	9.249
Ho ppm	1.950	1.836	1.954
Er ppm	5.521	4.974	5.345
Tm ppm	0.834	0.713	0.783
Yb ppm	5.290	4.569	4.923
Lu ppm	0.819	0.741	0.788
Ba ppm	1733.603	846.618	981.683
Th ppm	7.749	4.938	6.577
Nb ppm	22.822	14.859	19.383
Y ppm	49.117	47.151	49.212
Hf ppm	11.196	6.102	8.040
Ta ppm	1.449	0.995	1.282
U ppm	2.406	2.578	2.808
Pb ppm	14.299	9.413	12.758
Rb ppm	71.915	41.050	64.316
Cs ppm	1.495	1.580	2.926
Sr ppm	94.478	345.392	210.671
Sc ppm	2.794	21.615	14.734
Zr ppm	433.472	237.256	311.453

All other units that are not the Strawberry Rhyolites

Sample ID	CD1982	MS-18-01	RS20MPT29	ASSV111	ASSV137
Quadrangle Unit	BC	JOJ	MPT		
Abbreviation Latitude	Tdct	Tdct	Tdct	Tdct	Tdct
Longitude	44.1704	44.0332	44.0343	44° 5'45.90"	44° 7'45.00"
Thin Section Available	-118.8618	-118.7516	-118.6958	118°39'24.90"	118°48'56.30"
Age Date					
XRF	Normalized Major Elements (Weight %):				
SiO2	77.040	76.906	76.978	76.624	76.994
TiO2	0.204	0.194	0.190	0.214	0.248
Al2O3	11.028	10.924	10.851	11.093	11.857
FeO*	2.502	2.850	2.862	2.724	2.090
MnO	0.053	0.061	0.054	0.044	0.035
MgO	0.024	0.000	0.062	0.027	0.022
CaO	0.108	0.171	0.160	0.152	0.350
Na2O	3.906	3.884	3.574	3.577	2.959
K2O	5.125	5.005	5.253	5.534	5.430
P2O5	0.009	0.006	0.015	0.012	0.014
*Pre Normalized Sum	96.502	96.291	97.149		
LOI %	3.001	2.988	2.157		
	Unnormalized Trace Elements (ppm):				
Ni	2.692	3.317	1.504	2.500	3.100
Cr	3.141	2.513	2.638	3.800	4.300
Sc	0.300	1.508	0.558	0.600	1.800
V	2.790	0.000	3.957	3.600	5.500
Ba	49.352	36.281	53.969	60.700	592.300
Rb	122.529	137.112	132.407	117.100	112.100
Sr	3.483	3.518	6.598	7.800	45.400
Zr	1038.745	1182.684	1176.276	937.100	799.000
Y	127.431	146.730	140.001	134.100	99.900
Nb	73.216	84.018	80.247	67.300	58.200
Ga	26.783	27.638	28.847	27.400	28.900
Cu	4.938	5.729	11.109	5.800	3.700
Zn	203.592	239.291	233.589	214.900	153.000
Pb	26.883	31.356	30.181	25.500	22.900
Ce	100.400	103.616	87.500	106.600	101.600
La	195.319	203.010	172.467	193.500	199.800
Th	11.200	13.769	13.182	11.300	10.500
Nd	96.600	93.063	91.564	97.600	94.500
U	3.941	4.824	5.580	3.400	3.900

All other units that are not the Strawberry Rhyolites

Sample ID	ASSV243	ASSV246	R20MPT38	RS20MPT40	RS20MPT41
Quadrangle Unit			MPT	MPT	MPT
Abbreviation	Tdct	Tdct	Trst	Trst	Trst
Latitude	43°47'52.00"	43°51'6.00"	44.0348	44.0317	44.0294
Longitude	118°50'41.00	118°48'23.00	-118.6829	-118.6801	-118.6841
Thin Section Available					
Age Date					
XRF	Normalized Major Elements (Weight %):				
SiO2	76.802	76.459	76.814	76.840	76.803
TiO2	0.208	0.252	0.156	0.169	0.178
Al2O3	11.284	11.560	12.386	12.126	12.642
FeO*	2.633	2.580	1.567	1.669	1.799
MnO	0.062	0.034	0.078	0.061	0.059
MgO	0.011	0.030	0.069	0.068	0.061
CaO	0.137	0.195	0.218	0.301	0.131
Na2O	4.192	2.882	3.148	3.403	3.750
K2O	4.644	5.993	5.550	5.339	4.566
P2O5	0.026	0.015	0.013	0.023	0.010
*Pre Normalized Sum			96.064	96.416	98.457
LOI %			3.425	3.262	1.260
	Unnormalized Trace Elements (ppm):				
Ni	1.796	2.494	2.370	1.665	1.180
Cr	3.691	4.190	3.486	3.658	3.884
Sc	1.397	0.698	4.242	5.380	4.939
V	7.980	5.287	4.446	4.370	7.417
Ba	63.740	112.119	672.735	794.666	727.115
Rb	115.511	108.927	88.063	85.566	86.005
Sr	6.983	15.362	13.029	17.289	12.423
Zr	768.674	843.486	313.641	322.322	347.938
Y	56.459	111.421	87.812	107.239	28.202
Nb	55.760	62.444	29.709	28.194	30.320
Ga	28.130	28.828	19.467	18.959	21.155
Cu	3.292	5.48625	4.5475	4.31795	4.4894
Zn	186.732	185.23575	104.3845	105.867	96.3095
Pb	26.534	23.3415	18.44155	17.9826	18.5664
Ce	61.346	102.543	40.21825	80.82375	6.7119
La	149.625	203.6895	85.58895	91.0455	55.2384
Th	10.973	10.07475	7.979	6.902	7.878
Nd	63.341	93.5655	48.95855	89.7139	5.1408
U	2.095	4.9875	4.04	3.3495	2.626

All other units that are not the Strawberry Rhyolites

ICP-MS

Sample ID	CD1982	MS-18-01	RS20MPT29	ASSV111	ASSV137
La ppm	105.194	93.291	91.938		
Ce ppm	203.700	196.106	179.416		
Pr ppm	26.322	24.503	24.082		
Nd ppm	102.077	96.525	95.797		
Sm ppm	22.602	22.792	21.639		
Eu ppm	0.760	0.708	0.738		
Gd ppm	22.071	23.323	22.086		
Tb ppm	3.858	4.214	3.964		
Dy ppm	24.548	27.281	24.069		
Ho ppm	5.069	5.712	5.179		
Er ppm	14.410	16.231	14.850		
Tm ppm	2.147	2.422	2.373		
Yb ppm	13.621	15.422	15.022		
Lu ppm	2.148	2.444	2.363		
Ba ppm	48.516	32.785	55.542		
Th ppm	12.815	14.028	13.830		
Nb ppm	72.338	81.285	77.117		
Y ppm	129.322	146.711	141.561		
Hf ppm	23.257	25.936	25.580		
Ta ppm	4.435	5.017	4.919		
U ppm	4.885	5.537	5.477		
Pb ppm	26.773	31.142	30.484		
Rb ppm	123.335	142.296	132.333		
Cs ppm	3.586	4.113	4.135		
Sr ppm	4.665	4.771	9.048		
Sc ppm	0.088	-0.703	0.546		
Zr ppm	1059.549	1194.361	1137.841		

All other units that are not the Strawberry Rhyolites

ICP-MS

Sample ID	ASSV243	ASSV246	R20MPT38	RS20MPT40	RS20MPT41
La ppm			41.555497	83.223487	5.9748182
Ce ppm			90.052112	93.020917	57.157703
Pr ppm			12.606219	23.805329	1.4361753
Nd ppm			50.135874	92.007588	5.7035934
Sm ppm			12.515152	20.627517	1.7168892
Eu ppm			1.3601718	2.9369858	0.8384912
Gd ppm			12.951728	18.859818	2.3170839
Tb ppm			2.4141557	3.3723211	0.5644298
Dy ppm			14.856804	19.61154	4.0795974
Ho ppm			3.2026928	4.019999	1.0286308
Er ppm			9.1392972	11.045783	3.3631124
Tm ppm			1.4474098	1.7248143	0.607205
Yb ppm			9.3825811	10.941973	4.3813012
Lu ppm			1.468861	1.6574712	0.7136439
Ba ppm			692.33142	818.90193	755.37985
Th ppm			8.1818275	7.7201341	8.4385259
Nb ppm			28.723561	27.480509	29.753804
Y ppm			87.576623	107.62645	28.604115
Hf ppm			9.4664523	9.5235258	10.337887
Ta ppm			1.8548662	1.7651473	1.8917641
U ppm			3.4898905	3.4251568	2.7920689
Pb ppm			19.08714	18.169965	18.472452
Rb ppm			88.288504	86.391573	85.523884
Cs ppm			3.2895355	3.2331256	1.6976659
Sr ppm			14.198155	19.64625	13.978138
Sc ppm			4.397446	4.7496455	4.2588662
Zr ppm			310.87636	324.58985	349.19829

All other units that are not the Strawberry Rhyolites

Sample ID	ASSV135	CD1938	BC19B36	CD18125	CD18109
Quadrangle Unit		BC	BC	JOJ	JOJ
Abbreviation	Trst	Tbsv	Tbsv	Ttsb	Ttsb
Latitude	44°10'4.10"	44.2369	44.2454	44.0205	44.0067
Longitude	118°48'20.40	-118.8475	-118.8054	-118.7582	-118.8676
Thin Section Available			yes		
Age Date					
XRF	Normalized Major Elements (Weight %):				
SiO ₂	76.864	50.722	50.903	53.560	50.757
TiO ₂	0.138	1.256	1.453	1.349	1.415
Al ₂ O ₃	12.014	17.150	16.663	17.494	17.412
FeO*	1.478	9.718	9.746	8.659	9.861
MnO	0.068	0.118	0.158	0.143	0.182
MgO	0.068	7.130	7.344	5.503	6.846
CaO	0.299	10.320	9.543	8.835	9.224
Na ₂ O	2.743	2.693	2.996	3.218	3.166
K ₂ O	6.318	0.597	0.840	0.835	0.641
P ₂ O ₅	0.011	0.297	0.353	0.404	0.495
*Pre Normalized Sum		95.682	98.964	98.047	97.567
LOI %		3.889	0.621	1.628	1.789
Unnormalized Trace Elements (ppm):					
Ni	2.600	142.200	138.787	49.949	93.331
Cr	3.100	303.026	202.762	132.335	111.540
Sc	3.600	31.699	27.038	25.572	26.268
V	4.200	258.620	236.006	218.104	244.472
Ba	626.900	272.996	282.547	544.564	328.549
Rb	98.300	11.640	10.326	10.335	6.728
Sr	12.700	372.977	469.747	516.604	521.878
Zr	281.800	79.691	108.421	139.644	115.958
Y	92.600	23.206	23.295	27.064	26.766
Nb	29.600	6.222	8.668	9.552	9.751
Ga	19.900	16.293	17.927	18.607	18.806
Cu	1.1	49.5735	63.730	24.378	67.063
Zn	104	74.60725	86.188	99.500	99.003
Pb	20.7	2.079	3.054	5.871	4.975
Ce	38.1	11.385	12.214	16.716	17.015
La	86.2	24.428	30.289	42.984	40.198
Th	7.2	0.394	0.690	1.791	0.697
Nd	47.8	14.3326667	18.321	22.189	23.781
U	2.9	0.83725	2.315	0.995	0.796

All other units that are not the Strawberry Rhyolites

ICP-MS

Sample ID	ASSV135	CD1938	BC19B36	CD18125	CD18109
La ppm		11.0736761	13.179	18.837	16.296
Ce ppm		22.9207825	30.226	39.680	37.612
Pr ppm		3.25920014	4.091	5.231	5.151
Nd ppm		14.3894944	17.911	22.019	22.486
Sm ppm		3.38979263	4.465	5.080	5.144
Eu ppm		1.24086089	1.529	1.571	1.663
Gd ppm		3.88422533	4.653	4.956	5.053
Tb ppm		0.64218132	0.743	0.791	0.841
Dy ppm		4.03651582	4.537	4.781	4.987
Ho ppm		0.83836677	0.933	0.980	1.018
Er ppm		2.27083047	2.509	2.636	2.728
Tm ppm		0.31555406	0.349	0.384	0.383
Yb ppm		1.99349769	2.170	2.337	2.380
Lu ppm		0.29715845	0.330	0.380	0.382
Ba ppm		271.037211	277.653	542.830	319.866
Th ppm		0.69880809	0.979	1.608	0.726
Nb ppm		6.41768544	8.938	9.430	8.986
Y ppm		23.0709966	23.369	26.363	26.419
Hf ppm		2.02294347	2.719	3.429	2.823
Ta ppm		0.39414523	0.577	0.568	0.487
U ppm		0.26163232	0.347	0.489	0.263
Pb ppm		1.94870467	2.451	4.648	3.024
Rb ppm		10.3883791	7.461	9.478	6.466
Cs ppm		0.90635427	0.206	0.389	0.206
Sr ppm		377.65969	473.049	522.060	533.534
Sc ppm		31.0101284	27.586	25.115	28.655
Zr ppm		80.2670699	109.208	141.569	119.184

All other units that are not the Strawberry Rhyolites

Sample ID	SW-JJ17-9	MS-17-08	BC19B07	BC19C15	MS-15-23A
Quadrangle Unit	JOJ	JOJ	BC	BC	JOJ
Abbreviation	Ttsb	Ttsb	Tvpd	Tvpd	Tvpd
Latitude	44.0225	44.1154	44.2285	44.2020	44.0086
Longitude	-118.8406	-118.8712	-118.8135	-118.7922	-118.8280
Thin Section Available			yes	yes	
Age Date					
XRF	Normalized Major Elements (Weight %):				
SiO2	50.265	48.922	53.655	54.399	59.588
TiO2	1.453	1.108	1.439	1.254	1.859
Al2O3	17.262	17.923	17.354	16.703	15.304
FeO*	10.484	10.117	9.856	8.603	8.921
MnO	0.179	0.285	0.166	0.163	0.176
MgO	6.415	9.211	4.887	5.789	1.791
CaO	9.284	9.316	8.459	7.981	5.383
Na2O	3.423	2.694	3.143	3.464	3.872
K2O	0.674	0.287	0.626	1.116	1.989
P2O5	0.559	0.136	0.415	0.527	1.118
*Pre Normalized Sum	98.203	96.126	94.132	98.922	95.122
LOI %	1.051	3.394	5.392	0.522	3.716
	Unnormalized Trace Elements (ppm):				
Ni	97.220	147.980	72.602	108.429	5.462
Cr	87.961	147.882	128.726	176.065	1.192
Sc	26.891	33.908	24.439	23.422	22.740
V	240.931	186.298	140.842	191.600	114.096
Ba	382.968	149.548	479.259	597.729	1004.916
Rb	7.913	4.320	5.363	11.310	45.479
Sr	573.432	313.074	520.515	515.702	406.832
Zr	125.395	75.362	113.972	153.622	196.300
Y	27.876	24.794	23.571	32.604	42.997
Nb	10.540	1.666	7.395	11.612	13.406
Ga	18.223	14.896	17.519	17.913	18.867
Cu	75.550	71.442	45.358	34.091	8.341
Zn	101.554	71.148	90.764	90.865	124.423
Pb	3.152	2.352	3.582	5.308	6.057
Ce	17.238	2.450	15.433	27.540	26.910
La	43.439	15.288	29.284	48.140	60.970
Th	1.281	0.392	0.990	1.683	4.071
Nd	23.246	12.054	19.005	27.691	35.649
U	2.561	0.490	1.787	1.391	3.575

All other units that are not the Strawberry Rhyolites

ICP-MS

Sample ID	SW-JJ17-9	MS-17-08	BC19B07	BC19C15	MS-15-23A
La ppm	17.432	5.578	14.962	27.255	28.832
Ce ppm	41.095	14.523	30.852	47.644	63.084
Pr ppm	5.712	2.218	4.460	7.045	8.583
Nd ppm	24.415	10.392	19.076	28.919	36.769
Sm ppm	5.646	2.972	4.624	6.335	8.670
Eu ppm	1.781	1.194	1.480	1.937	2.837
Gd ppm	5.462	3.659	4.624	6.277	8.649
Tb ppm	0.901	0.670	0.726	0.993	1.392
Dy ppm	5.424	4.486	4.441	5.902	8.430
Ho ppm	1.086	0.985	0.901	1.233	1.710
Er ppm	2.936	2.821	2.461	3.191	4.617
Tm ppm	0.417	0.406	0.347	0.463	0.654
Yb ppm	2.607	2.637	2.189	2.947	4.075
Lu ppm	0.405	0.414	0.346	0.476	0.646
Ba ppm	384.085	143.619	483.873	591.303	1028.849
Th ppm	0.620	0.370	1.166	1.785	4.039
Nb ppm	9.685	1.846	7.715	11.803	13.878
Y ppm	27.703	24.825	23.656	32.171	44.029
Hf ppm	2.993	1.921	2.763	3.624	5.217
Ta ppm	0.515	0.130	0.481	0.677	0.917
U ppm	0.229	0.132	0.406	0.560	2.370
Pb ppm	2.793	1.172	3.479	5.403	7.211
Rb ppm	5.962	2.964	2.217	9.619	44.662
Cs ppm	0.137	0.516	0.190	0.176	2.030
Sr ppm	579.232	319.205	513.660	516.355	417.106
Sc ppm	27.112	35.797	24.339	22.760	23.960
Zr ppm	123.593	76.502	114.492	153.640	202.141

All other units that are not the Strawberry Rhyolites

Sample ID	MS-15-23B	MS-15-23C	MS-18-03b	MS-14-17	CD1972
Quadrangle Unit	JOJ	JOJ	JOJ	JOJ	BC
Abbreviation	Tvpd	Tvpd	Tvpd	Tvpd	Tasv
Latitude	44.0086	44.0086	44.0293	44.0118	44.1867
Longitude	-118.8280	-118.8280	-118.7967	-118.8410	-118.7853
Thin Section Available					
Age Date					
XRF	Normalized Major Elements (Weight %):				
SiO2	59.782	57.906	61.793	59.582	61.170
TiO2	1.875	1.838	1.905	1.933	1.000
Al2O3	15.000	16.088	16.242	15.255	16.104
FeO*	9.102	9.362	6.228	9.068	6.672
MnO	0.172	0.185	0.113	0.171	0.127
MgO	1.932	1.514	0.696	1.842	2.849
CaO	5.194	5.766	5.154	5.095	6.193
Na2O	4.254	4.323	4.324	4.274	3.747
K2O	1.811	1.395	2.156	1.912	1.790
P2O5	0.879	1.623	1.390	0.868	0.348
*Pre Normalized Sum	97.661	94.647	95.040	97.461	99.531
LOI %	2.235	5.205	4.204		0.000
	Unnormalized Trace Elements (ppm):				
Ni	7.348	7.979	7.700	5.174	8.767
Cr	0.000	0.000	2.700	12.040	17.139
Sc	24.130	24.231	24.600	24.179	18.124
V	120.054	66.094	114.300	135.818	155.778
Ba	1072.043	1106.057	1183.500	998.284	901.571
Rb	38.826	11.525	41.062	37.313	35.367
Sr	415.769	411.336	427.100	409.343	456.400
Zr	192.300	208.100	211.761	196.513	147.569
Y	42.401	51.713	74.700	47.462	25.758
Nb	13.505	15.169	15.100	14.428	8.126
Ga	19.264	19.799	20.800	19.502	17.878
Cu	7.050	9.653	9.800	11.542	19.700
Zn	133.360	122.633	130.600	145.071	80.524
Pb	8.043	6.895	8.000	8.756	8.274
Ce	27.605	30.732	38.600	31.044	19.306
La	59.183	67.177	69.500	58.506	44.768
Th	3.078	4.137	4.500	3.881	2.955
Nd	33.266	40.287	49.900	38.706	22.458
U	2.681	3.349	3.500	0.597	1.970

All other units that are not the Strawberry Rhyolites

ICP-MS

Sample ID	MS-15-23B	MS-15-23C	MS-18-03b	MS-14-17	CD1972
La ppm	27.825	34.400	40.496	29.618	21.278
Ce ppm	61.222	65.752	72.990	60.435	43.241
Pr ppm	8.413	9.770	11.504	8.879	5.505
Nd ppm	36.436	41.488	50.235	38.263	22.217
Sm ppm	8.609	9.656	11.835	9.183	5.006
Eu ppm	2.878	3.004	3.587	2.929	1.445
Gd ppm	8.489	9.524	12.778	9.500	4.826
Tb ppm	1.381	1.562	2.111	1.514	0.772
Dy ppm	8.475	9.487	13.155	9.101	4.862
Ho ppm	1.687	1.971	2.730	1.858	0.975
Er ppm	4.525	5.299	7.533	5.035	2.618
Tm ppm	0.634	0.755	1.111	0.719	0.385
Yb ppm	3.868	4.717	7.190	4.521	2.381
Lu ppm	0.625	0.760	1.178	0.702	0.362
Ba ppm	1094.390	1148.062	1193.803	1000.155	906.442
Th ppm	3.801	4.162	4.197	3.884	3.113
Nb ppm	13.599	14.883	14.715	13.282	8.202
Y ppm	43.438	52.538	75.805	46.916	25.334
Hf ppm	5.023	5.525	5.531	4.979	3.761
Ta ppm	0.842	0.913	0.930	0.859	0.549
U ppm	1.739	3.535	3.274	1.895	1.132
Pb ppm	7.636	5.867	7.032	7.731	7.493
Rb ppm	37.934	10.848	43.603	35.821	34.851
Cs ppm	2.432	0.401	1.482	1.811	1.092
Sr ppm	431.272	428.313	433.078	409.783	461.810
Sc ppm	25.178	24.978	26.766	24.614	18.639
Zr ppm	197.761	214.302	217.865	193.056	147.850

All other units that are not the Strawberry Rhyolites

Sample ID	BC19A22	BC19B45	CD1852	CD1841	CD18124
Quadrangle	BC	BC	JJO	JJO	JJO
Unit Abbreviation	Tasv	Tasv	Tsva	Tsva	Tsva
Latitude	44.1911	44.2370	44.1093	44.0926	44.1087
Longitude	-118.8419	-118.8091	-118.8739	-118.8229	-118.7829
Thin Section	yes	yes			
Available Age Date			~16-12 ma	~16-12 ma	~16-12 ma
XRF	Normalized Major Elements (Weight %):				
SiO2	60.868	62.276	61.279	62.456	59.167
TiO2	1.010	0.731	1.318	0.763	0.869
Al2O3	16.085	16.481	15.714	16.582	18.155
FeO*	6.811	5.593	7.193	5.457	6.568
MnO	0.131	0.111	0.141	0.102	0.146
MgO	2.923	3.011	2.417	3.019	3.819
CaO	6.262	5.993	5.557	5.718	6.409
Na2O	3.780	3.484	3.918	3.372	3.347
K2O	1.773	2.047	1.956	2.310	1.289
P2O5	0.358	0.273	0.508	0.221	0.231
*Pre Normalized Sum	99.483	97.052	99.124	98.326	97.722
LOI %	0.000	2.626	0.289	1.144	2.008
	Unnormalized Trace Elements (ppm):				
Ni	11.623	27.770	6.965	35.621	46.069
Cr	22.015	48.659	13.234	60.098	75.322
Sc	18.272	15.741	17.612	17.114	21.890
V	150.213	120.830	141.788	128.256	121.092
Ba	884.727	894.465	949.031	818.587	701.077
Rb	35.271	38.703	35.393	45.435	22.133
Sr	459.650	460.152	442.875	378.100	410.438
Zr	148.538	167.889	179.498	157.357	150.148
Y	25.462	23.018	33.731	23.980	25.273
Nb	8.520	8.712	11.940	7.463	7.562
Ga	18.617	16.880	19.502	17.114	18.806
Cu	20.390	35.442	13.831	28.457	22.487
Zn	81.854	70.488	96.913	65.372	77.411
Pb	7.782	8.514	8.557	8.259	6.070
Ce	22.261	23.562	26.268	15.622	25.870
La	41.961	46.184	53.034	45.472	39.303
Th	2.463	3.366	3.483	4.179	3.085
Nd	22.951	22.671	28.955	22.388	25.373
U	2.906	2.376	2.587	2.090	1.095

All other units that are not the Strawberry Rhyolites

ICP-MS

Sample ID	BC19A22	BC19B45	CD1852	CD1841	CD18124
La ppm	21.985	24.540	25.530	20.531	24.533
Ce ppm	43.834	48.097	52.854	40.785	42.092
Pr ppm	5.768	5.833	6.850	5.060	6.266
Nd ppm	23.231	22.615	28.182	20.214	24.361
Sm ppm	5.048	4.666	6.266	4.346	5.265
Eu ppm	1.498	1.277	1.828	1.199	1.438
Gd ppm	5.013	4.345	6.161	4.189	4.851
Tb ppm	0.810	0.673	1.018	0.707	0.805
Dy ppm	5.001	4.254	6.255	4.330	4.906
Ho ppm	1.004	0.853	1.270	0.866	0.945
Er ppm	2.722	2.383	3.371	2.481	2.567
Tm ppm	0.386	0.352	0.496	0.372	0.387
Yb ppm	2.490	2.175	3.119	2.317	2.383
Lu ppm	0.390	0.357	0.486	0.369	0.374
Ba ppm	894.734	899.461	951.601	820.942	699.120
Th ppm	3.081	3.561	3.306	3.938	3.529
Nb ppm	8.414	9.047	11.619	7.811	7.339
Y ppm	26.431	23.002	32.627	23.293	24.783
Hf ppm	3.754	4.146	4.512	3.992	3.802
Ta ppm	0.548	0.592	0.745	0.549	0.500
U ppm	1.174	1.300	1.319	1.477	1.212
Pb ppm	7.557	8.577	7.937	8.074	6.308
Rb ppm	34.472	35.529	36.490	47.086	22.880
Cs ppm	1.123	1.158	1.244	1.472	0.796
Sr ppm	467.606	452.055	440.685	379.533	417.871
Sc ppm	18.712	15.731	18.723	17.644	21.749
Zr ppm	149.957	169.393	183.390	160.796	153.737

All other units that are not the Strawberry Rhyolites

Sample ID	BC19A45	BC19A01	BC19A07
Quadrangle	BC	BC	BC
Unit Abbreviation	Itss	Itss	Kpm
Latitude	44.2224	44.2073	44.2206
Longitude	-118.8697	-118.8715	-118.8681
Thin Section Available	yes	yes	yes
Age Date			
XRF	Normalized Major Elements (Weight %):		
SiO2	57.907	71.255	47.492
TiO2	0.904	0.553	0.012
Al2O3	16.515	13.864	0.843
FeO*	7.347	2.995	8.560
MnO	0.148	0.039	0.250
MgO	3.751	1.378	42.604
CaO	7.550	5.918	0.209
Na2O	3.699	1.722	0.000
K2O	2.003	2.149	0.015
P2O5	0.176	0.128	0.016
*Pre Normalized Sum	94.368	95.888	84.444
LOI %	5.114	3.613	14.399
	Unnormalized Trace Elements (ppm):		
Ni	15.821	11.406	2233.479
Cr	41.939	20.689	2872.008
Sc	24.527	14.317	11.250
V	178.652	83.687	44.521
Ba	697.296	362.417	31.419
Rb	73.954	86.930	2.419
Sr	442.924	383.543	5.900
Zr	148.552	141.657	7.195
Y	26.766	24.886	2.332
Nb	4.229	3.949	0.000
Ga	16.318	13.873	2.538
Cu	44.526	29.528	8.506
Zn	70.446	55.891	59.065
Pb	7.761	8.739	1.235
Ce	12.537	13.563	0.823
La	27.114	22.557	0.137
Th	5.274	6.565	0.137
Nd	15.323	13.790	0.000
U	2.736	3.013	1.372

All other units that are not the Strawberry Rhyolites

ICP-MS

Sample ID	BC19A45	BC19A01	BC19A07
La ppm	12.179	12.040	0.319
Ce ppm	26.991	25.967	0.142
Pr ppm	3.678	3.514	0.087
Nd ppm	15.722	14.918	0.426
Sm ppm	4.176	3.829	0.102
Eu ppm	1.039	0.918	0.028
Gd ppm	4.398	4.058	0.123
Tb ppm	0.751	0.686	0.021
Dy ppm	4.770	4.563	0.116
Ho ppm	1.015	0.957	0.023
Er ppm	2.902	2.630	0.065
Tm ppm	0.426	0.401	0.010
Yb ppm	2.650	2.635	0.059
Lu ppm	0.426	0.412	0.007
Ba ppm	691.180	361.522	22.840
Th ppm	5.395	6.419	0.041
Nb ppm	4.233	3.891	0.080
Y ppm	27.199	24.874	0.906
Hf ppm	4.075	4.107	0.013
Ta ppm	0.329	0.349	0.027
U ppm	2.443	2.936	0.003
Pb ppm	7.839	8.789	0.013
Rb ppm	72.874	83.991	-0.588 0.396
Cs ppm	6.328	1.617	
Sr ppm	442.569	377.046	6.816
Sc ppm	24.982	13.738	11.634
Zr ppm	149.497	141.163	1.740

APPENDIX B:

Actual Area Sums per Outcrop Mapped

Table showing the actual calculated values of each unit by their outcrops determined by field mapping. Geometry for the areas was calculated using the sum of each units' polygon produced in ArcMap. Unit thicknesses and volume are estimates, which allow an average volume per unit to be estimated.

*Area values are for the true field mapped polygons generated in ArcMap

Unit Name	Area Sum (Km2)	Estimated Unit Thickness (m)		Estimated Volume (Km3)		Average Volume (km3)
		Min	Max	Min	Max	
Qa Alluvium	35.52	0.10	1.00	0.00	0.04	0.02
Trst Rattlesnake Tuff	13.96	5.00	20.00	0.07	0.28	0.17
Tdet Devine Canyon Tuff	7.27	5.00	15.00	0.04	0.11	0.07
Tbsv Basalt to Basaltic Andesite	2.22	3.00	30.00	0.01	0.07	0.04
Tpvd Near Vent Pyroclastic Deposits	1.53	3.00	10.00	0.00	0.02	0.01
Tasv Andesite of Strawberry Volcanics	163.66	5.00	180.00	0.82	29.46	15.14
Ttms Milk Spring Tuff	5.49	5.00	30.00	0.03	0.16	0.10
Trbs Buckhorn Spring Rhyolite	1.08	20.00	120.00	0.02	0.13	0.08
Trbb Big Bend Rhyolite	0.85	20.00	40.00	0.02	0.03	0.03
Trbc Bridge Creek Rhyolite	19.93	40.00	100.00	0.80	1.99	1.40
Trews Elk Wallow Spring Rhyolite	16.97	40.00	200.00	0.68	3.39	2.04
Trks Kent Spring Rhyolite	21.87	40.00	200.00	0.87	4.37	2.62
Trac Antelope Creek Rhyolite	11.65	3.00	70.00	0.03	0.82	0.43
Trcc Canyon Creek Rhyolite	7.72	40.00	100.00	0.31	0.77	0.54
Trtes Three Canyon Spring Rhyolite	40.90	40.00	180.00	1.64	7.36	4.50
Trwm Wolf Mountain Rhyolite	59.45	50.00	200.00	2.97	11.89	7.43
Tdit4 Dinner Creek Tuff, unit 4	3.26	3.00	8.00	0.01	0.03	0.02
Tdit2 Dinner Creek Tuff, unit 2	2.18	3.00	10.00	0.01	0.02	0.01
Tdit1 Dinner Creek Tuff, unit 1	20.23	3.00	30.00	0.06	0.61	0.33
Tmus Mullen Spring Volcanic Clastics	0.22	8.00	20.00	0.00	0.00	0.00
Thsd Holdout Spring Dacite	0.14	4.00	8.00	0.00	0.00	0.00
Itss Clastic Sedimentary Rocks	28.33	10.00	400.00	0.28	11.33	5.81
Kpm Ultramafic Rocks	0.31	3.00	10.00	0.00	0.00	0.00
Total area of all units:					464.75	km2
Total area of the SV Rhyolites:					180.79	km2

APPENDIX C:

List of abbreviations found throughout this study.

LIST OF ABBREVIATIONS

Map Units:

Qa	Qaternary Alluvium
Trst	Rattlesnake Tuff
Tdct	Devine Canyon Tuff
Tbsv	Basalt to Basaltic Andesite
Tpvd	Near Vent Pyroclastic Deposits
Tasv	Andesite of Strawberry Volcanics
Ttms	Milk Spring Tuff
Ttms1	Milk Spring Tuff, unit 1
Trbs	Buckhorn Spring Rhyolite
Trbb	Big Bend Rhyolite
Trbc	Bridge Creek Rhyolite
Trews	Elk Wallow Spring Rhyolite
Trks	Kent Spring Rhyolite
Trac	Antelope Creek Rhyolite
Trcc	Canyon Creek Rhyolite
Trtcs	Three Canyon Spring Rhyolite
Trwm	Wolf Mountain Rhyolite
Tdit4	Dinner Creek Tuff, unit 4
Tdit2	Dinner Creek Tuff, unit 2
Tdit1	Dinner Creek Tuff, unit 1
Tmus	Mullen Spring Volcanic Clastics
Thsd	Holdout Spring Dacite
Itss	Clastic Sedimentary Rocks
Kpm	Ultramafic Rocks

LIST OF ABBREVIATIONS

Other Abbreviations Mentioned:

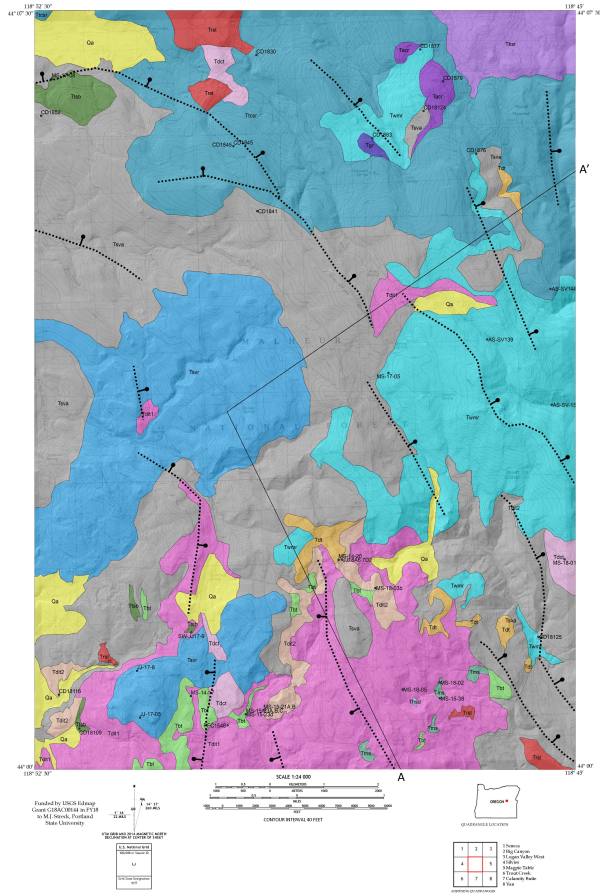
JOJM	Jump-off Joe Mountain Quadrangle
BC	Big Canyon Quadrangle
MPT	Magpie Table Quadrangle
LVW	Logan Valley West Quadrangle
SR	Strawberry Rhyolites
CRBG	Columbia River Basalt Group
HLP	High Lava Plains
XRF	X-ray fluorescence spectrometer
ICP-MS	Inductively coupled plasma mass spectrometry
ArcGIS	Aeronautical Reconnaissance Coverage Geographic Information System, made up of four fundamental applications with ArcMap being one for viewing and editing spatial and geographic data.
XPL	Cross Polarized Light
PSU	Portland State University, Oregon USA
USGS	United States Geological Survey
PPL	Plane Polarized Light
EDMAP	EDMAP is the component of the NCGMP that funds universities to train the next generation of geologic mappers. EDMAP is a one-year, mentor-guided program designed to teach students geologic mapping techniques through rigorous field mapping. Colleges and universities in the United States and Puerto Rico are eligible to apply through an annual competitive grants process. Every Federal dollar that is awarded is matched with university funds. Geology professors, who are skilled in geologic mapping, request EDMAP funding to support undergraduate and graduate students at their college or university in a one-year mentored geologic mapping project. Although individual projects last for only one year, they may build upon the results of previous years' efforts. EDMAP geology professors and their students frequently work closely with STATEMAP and FEDMAP geologists who may be mapping nearby.

APPENDIX D:

Geologic Map of the Jump-Off Joe Mountain Quadrangle, Oregon, USGS EdMap project. (Dvorak, C.L. and Streck, M.J., 2018)

Geologic Map of the Big Canyon Quadrangle, Oregon, USGS EdMap project. (Dvorak, C.L. and Streck, M.J., 2018)

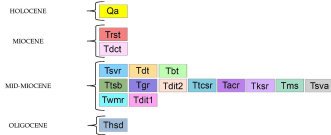
GEOLOGIC MAP OF THE JUMP-OFF JOE QUADRANGLE, OREGON
 Chanel L. Dvorak and Martin J. Streck
 2019



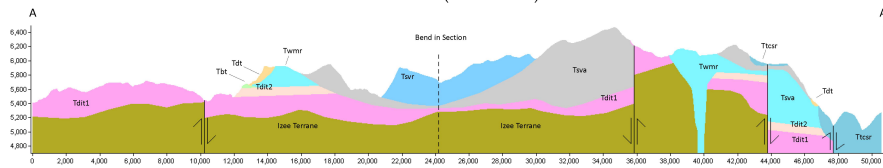
DESCRIPTION OF MAP UNITS

- Qa** ALLUVIUM (Holocene) - Composed largely of clay, silt, and fine to coarse sand.
 - Trst** RATTLESNAKE TUFF (7.1 Ma) - High-silica rhyolitic tuff, ranging from incipiently welded to densely welded and less than 20 m thick. The tuff is often vitric and contains ~1% phenocryst.
 - Tdct** DEVINE CANYON TUFF (9.7 Ma) - Crystal-rich (25%) to crystal-poor (4%), high-silica rhyolite. Partially to densely welded, observed thickness is up to a few meters.
 - Tdt** MILK SPRING TUFF (Mid-Miocene) - Stratified member (mostly 1-2 m, up to 10 m consisting of thinly bedded fallout and surge) overlain by ash-flow tuff (up to ~10 m) with small, lapilli-sized pumices. Lithics include Tdt and Tsvr. White to light gray matrix.
 - Tbt** SCORIA PYROCLASTIC FLOW DEPOSIT (Mid-Miocene) - Vesiculated lapilli to bomb-sized, red to black scoria, includes locally fallout spatter deposits.
 - Ttsb** TAMARACK SPRING BASALT (Mid-Miocene) - Dark colored, coarse grained groundmass, with 20% plagioclase.
 - Tsva** ANDESITE OF STRAWBERRY VOLCANICS (16-12 Ma) -Aphyric to phenocryst-poor lavas throughout map extent. Phenocryst content ranges from 0-15% plagioclase <1 mm in length. Outcrops are platy to blocky in habit. Occasionally intercalated basalt lavas that can be vesiculated and light gray.
 - Tsvr** STRAWBERRY BIOTITE-AMPHIBOLE RHYOLITE (14 Ma) - 3%-5% biotite and amphibole phenocrysts. Groundmass is often glassy, porous to give rock a light greenish gray appearance. Outcrops are large and blocky.
 - Ttcsr** THREE CABIN SPRING RHYOLITE (Mid-Miocene) -Mostly aphyric, flow banded rhyolite; occurs as glassy (lob-sided) or light colored, devitrified rock, found in close proximity to glassy member.
 - Twmr** WOLF MOUNTAIN RHYOLITE (15 Ma) - Dark gray glassy or pinkish devitrified, plagioclase rich (up to 30%) rhyolite, typically flow banded.
 - Tacr** ANTELOPE CREEK RHYOLITE (Mid-Miocene) - Glassy to devitrified rhyolite with 1% plagioclase (does not contain biotite).
 - Tksr** KENT SPRING RHYOLITE (Mid-Miocene) - Light gray groundmass with 1% biotite and 3% plagioclase.
 - Tgr** UNDIFFERENTIATED RHYOLITE (Mid-Miocene) - Undifferentiated glassy groundmass.
 - Tms** MULLEN SPRING (Mid-Miocene) -Undifferentiated volcanic clastics - epiclastic, pyroclastic, debris flow deposits. Epiclastic member is crystal rich with distinctive quartz phenocrysts. Debris flow member with blocks of dacite (Thsd) and rhyolite and is overlain by non-welded ignimbrite.
 - Tdit2** DINNER CREEK UNIT II (12.5 Ma) - Incipiently to partially welded tuff. Gray with <5% plagioclase phenocrysts. Abundant white to gray pumices up to 10 cm in length. Typically contains glassy lithic fragments. On west side of map with distinctive scoria. Less than 10 meters thick.
 - Tdit1** DINNER CREEK TUFF UNIT (16.1 Ma) - High-silica rhyolitic tuff, partially to densely welded, containing 1-5% crystals with a pinkish devitrified or dark gray glassy groundmass. Rheomorphic sections 20-80 m thick. Lithophyses and spherulites are common in outcrop.
 - Thsd** HOLDOUT SPRING DACITE (Oligocene) - Greenish in color, containing large (up to ~1 cm) plagioclase phenocrysts.
- Approximate location of fault
● Sample location with geo-analytical data

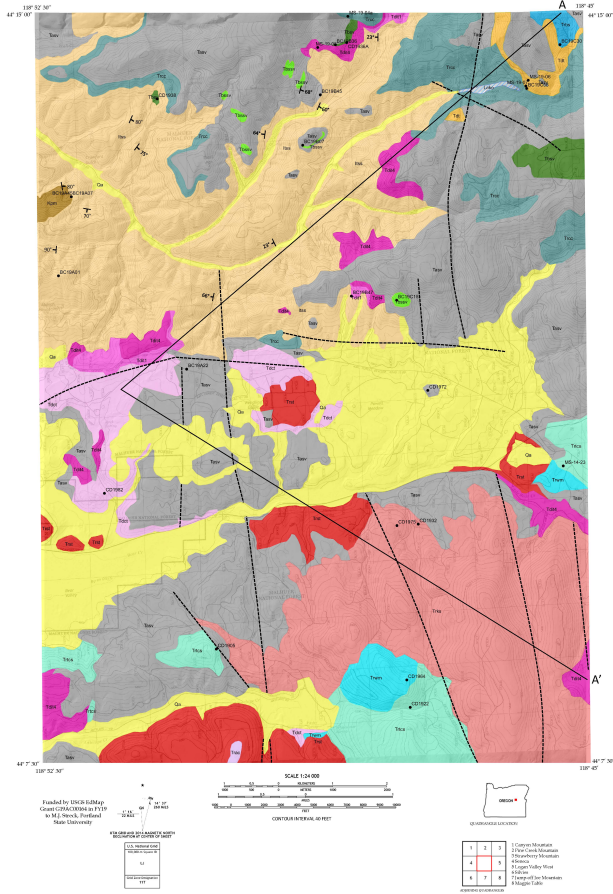
CORRELATION OF MAP UNITS



Cross-section (units in feet)



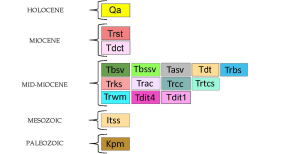
GEOLOGIC MAP OF THE BIG CANYON QUADRANGLE, OREGON
 Chanel L. Dvorak and Martin J. Streck
 2020



DESCRIPTION OF MAP UNITS

- Qa** ALLUVIUM (Holocene) - Composed largely of clay, silt, and fine to coarse sand.
 - Trst** RATTLESNAKE TUFF (7.1 Ma) - High-silica rhyolitic tuff, ranging from incipiently welded to densely welded and less than 20 m thick. The tuff is often vitric and contains ~1% phenocrysts.
 - Tdct** DEVINE CANYON TUFF (9.7 Ma) - Crystal-rich (25%) to crystal-poor (~5%), high-silica rhyolite. Partially to densely welded, observed thickness is up to a few meters.
 - Tbstv** BASALT TO BASALTIC ANDESITE LAVAS OF STRAWBERRY VOLCANICS (Mid-Miocene) - Dark colored lavas with coarse grained groundmass. Lavas are often vesicular with plagioclase and olivine phenocrysts, variably altered to iddingsite.
 - Tbssv** STROMBOLIAN VENT FACIES OF BASALTIC ANDESITE OF STRAWBERRY VOLCANICS (Mid-Miocene) - Vent facies of flow consisting of highly vesiculated, not basaltic andesitic scoria deposits consisting of lapilli- to bomb-sized scoria with occasional plagioclase and olivine phenocrysts that are often sieve-textured and altered to iddingsite, respectively. Thickness is roughly 3-10 m.
 - Tasv** ANDESITE OF STRAWBERRY VOLCANICS (16-12 Ma) - Aphyric to phenocryst-poor lavas throughout map extent. Phenocryst content ranges from 0-15% plagioclase <1 mm in length. Outcrops are pipe to blocky in habit. Occasionally intercalated basaltic lava that can be vesiculated and light gray.
 - Tdt** MILK SPRING TUFF (Mid-Miocene) - Variably thick. Stratified member (mostly 1-2 m, up to 15 m consisting of thinly bedded fallout and surge) overlain by ash-flow tuff (up to ~30 m) with small, lapilli-sized pumices but large lithic blocks (up to ~30 cm). Lithic fragments include Tdt (Dinner Creek Tuff), rhyolite of Canyon Creek, and andesites to basaltic lithologies of Strawberry Volcanics. White to light gray matrix.
 - Trbs** RHYOLITE OF BIRCHHORN SPRING (Mid-Miocene) - Stratigraphically the youngest rhyolite and overlies Tdt. Light in color pale pink with white elongated streaks along parallel fractures. Devitrified and mostly aphyric with flow banding. Fine grained groundmass with ~1% plagioclase phenocrysts.
 - Trks** RHYOLITE OF KENT SPRING (3.4 Ma) - Overall a crystal gray rhyolite that is often porous containing 1% biotite phenocrysts in addition to occasional plagioclase.
 - Trac** RHYOLITE OF ANTELOPE CREEK (Mid-Miocene) - Glassy (obsidian) to devitrified rhyolite with ~5% plagioclase but without biotite. The Trac is distinct with white speckles (plagioclase) set in the black matrix.
 - Trcc** RHYOLITE OF CANYON CREEK (Mid-Miocene) - Aphyric rhyolite that is black to light gray in color where glassy or white-ashy when devitrified. Unit thickness is on the order of 80 m.
 - Trtcs** RHYOLITE OF THREE CABIN SPRING RHYOLITE (3.4 Ma) - Mostly aphyric, flow banded rhyolite; occurs as glassy (obsidian) or light colored, devitrified rock, continuously found in close proximity to glassy member. The devitrified portion is typically fine grained, crystal poor, and light grey to cream in color.
 - Trwm** RHYOLITE OF WOLF MOUNTAIN (15 Ma) - Dark gray glassy or pinkish devitrified, plagioclase rich (up to 30%) rhyolite, typically flow banded. Trwm is distinct in how crystal rich it is, dark to light grey or pinkish in color, and does not contain biotite.
 - Tdit4** DINNER CREEK TUFF, UNIT 4 (5 Ma) - Low-silica rhyolitic tuff, welded vitrophyre, containing 1-5% plagioclase and ~1% pyroxene phenocryst. The unit is roughly 3-8 m in thickness and very dark colored in outcrop.
 - Tdit1** DINNER CREEK TUFFS, UNIT 1 (16.1 Ma) - High-silica rhyolitic tuff, partially to densely welded, containing 1-5% crystals with a pinkish devitrified or dark gray glassy groundmass. Rheomorphic sections 20-80 m thick. Lithophyses and spherulites are common in outcrop.
 - Itss** CLASTIC SEDIMENTARY ROCKS: Conglomerate, Sandstone, Siltstone, and Minor Carbonates (Mesozoic ~252-66 Ma) - Medium bedded mudstone, shale, siltstone, and massive volcanic graywacke; contains lenses of limestone breccia and cobble mudstone. Paleozoic and Triassic fossils have been reported in detrital blocks.
 - Kpm** ULTRAMAFIC ROCKS (Paleozoic ~343-251 Ma) - Sheared serpentine, mostly derived from peridotite, but original rock type not readily determinable. Small masses of garnet, pyroxene, and meta-volcanic rocks undivided.
- Approximate location of fault
 • Sample location with geo-analytical data

CORRELATION OF MAP UNITS



Cross-section (units in feet)

